ABSTRACT

KOLLMAN, MATTHEW STEPHEN. Amination and Reductive Depolymerization of Technical Lignins to Renewable Materials and Chemicals. (Under the direction of Dr. Hasan Jameel and Dr. Hou-min Chang).

Lignins are a highly abundant class of natural polymers representing the largest source of renewable aromatic carbon on land. Lignin-rich side streams are generated during the processing of woody plants to produce pulp, paper, and advanced biofuels. Impurities, heterogeneous chemical and physical properties, and relatively low reactivity have complicated the widespread adoption of these technical lignins as raw materials for value-added products. The purpose of the research presented here was to improve fundamental understanding of factors involved in the development of three potential technical lignin applications: natural-synthetic polymer blends, amine-modified lignin, and lignin-derived chemicals and fuels. The goal in each case was to identify structure-property relationships using comprehensive characterization methodologies to help inform product and process development efforts.

First, lignin isolated from a commercial pine kraft pulp mill was melt blended with polyethylene terephthalate (PET), the main thermoplastic used in carbonated beverage bottles and polyester textiles. Lignin was refined through separation into two more uniform fractions to isolate effects observed when blending the whole sample. The high molecular weight fraction would not flow by heating, but original lignin was able to. Thus, the low molecular weight fraction acted as a plasticizer to improve the free volume of the whole lignin sample and allow for melt processability. The fraction with a lower average molecular weight blended well with PET despite its lower thermal stability. PET crystallization was disrupted when blended with lignin, thereby facilitating the production of more flexible PET materials while reducing petroleum-derived content.

Similar fractionated pine kraft lignin samples were used in the second project. Adding amine groups to this type of lignin enables new functionalities, including improved water solubility, reactivity, and metal ion adsorption capacity. Gaps in literature prompted a comprehensive examination of different factors and their effect on the degree of amine substitution. Elemental analysis was shown to overestimate substitution. Carbon-13 and two-dimensional nuclear magnetic resonance (NMR) spectroscopy were combined in one technique to directly identify the number and location of amine groups that reacted with lignin. Low molecular weight lignin was more reactive towards amination, which occurred at free positions *ortho* to non-etherified phenolic hydroxyl groups and by displacing carboxylic acid groups of benzoic- and cinnamic-type subunits.

In the final project, deconstruction of three types of technical lignins (pine kraft, mixed hardwood kraft, and hardwood biorefinery) was achieved in solution at elevated temperature and pressure using three solid catalysts under a pure hydrogen atmosphere. A relatively mild (250 °C to 300 °C) and reductive environment was selected to target stable liquid phase products that were partially deoxygenated and hydrogenated. Despite improved knowledge in the conversion of simple chemicals that model lignin, how different types of real technical lignins are reductively depolymerized and the role of various catalysts remains poorly understood. Biorefinery lignin was highly depolymerized by a strong acid and base catalyst, but 20% to 25% solid residue remained when using a milder acid. Ruthenium-containing catalysts were most selective towards liquid products for all lignin types either by preventing recondensation through hydrogenation or promoting hydrogenolysis. Ru-Zn catalyst converted 18% of hardwood kraft lignin to monomers or dimers and 79% to oligomeric products with the lowest abundance of stilbenes and target molecular weight for downstream upgrading to jet fuel-range hydrocarbons.

Amination and Reductive Depolymerization of Technical Lignins to Renewable Materials and Chemicals

by
Matthew Stephen Kollman

A dissertation submitted to the Graduate Faculty of
North Carolina State University
in partial fulfillment of the
requirements for the degree of
Doctor of Philosophy

Forest Biomaterials

Raleigh, North Carolina
2021

APPROVED BY:

_____	_____
Dr. Hasan Jameel Committee Co-chair	Dr. Hou-min Chang Committee Co-chair
_____	_____
Dr. Sunkyu Park	Dr. Fanxing Li

DEDICATION

To Amanda, who has brought so much beauty and joy into my life through her art, incredible wealth of knowledge, and stopping us on hikes to marvel at the tiniest of flowers.

To my parents, whose love, support, and unwavering faith convinced me that I could.

BIOGRAPHY

Matthew Kollman grew up in North Carolina where he gained an appreciation for the natural world by scrambling up smoky mountains, peaking under the rocks of Piedmont creeks, and clamming along the coast. His love for our environment and desire to protect it sent him to NC State University to study chemical engineering and paper science, where he became convinced that green engineering is good engineering. At Georgia Tech, he got to dive into the science that drives our environment, specializing in atmospheric chemistry. After graduating from GT with a masters, Matthew began practicing engineering at a firm where he had the exciting and fortunate opportunity to put into action all that school had taught him.

After a few years he reached a crossroads and accepted an offer to work with a former professor at NC State. Dr. Jameel intrigued Matt with a question, “what can we do with lignin?” A fitting question to ask someone about to pursue a degree in philosophy. Through the past five years, Matthew has interned with a private research institute, traveled the world from Seoul to Seattle, and persevered through a global pandemic pondering this question. He hopes this dissertation may suffice as at least a partial response.

Along with his graduate studies, Matthew had the opportunity to create a departmental chapter of the NC State Graduate Student Association and serve on a legislative affairs committee. This foray into policy piqued his interest and Matthew currently serves as a STEM policy fellow in the NC Office of Science, Technology, and Innovation.

Matt is fascinated by the local histories of NC towns and all the places through which he travels. On free weekends he may be found hiking, camping, brewing, or trying his hand at home repair. He plays saxophone, guitar, bass, and has serious intentions to learn the banjo - one day.

ACKNOWLEDGMENTS

Doctoral work is perhaps one of the most personal, independent, and at times lonely, pursuits. Yet, it is also one pursuit in which success is impossible without the support of innumerous people.

I first wish to offer my deepest gratitude to Prof. Hou-min Chang and Prof. Hasan Jameel for taking me on as their student, allowing me the freedom to explore, the time to fail and learn, and the patience to teach me chemistry, scientific research, communication, and leadership.

I want to thank my committee members, Dr. Sunkyu Park, Dr. Fanxing Li, Dr. David Dayton, and Dr. Ofei Mante for your valuable feedback and suggestions in improving the quality of this work. I'd additionally like to thank Drs. Dayton and Mante for hosting me as an intern at RTI International, which inspired much of this work and improved my confidence as an independent researcher.

Many colleagues have contributed directly to the concepts, data, and discussion included in this dissertation: Dr. Xiao Jiang, Dr. Robert Narron, and Dr. Runkun Sun in the Department of Forest Biomaterials; Dr. Peter Thompson and Dr. Xiaoyan Sun in the Molecular Education, Technology and Research Innovation Center at NC State; Ms. Lisa Lentz of the Environmental and Agricultural Testing Service at NC State; Dr. Samuel J. Thompson at Kao Specialties (formerly at RTI International), and Prof. Wenzhi Li and his research group at the University of Science and Technology of China. I am also indebted to the Jordan family and their generous support that funded this research through the Jordan Family Professorship.

My appreciation for the Forest Biomaterials staff (current and former) cannot be understated. Thank you to Ms. Melissa Rabil, Ms. Barbara White, Ms. Beverly Miller, Mr. Mike Maltby, Dr. Jie Liu, and Ms. Ambre Chiomento for all your assistance and dedication to the

department. I'd also like to recognize the work of housekeeping and facilities for maintaining a safe, functioning, and comfortable working environment, without which we could not do our work, specifically Mr. Nordoff, Ms. Gloria, and Mr. Ehab Asfari. Special thanks to Ehab who kept my eye on the prize by never failing to ask when I was going to graduate.

Many, many fellow graduate students, post-docs, and visiting scholars guided me in administrative matters, lent lab supplies, or simply offered support as a friend. Although I cannot acknowledge everyone here, I at least would like to thank Dr. Camilla Abbati de Assis for making me feel welcome when I first arrived and establishing such a positive energy for our office and department, which has since continued. And a special shoutout to Dr. Adam Scouse for always keeping it real.

I sincerely thank Xiao Jiang for never getting upset despite the numerous times I have asked for his advice and help, whether it be setting up a reaction apparatus, on wood chemistry fundamentals, or the many times in the evening when the NMR was acting up. Without our long talks on history, politics, and solving the world's problems my experience would not nearly have been so enjoyable.

And finally, last but most importantly, I thank my family and friends: Amanda for your seemingly endless patience, compassion, and guidance; Mom and Dad for the opportunities that have made this journey possible; Michael for teaching me my times table and including a blanket in the box; Lauren for reminding me to breathe and enjoy life, and the suite of 503 (Ryan, Trent, Jason, Jit, Taylor, and Kevin) for your honesty and keeping me grounded.

TABLE OF CONTENTS

LIST OF TABLES

LIST OF FIGURES

CHAPTER 1: Introduction

Background

2020 was recognized as the 100th anniversary of polymer science. One century earlier, Hermann Staudinger proposed that materials like natural rubber were comprised of very high molecular weight molecules of covalently bonded repeating units. Physical interactions between smaller molecules were thought to explain the viscoelastic behaviors of rubber, cellulose derivatives, phenol-formaldehyde resins, etc. before this. His seminal work, "On polymerization," was published in 1920 while the first world war accelerated the industrial revolution towards mass production of goods. This new knowledge of how organic materials were structured aided in the development of new, synthetic materials that could be produced in large amounts from petroleum resources, largely displacing products derived from biological sources by the 1950s.

The world of 2020 is quite different than 1920. Global human population has increased 4.2 times from 1.9 billion to 7.8 billion and atmospheric CO_2 concentration has increased by 35.6% to 410 ppm, whereas the highest recorded value before 1900 (spanning at least 800,000 years) was 299 ppm.[1–3] Climate change is arguably the single greatest threat to the survival of humans and multiple scientific, technological, and societal advancements are required to mitigate its effects.[4] The sustainable use of renewable resources as feedstocks to fuels, chemicals, and materials may be one such option. It is illogical to rely on a finite supply of petroleum resources to provide for a growing human population, while at the same time understanding the need to sequester atmospheric carbon to slow the effects of climate change.[5] The U.S Department of Energy (DOE) calculated that it should be possible to replace 30% of petroleum consumed in the U.S. with bioproducts with a shift in policy from a petroleum-based to a bio-based economy.[6]

The most accessible renewable sources of carbon are terrestrial, vascular plants, the cell walls of which are mainly comprised of three biopolymers: cellulose, hemicellulose, and lignin. Lignocellulosic materials are attractive renewable resources because they do not compete with food supplies and are available at large scales as residues or byproducts of current agricultural and industrial activities. Lignins represent 30% of terrestrial carbon in the biosphere and the largest source of renewable aromatic carbon.[7] A higher carbon-to-oxygen ratio on average relative to cellulose or other natural polysaccharides imparts a higher heat of combustion for fuel production. Up to 2 percent of global petrochemical production could be supplied with the current availability of commercial lignins.[8] However, of the 50 million metric tons of lignin extracted from wood as black liquor by the pulp and paper industry, only 2 percent is used in commercial applications; the remaining 98% of black liquor is combusted as a fuel for the production of steam and power.[9] The overall motivation of this doctoral research was to contribute towards the increased utilization and valorization of lignins.

Formation and Structure in Nature

Lignins are a class of natural polymer found within and between cell walls of all vascular plants.[10] Evolution of phenylpropanoid biosynthesis pathways allowed early terrestrial plants to thrive despite exposure to damaging UV radiation and pathogens; and, eventually the rigid aromatic network enabled upright growth of tracheophytes that have since diversified into more than 300,000 species of ferns, gymnosperms, and angiosperms.[11,12] The lignin polymeric network can be composed of three primary phenylpropane units: syringyl (S-type), guaiacyl (G-type), and *p*-hydroxyphenyl (H-type). These three repeat units correspond to three *p*-hydroxycinnamyl monomers known as monolignols (*p*-coumaryl, coniferyl, and sinapyl

alcohols) that are biosynthesized from L-tyrosine and L-phenylalanine (**Figure 1.1**). While only three main repeat units exist, the chemical structure of lignins is complex and varies between species, within a single plant, and between seasons depending on required functionality. For example, both gymnosperms and angiosperms contain G-type and H-type units, but only angiosperms contain S-type units in an appreciable quantity.

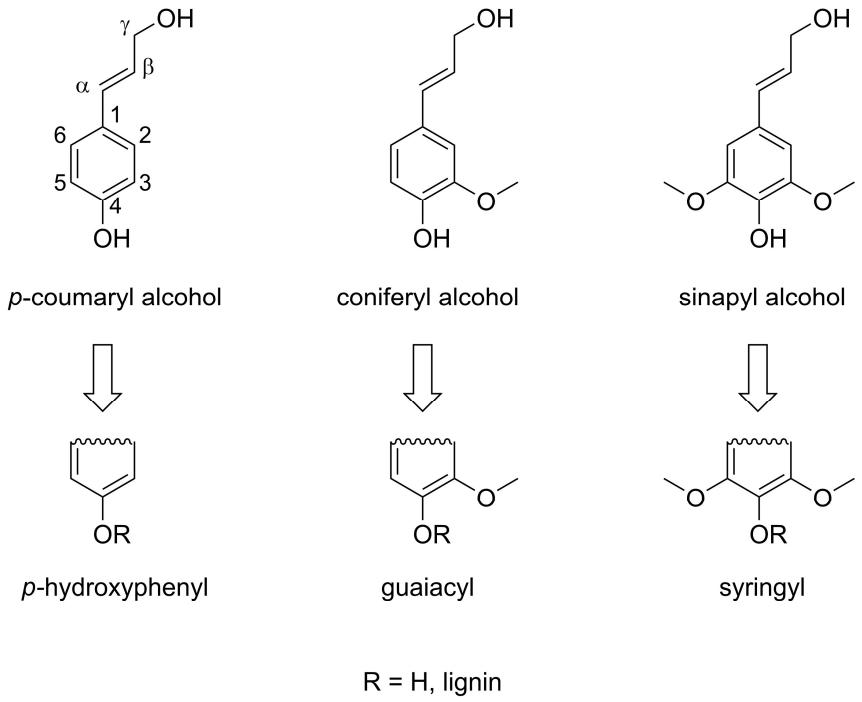

Figure 1.1. The three monolignol compounds and corresponding lignin molecule repeat units.

Lignin biosynthesis is initiated by enzyme-mediated dehydrogenation of the phenolic hydroxyl group of monolignols to form a phenolic radical. These resonance-stabilized radicals contain electron deficient centers at the phenoxy group, C5, C1, and Cβ. Dimers, or dilignols, are formed through radical coupling of different canonical forms. Lignification continues either through endwise coupling of monolignols to dimers/oligomers or bulk polymerization of

oligomers and dimers. Quinone methides are formed from Cβ coupling, to which any nucleophile may add to regenerate a phenolic hydroxyl group for further dehydrogenation. Thus, repetitive dehydrogenation, coupling, and addition to quinone methide eventually lead to the formation of lignin macromolecules as shown in **Figure 1.2**. Typical interunit linkages are shown in **Figure 1.3** and average distributions for softwood and hardwood lignins are given in **Table 1.1**. Boerjan *et al. o*ffer a more in-depth discussion of lignin biosynthesis.[7]

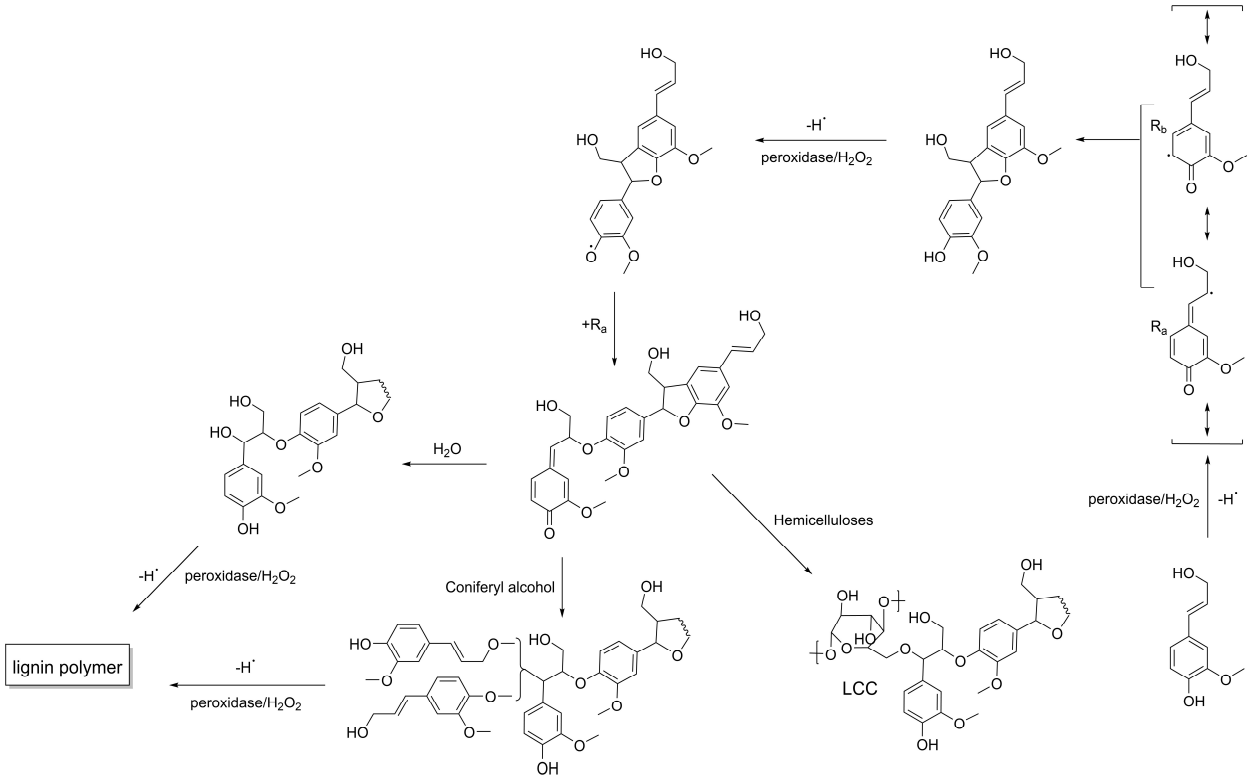

Figure 1.2. Lignification process. Reproduced from reference.[13]

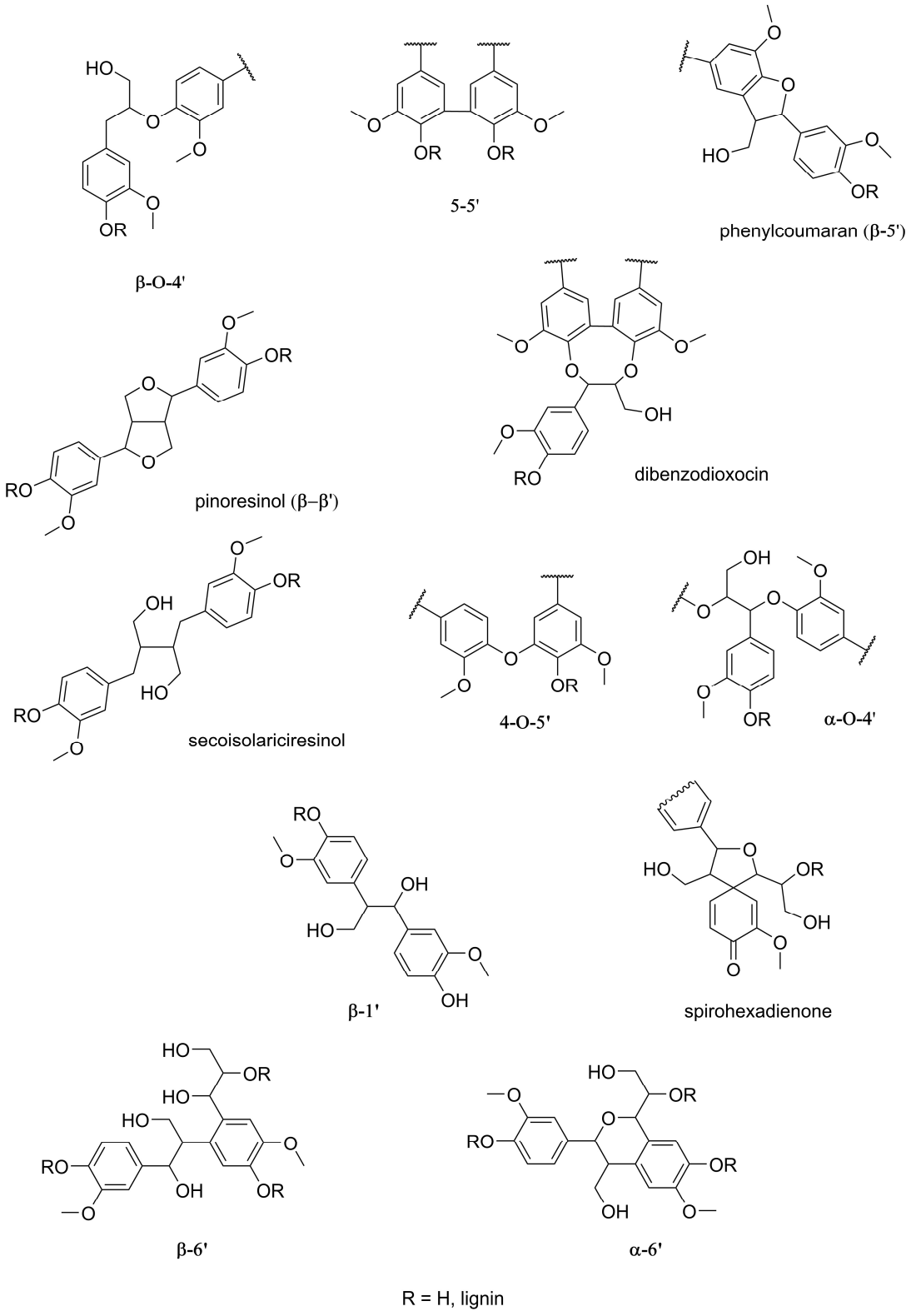

Figure 1.3. Common interunit linkages of lignin molecules.

Table 1.1. Approximate distribution of native lignin structural features found in softwood and hardwood tree species (mol/100 mol aromatic units).[14]

Structure	Softwood	Hardwood
Aromatic subunit[a]		
p-Hydroxyphenyl	4	2
Guaiacyl	95	50
Syringyl	1	50
Interunit[b]		
β-O-4'	44	48 to 53
Phenylcoumaran (β-5')	10	4
5-5'	23	9
Dibenzodioxocin (DBDO)	6	1
Pinoresinol (β-β')	4	8
β-1'	3	5
α-6', β-6'	3	2
4-O-5'	4	7
Cyclohexadienone Units	3	4
α-O-4'	1 to 3	1 to 5

a. Softwood lignins are similar, but the S:G of hardwood lignins ranges from 1 to 2 or higher.

b. DBDO quantities are included in β-O-4' and 5-5' estimates.

Industrial Isolation of Technical Lignins

Analytical lignins include Milled Wood Lignin (MWL), Mild Acidolysis Lignin (MAL), Cellulolytic Enzyme Lignin (CEL), and Enzymatic Mild Acidolysis Lignin (EMAL). These methods are performed on the lab scale and as such are not relevant to the development of commercial products. As the intention of the present work is to discuss the application of lignin towards development commercial products, analytical lignin will not be discussed further. However, information on these techniques can be found in many reviews or books, specifically the first three chapters of Methods in Lignin Chemistry.[15,16] Analytical lignins are produced at

small scales with little concern for economics. Several industrial-scale processes exist to remove lignin from biomass that are of more interest to applied research efforts. These processes are all designed to isolate carbohydrates either as fibers for downstream upgrading to paper, packaging, non-woven textiles; or, as sugars to feed fermentation processes or serve as platform chemicals. Lignin-rich side streams are burned, if possible, to recover the heat value and process chemicals. Lignin must be depolymerized and solubilized to be removed from biomass, thereby altering the chemical and physical properties compared to native lignins from which they are derived. These properties are highly dependent on the method of isolation and wood species, so it is necessary to understand the origins of a lignin sample before being used.

Soda

Soda or alkali pulping uses sodium hydroxide to swell biomass and fragment and dissolve lignin molecules. It was the first method of pulping wood and grasses with the first mill opening in 1866 but has largely been replaced by the kraft process.[17] Some soda pulp mills still exist that pulp hardwoods and non-woody grasses. Soda pulping hydrolyzes lignin ether bonds, and the pH (11 to 13) is high enough to ionize phenolic hydroxyl groups to facilitate dissolution. The soda process has fallen out of favor due to low selectivity towards lignin, which causes hydrolysis of carbohydrate polymers and low fiber strength. Furthermore, γ-hydroxymethyl groups from lignin side chains are liberated as formaldehyde molecules, which condense lignin aromatic units to form diphenylmethane structures that are not easily broken and limit depolymerization.[18] Soda lignins remain attractive as feedstocks to catalytic conversion processes for their lack of sulfur compounds, which act as poisons to many catalysts and must be removed from the final fuel or fine chemical mixture.[19]

Sulfite

Sulfite pulping liberates cellulose from wood chips using a base and sulfurous acid through two overall reactions: 1) formation of lignosulfonate groups on lignin, which increases solubility and 2) hydrolysis of the lignosulfonates to smaller molecules.[17] Cooking is performed under acidic conditions but base serves as a buffer, which prevents pulp darkening reactions and condensation of lignin fragments. Sulfite pulp is easier to bleach than other conventional pulps like soda and kraft and is used for bleached grades of packaging or to avoid bleaching where semi-white packaging is sufficient. Dissolving pulp is also mostly produced by the sulfite process. Lignin molecules obtained from spent pulping liquors are highly soluble in water across a wide range of pH and have relatively high average molecular weights compared to other technical lignins. Lignosulfonates have a weight-average molecular weight three to four times that of softwood kraft lignins.[20] They have found applications as anionic polyelectrolytes in cement formulations, animal feed, road dust suppressants, oil drilling thinners, and controlled release fertilizer granules.[21]

Lignosulfonates dominated the technical lignin market in 2018, accounting for 79% of commercial production, while kraft and soda lignins accounted for 16% and 5%, respectively.[22] Applications for kraft lignins are the focus of this dissertation and many research studies because of the rate at which production has accelerated and the potential supply are far greater than that of lignosulfonates. Kraft lignin production increased by 1.5 times from 2014 to 2018 versus an estimated 1% growth rate of lignosulfonates, and kraft cooking generates 90% of global pulp supply.[22]

Kraft

C.F. Dahl obtained a patent for the kraft pulping process in 1884 after experimenting with sodium sulfate as a make-up chemical and finding that it increased selectivity towards delignification and retained a higher carbohydrate degree of polymerization, thus producing a stronger pulp relative to the soda process.[17] Sodium hydroxide and sodium sulfide are the two main pulping chemicals used for the delignification of wood in the kraft process. Modern kraft pulp mills employ an integrated, closed process with high recovery rates of process chemicals, water re-use, and on-site production of steam and electricity (**Figure 1.4**). Wood chips and cooking chemicals (white liquor) are fed to either batch or continuous digesters that are heated to 170 °C for approximately 2 hours. During the cook, several reactions occur that will be discussed in more detail in the following section. The deconstructed wood chips are washed to remove dissolved lignin fragments and cooking chemicals (black liquor), which are fed to evaporators and a recovery boiler to burn the organics and recover the inorganics mostly as sodium carbonate and sodium sulfide (green liquor). Sodium carbonate is converted to sodium hydroxide through a process known as causticizing to regenerate white liquor needed for cooking.

Kraft lignin is typically isolated from black liquor by lowering pH using carbon dioxide to deionize phenolic hydroxyl groups, thus precipitating molecules out of solution. LignoForce System™ and LignoBoost® are two examples of commercialized processes that use this concept.[23,24] Subsequent filtration and washing of solids with sulfuric acid and water can lower the sulfur and ash contents to less than one or two percent. Softwood and hardwood kraft lignins are produced commercially, though hardwood kraft yields tend to be lower at least in lab scale studies.[25–27]

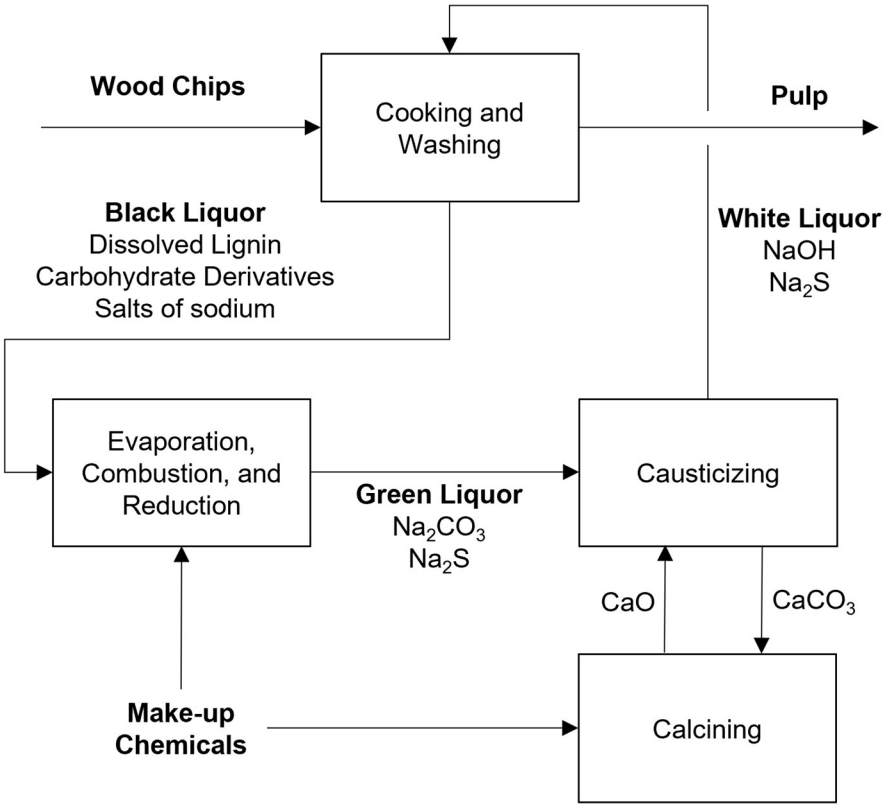

Figure 1.4. Process flow diagram of kraft pulping and chemical recovery.

Biorefinery lignins

Conventional pulp and paper mills are technically examples of biorefineries, but much of the literature refers to biorefinery lignin as a product of non-commercial lignocellulosic conversion processes like acid hydrolysis, steam explosion, and hot water extraction for which the main product is sugar or ethanol.[28] Organosolv is another method of pulping that will be discussed here as it is not currently commercialized and produces a similarly pure lignin product.[29] These processes are typically milder than the conventional pulping technologies (soda, kraft, sulfite) and result in lower chemical modifications of the molecular structure. Furthermore, steam explosion, hot water extraction, and organosolv pulping do not use sulfurous chemicals and are generally more environmentally benign than kraft or sulfite pulping.

Acid hydrolysis pretreatment of biomass typically uses mineral acids like sulfuric or hydrochloric as catalysts to hydrolyze carbohydrates to soluble sugars yielding a lignin-rich solid. Dilute and concentrated acid versions exist that each have their own advantages and disadvantages in terms of sugar yield and fermentation efficiency.[28] Steam explosion and hot water extraction are versions of hydrothermal pretreatment methods that rely on hemicellulose-derived acetic acid to catalyze hydrolysis. Steam explosion uses rapid depressurization to rupture the cell walls and the cellulose crystals to expose these polymers for enzymatic treatment downstream and is possibly the most popular hydrothermal method historically.[30] Hot water treatment followed by mechanical refining has been demonstrated as an alternative to steam explosion to achieve high sugar and ethanol yields using lower temperatures.[31,32] This latter process is used to generate sweetgum autohydrolysis, enzymatic-hydrolysis residue lignin used in the main body of this dissertation where the lignin chemical structure is discussed in detail. To understand the overall process a diagram and mass balance are provided here (**Figure 1.5**).

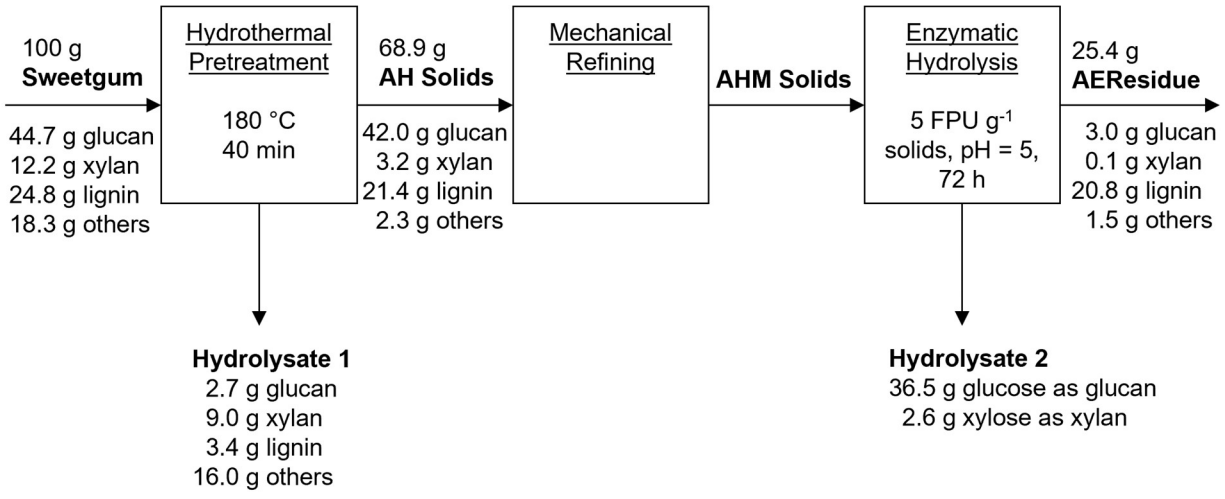

Figure 1.5. Process flow diagram of hot water treatment followed by mechanical refining to increase enzymatic hydrolysis conversion. Reproduced from reference.[32]

Kraft Lignin Chemistry

Kraft lignins isolated from softwood and hardwood black liquors are the main technical lignin samples used in the research that follows, therefore, a brief overview of the current knowledge on kraft pulping chemistry as it relates to dissolved lignins is presented here. The focus will be on softwood kraft lignins simply because more information exists. The main objective of kraft pulping is to selectively remove lignin from the biomass matrix and separate wood fibers with minimal cellulose degradation. Time, temperature, hydroxide and sulfide concentrations, and wood species are major variables that dictate the pulp yield, degree of delignification, and final physicochemical properties of the carbohydrate and lignin molecules. For bleachable grades, delignification up to 85% (dry weight basis) is typical for a kraft cook, which corresponds to a pulp containing 5% to 3% residual lignin for softwood and hardwood, respectively.[17] 40% to 45% (dry weight basis) of carbohydrate polymers are degraded and dissolved into the black liquor along with the dissolved lignin.[17] Though the majority (60% to 75%) of the carbohydrate losses are attributed to hemicellulose degradation.

The objective of delignification is to cleave enough interunit bonds to solubilize lignin fragments and separate fibers from each other. Minimizing interunit recondensation of fragments and precipitation back onto the fiber is equally important. Alkyl-aryl ether bond cleavage is the main pathway towards delignification during alkaline pulping. 50 to 60 percent of interunit bonds in the lignin polymeric structure are susceptible to cleavage given estimated β-O-4' and α-O-4' abundances (**Table 1.1**). Aryl-aryl ether and carbon-carbon interunit bonds are stable during alkaline pulping.

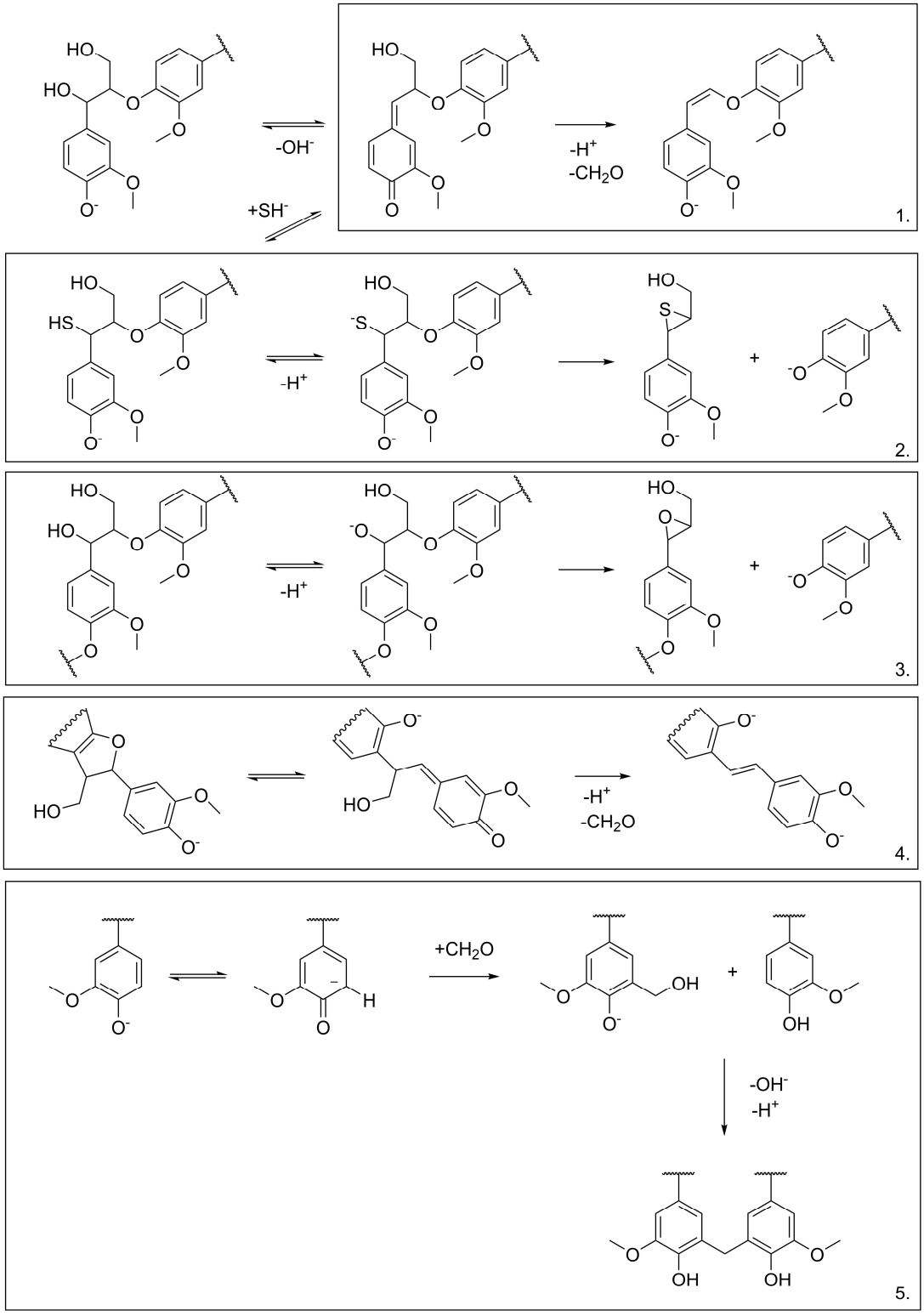

Figure 1.6. Reactions involving lignin during kraft pulping.

β-O-4’ hydrolysis proceeds through two routes depending on whether or not the other phenolic hydroxyl group is etherified. The reaction of free phenolic units proceeds at a faster rate, while etherified phenolic unit hydrolysis is slower and determines overall reaction rate. Free phenolic hydroxyl groups are not common in the native lignin structure, accounting for between 10 and 13 mol per 100 mol C9 units in spruce and aspen wood samples.[33,34] Etherified phenolic units must natively have a hydroxyl group present at the benzylic carbon and/or Cγ to be reactive towards beta-aryl ether cleavage via epoxide formation, though epoxide formation from α-hydroxyl groups is faster than from γ-hydroxyl groups (**Figure 1.6**, reaction 3).[35] These rate-determining reactions are common to both kraft and soda pulping processes since no hydrosulfide is involved in formation of these epoxides. However, new phenolic units are formed as alkyl-aryl ether bonds are cleaved, which increases overall rate of reaction as the cook proceeds. Free phenolic units are first ionized to form quinone methides (**Figure 1.6**, reaction 2). Either OH^- or SH^- may attack the quinone methide to restore aromaticity, but the resulting benzyl hydrosulfide is a stronger acid and a much better nucleophile than the corresponding benzyl alcohol. Ionization of the hydroxyl or thiol group leads to epoxide or episulfide formation and cleavage of the beta-ether bond (**Figure 1.6**, reaction 2), which generates a new phenolic hydroxyl group to continue the process.

Other degradation reactions occur that do not contribute towards delignification, like demethylation and demethoxylation of methoxyl groups and elimination of γ-hydroxymethyl groups. γ-elimination of β-O-4’ yields enol ether and β-1’ and β-5’ interunit structures yield stilbenes (**Figure 1.6**, reactions 1 and 4). Neither of these structures can be hydrolyzed during alkaline pulping. Additionally, formaldehyde molecules are generated that readily participate in condensation reactions given the reactivity of quinone methide and carbanions that exist in

equilibrium with phenolate anions (**Figure 1.6,** reaction 5). Approximate interunit linkages and subunit abundances of a dissolved softwood kraft lignin sample (as determined by nuclear magnetic resonance spectroscopy, NMR) are presented to demonstrate the effects of these reactions on the overall structure (**Table 1.2**). Two sets of data are presented for Indulin AT to illustrate results of two different quantitative NMR techniques from different labs.

Table 1.2. Structural feature abundances for dissolved softwood kraft lignin compared with approximations of native lignin as determined by NMR (mol/100 mol aromatic units).

Structure	Native Appx.[36]	Lab scale cook[37,a]	Indulin AT[38,b]	Indulin AT[39,b]	BCL[39,b]
β-O-4’	41	3.2	7.1	8.2	2.2
DBDO	8	ND[c]	0.2	0.6	0.8
β-5’	9	0.8	1.5	1.1	1.6
β-β’ pinoresinol	2	2.4	1.6	1.2	2.5
Secoisolariciresinols	2[40]	3.2	2.3	3.1	3.5
Stilbenes	-	4.8	9.8	6.7	7.3
Enol ethers	-	1.3	3.9	1.5	2.2
Coniferyl alcohol	4	0.8	1.8	0.3	0.7
Methoxyl groups	95	80	75	68	63

a. Lab scale pulping to 1700 H-factor and acidification of black liquor to pH = 2.

b. The first column of Indulin AT data[38] was obtained by $HSQC_0$ experiments, while the right two columns were obtained by combining ^{13}C and HSQC NMR.[39]

c. ND = not detected.

The average molecular weight reduction of lignins during kraft pulping is an indication of the extent of depolymerization when coupled with mass balance information. Isolation from black liquor is usually incomplete because smaller molecules are more difficult to precipitate and

filter out of solution, therefore kraft lignin samples usually represent a higher MW portion of total dissolved lignin. Mass balance data is not usually presented along with molar mass determinations. Additionally, the correct method to determine absolute molecular weight of lignins continues to be a topic of debate.[20,41,42] Nonetheless, number- and weight-average molecular weight data can be useful for predicting trends in structure-property relationships when developing kraft lignin applications. Relative comparisons can be made given consistent methodology, similar polymer-solvent interaction energies, and complete dissolution of the sample. Molecular weight distribution data for milled wood and dissolved kraft lignins are given for both softwood and hardwood species in **Table 1.3**. Number-average and weight-average molecular weights of MWL samples dissolved in dimethylformamide were determined by osmotic pressure and ultracentrifugation techniques, respectively. Hardwood lignins are typically comprised of smaller molecules given the presence of syringyl moieties that prevent intermolecular condensation during lignification and pulping. The measured molecular weight of sweetgum MWL presented in **Table 1.3** was higher than that of spruce because 96% dioxane is a better solvent for sweetgum lignin.[43] Both kraft lignins presented in **Table 1.3** were first acetylated with acetic anhydride and dissolved in tetrahydrofuran. Molecular weight information was derived by correlating the elution times of lignin samples with polystyrene calibration standards using gel permeation chromatography.[44,45]

Table 1.3. Molecular weight distribution of milled wood and dissolved kraft softwood and hardwood lignins.

Sample	M_n (g mol^{-1})	M_w (g mol^{-1})	$Đ$	Reference
Spruce MWL	3,420	15,000	4.4	(*43*)
Pine Kraft	1,660	6,650	4.0	(*44*)
Sweetgum MWL	4,260	16,000	3.8	(*43*)
Mixed HW Kraft	1,260	2,400	1.9	(*45*)

Kraft Lignin Applications and Challenges

Kraft lignin-based products have not been commercialized to the extent lignosulfonates have. Sulfonated kraft lignins are produced commercially, which have similar applications to lignosulfonates like road dust binder and cement or oil well dispersants.[8] These are relatively low value, as is kraft lignin's main use as a solid fuel for pulp and paper mill steam and electricity generation. Many reviews summarizing lignin applications have been published. Holladay *et al*. covered these products along with potential market penetration and risk.[46] The purpose of this section is not to relist these, but to offer a brief survey of recent applied research efforts specifically related to kraft lignin to acknowledge challenges to valorization and potential solutions.

Fractionation and chemical modification

Several challenges exist for using kraft lignins in material applications. Highly disperse molecular weight distributions ($Đ > 2$) and heterogeneous chemical structures complicate efforts to control polymerization and develop a product of uniform structure and properties. Pure synthetic, petroleum-derived monomers and platform chemicals are readily available and

inexpensive, but that is not because the crude material is homogenous and uniform; instead, it is because extensive research and development have developed a petroleum refining industry to reach that goal. Different methods of fractionation have been developed for improving the uniformity of lignin samples, including solvent-based, precipitation, and membrane filtration.[26,47–49] Adoption of crude kraft lignin as a feedstock for material applications is hindered by other factors, including low average molecular weight relative to synthetic polymers, low reactivity and functionality (reactive sites per molecule), and they are highly branched with poorly-defined glass-transition temperatures that exist close to degradation temperature (two factors specifically relevant to thermoplastic product development). Chemical modifications can overcome many of these limitations for kraft lignin to be used as functional material or to be physical incorporated into polymer blends and composites.[50–54]

Some examples of chemical modifications include phenolation, esterification, etherification, amination, and graft polymerization. Phenolation increases the number of reactive sites (C3 and C5 positions) and the free volume of the modified lignin. A promising application of phenolation is to improve the functionality of lignin as a phenol substitute in phenol-formaldehyde resins to partially reduce the total amount of phenol monomer required, which is toxic.[55] Alternatively, depolymerization can also increase the number of free sites and has been reviewed as a method for polymerization of rigid polyurethane foams.[56] Esterification and etherification reduce polarity and reactivity of the lignin molecule, whether the latter is an intended effect or not. Reduction of polarity is useful in modifying interfacial energy to improve polymer blend stability.[57] Esterification and alkylation for polarity and reactivity reduction has been successfully used as a means for lowering glass transition temperature (reduced hydrogen bonding) and limiting condensation reactions during melt processing of softwood kraft

lignin.[58,59] Amination adds cationic functionality and improves hydrophilicity. Amination of kraft lignins has been shown to improve dispersion in epoxy composites[60] or simply as a method for creating a bio-based nitrogen fertilizer.[61] Many different graft polymerization chemistries have been used to increase the molecular weight and thermal stability of kraft lignin molecules, linearize the starting polymeric network to impart thermoplastic properties, or to develop thermosets given a sufficiently high degree of crosslinking.[62–67]

Carbon materials

Lignins' cyclical structure and high carbon yield after pyrolysis have inspired researchers to study their potential as precursors for carbon fibers.[68–71] The main advantage of lignins over PAN is cost. In 2010, PAN-derived carbon fibers cost roughly $30/kg, and the DOE estimated that at a yield of 35%, lignin-based fibers would cost $6.27/kg or $4/kg if the yield improved to 55%.[68] The first demonstration of any lignin as a precursor for carbon fibers was in 1965 at Nippon Kayaku, a chemical company in Japan.[72] The Nippon Kayaku fibers were sold commercially until the late 1970s. After a hiatus of lignin-based carbon fiber research, interest in the subject reemerged in the early 1990s with melt spinning as a focus, as this was (and is) considered more economical for scale-up and possibly one reason the Kayaku commercial enterprise failed. One of the first of this second wave of studies investigated steam-exploded birch lignin modified via hydrogenolysis.[73] This modification removed moieties that participated in crosslinking upon heating, thereby maintaining a low glass transition temperature that facilitated melt spinning. Most studies afterwards relied similarly on performing some modification of the lignin to be melt processed. In 2002, Kadla *et al*. demonstrated melt spinning of hardwood kraft lignin fibers without modification by using poly(ethylene oxide) (PEO) as a

plasticizer at 5% loading.[74] The reduced glass transition temperature allowed for melt spinning and the carbonized fibers achieved a carbon yield of 45%, close to that of PAN-derived fibers. However, many drawbacks exist that have prevented their commercialization. For one, the highest published tensile strength of an unmodified, lignin carbon fiber was 1070 MPa with a modulus of 83 GPa compared to 7 GPa and 500 GPa for PAN tensile and modulus, respectively.[69] Poor orientation of polymer chains in the axial direction and presence of defects are two characteristics of lignin carbon fibers that limit their strength.

Carbon material applications that do not rely on strength have also shown early promise. Activation of carbonized fibrous mats or volatilization of sacrificial polymers during carbonization creates microporous fibers with high surface area, which is attractive for applications in water treatment, gas separation, or power storage. Most applied research of lignin-based carbon fiber mats focused on power storage applications, with goals to produce either capacitors or battery anodes.[75–77]

Chemicals and liquid fuels

Some challenges associated with lignin-based materials like incompatibility, low molecular weight, and low reactivity can be avoided through depolymerization to a liquid mixture of uniform molecular weight that can be separated based on chemical classes, upgraded to hydrocarbon fuels, or ideally used as is. Methoxy phenolic compounds and platform chemicals like benzene, toluene, and xylenes are potential kraft lignin-derived chmicals.[78–80] Gasoline, diesel, jet fuel-range hydrocarbons have also been explored extensively given the relatively low carbon-to-oxygen ratio and aromatic backbone of lignins.[81,82] Heterogeneity of interunit linkages and subunits makes depolymerization of lignins difficult and has evolved in nature to be so. One

biocatalyst or mechanism is not sufficient for total degradation of the lignin polymeric network. The lack of alkyl-aryl ether bonding in kraft lignin makes it relatively more recalcitrant than native, which challenges biochemical conversion, although advances in bioengineering will likely provide solutions.[83] Thermochemcial processes like pyrolysis, hydropyrolysis, (photo)oxidation, liquid-phase hydroprocessing (hydrogenolysis, hydrodeoxygenation, and hydrogenation), and gasification offer the advantages of lower process times and higher yields than biological routes. Each technology is briefly reviewed in chapter five. Reductive depolymerization was selected because of higher liquid yields, more stable liquid product, and product tunability (**Figure 1.7**).

Hydrogenolysis of lignins has been studied for many years as an analytical tool but the focus has shifted to applied research over time.[15] Much work has been performed to assist in our understanding of reaction mechanisms using model compounds, to a lesser extent milled wood lignin and biorefinery lignin, and to a much lesser extent kraft lignins. Advances in nuclear magnetic resonance spectroscopy have allowed for characterization of higher molecular weight products which will assist in elucidation of reaction pathways. More can be learned about the relationships between technical lignins, catalysts, process conditions, and products, which will inform the design of more selective and robust solid catalysts.

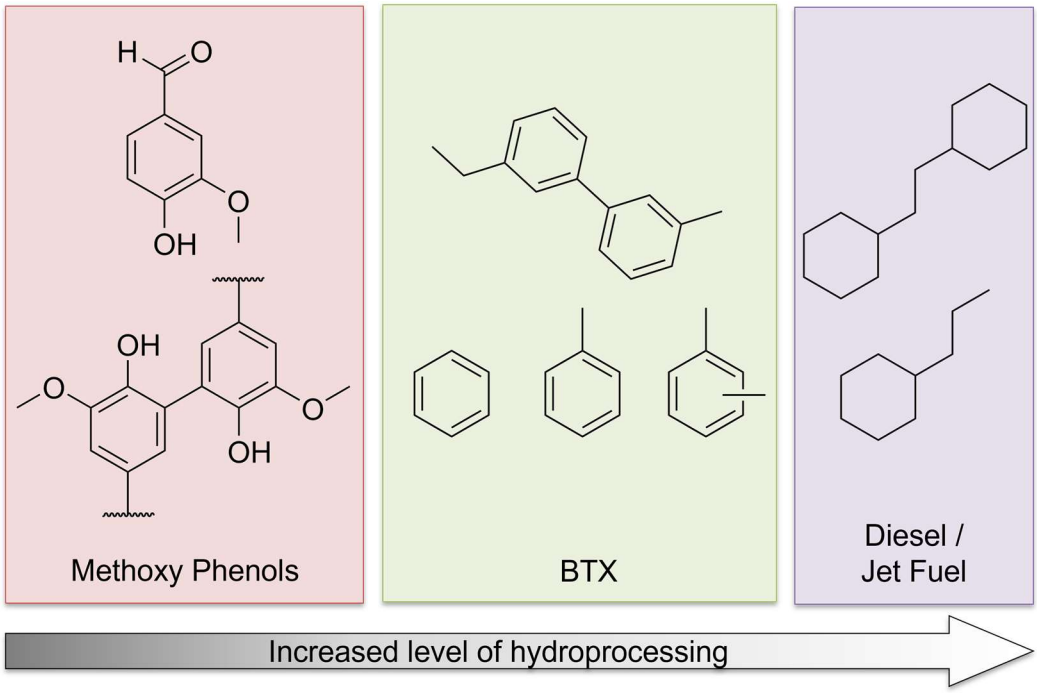

Figure 1.7. Liquid-phase hydroprocessing product tunability.

Analytical methods

For much organic chemistry research physical and chemical properties of the starting materials are well-defined and certified by the manufacturer in many cases. Natural polymer chemists start with a package of unknowns. This may sound hyperbolic or obvious to seasoned researchers. Still, many results found in applied lignin research literature are not discussed in relation to the properties of the starting material because source of origin and appropriate characterization of the starting lignin were unknown. Studies have claimed to have used "kraft" lignin purchased from a chemical supplier and assume that because it has a product number it is a standard, pure lignin when in fact Aldrich lignin contains more than 60% ash.[84] Often this is a result of non-lignin chemists wishing to use a renewable material in their research but it serves as a reminder not to assume that the batch of lignin we are currently working with will look like the next, especially when received from a supplier or pulp mill.

Lupoi *et al.* compiled an excellent comprehensive survey of current lignin characterization techniques, including spectroscopy, chromatography, and wet methods, and reviewed the advantages and limitations of each.[85] Instead of reproducing that review here, relevant analytical procedures and discussion are given within each of the main chapters that follow. Analytical lignins have received a lot of attention but kraft lignins not as much. Techniques that were developed for analytical lignins may or may not apply to kraft lignins or other technical lignins. Even as understanding of the abundance and type of structural components increases, the order of assembly remains less clear. It is important to remain cognizant of the limitations of analytical methods and gaps in knowledge when making conclusions about structure-property relationships. Continued development and testing of new techniques specifically for technical lignin research should be encouraged.

Research Goals and Objectives

Research projects focused on industrial lignin applications. Projects involved many disciplines like polymer science and catalysis but emphasized the perspective of lignin and wood chemistry. Research goals and specific objectives are listed below.

Goals:

- Explore value-added applications using technical lignins as main raw material.
- Execute comprehensive characterization of starting material and products to make informed explanations of observed physicochemical properties.
- Contribute to the lignin chemistry and wider biorefinery research and development community.

- Remain cognizant of technical and economic feasibility while developing and carrying out experimental plans.

Objectives:

1. Carry out proof of concept testing of polyethylene terephthalate kraft lignin melt blending.
2. Study modification of different technical lignins by amination, the factors that affect degree and location of substitution, and evaluate analytical technique accuracy.
3. Identify reductive lignin depolymerization structure-catalyst-product relationships that exist by testing different lignin types, catalysts, and process conditions.

REFERENCES

(1) United Nations Population Division. *The World at Six Billion*; 1999.

(2) Population Reference Bureau. 2020 World Population Data Sheet. https://interactives.prb.org/2020-wpds/ (accessed Aug 29, 2021).

(3) US EPA. Global Atmospheric Concentrations of Carbon Dioxide over Time. https://www.epa.gov/climate-indicators (accessed Aug 29, 2021).

(4) Watson, R. T.; Zinyowera, M. C.; Moss, R. H. *Technologies, Policies and Measures for Mitigating Climate Change*; 1996.

(5) Pachauir, R. K.; Meyer, L. A. *Climate Change 2014: Synthesis Report. Contribution of Working Groups I, II and III to the Fifth Assessment Rport of the Intergovernmental Panel on Climate Change*; Geneva, 2014.

(6) Langholtz, M. H.; Stokes, B. J.; Eaton, L. M. *2016 Billion-Ton Report: Advancing Domestic Resources for a Thriving Bioeconomy, Volume 1: Economic Availability of Feedstocks*; Oak Ridge, 2016. https://doi.org/10.2172/1271651.

(7) Boerjan, W.; Ralph, J.; Baucher, M. Lignin Biosynthesis. *Annu. Rev. Plant Biol.* **2003**, *54*, 519–546. https://doi.org/10.1146/annurev.arplant.54.031902.134938.

(8) Berlin, A.; Balakshin, M. Industrial Lignins: Analysis, Properties, and Applications. In *Bioenergy Research: Advances and Applications*; Gupta, V. K., Tuohy, M. G., Kubicek, C. P., Saddler, J., Xu, F., Eds.; Elsevier: Oxford, UK, 2014; pp 315–336.

(9) Frost & Sullivan: High-value Opportunities for Lignin http://www.frost.com/prod/servlet/press-release.pag?docid=269974856 (accessed Jan 1, 2016).

(10) Sarkanen, K. V; Ludwig, C. H. Definition and Nomenclature. In *Lignins: Occurrence,*

Formation, Structure and Reactions; Sarkanen, S. V, Ludwig, C. H., Eds.; John Wiley & Sons, Inc.: New York, 1971; pp 1–17.

(11) Weng, J.-K.; Chapple, C. The Origin and Evolution of Lignin Biosynthesis. *New Phytol.* **2010**, *187* (2), 273–285. https://doi.org/10.1111/j.1469-8137.2010.03327.x.

(12) Christenhusz, M. J. M.; Byng, J. W. The Number of Known Plants Species in the World and Its Annual Increase. *Phytotaxa* **2016**, *261* (3), 201–217. https://doi.org/10.11646/phytotaxa.261.3.1.

(13) Higuchi, T. The Discovery of Lignin. In *Discoveries in Plant Biology: Volume II*; Kung, S.-D., Yang, S.-F., Eds.; World Scientific: Singapore, 1998; p 252. https://doi.org/10.1142/3860.

(14) Brunow, G.; Lundquist, K. Functional Groups and Bonding Patterns in Lignin. In *Lignin and Lignans: Advances in Chemistry*; Heitner, C., Dimmel, D. R., Schmidt, J. A., Eds.; CRC Press: Boca Raton, 2010; pp 267–300.

(15) Lin, S. Y.; Dence, C. W., Eds. *Methods in Lignin Chemistry*; Springer: New York, 1992.

(16) Duval, A.; Lawoko, M. A Review on Lignin-Based Polymeric, Micro- and Nano-Structured Materials. *React. Funct. Polym.* **2014**, *85*, 78–96. https://doi.org/10.1016/j.reactfunctpolym.2014.09.017.

(17) Smook, G. A. *Handbook for Pulp & Paper Technologists*, 3rd ed.; Angus Wilde Publications Inc.: Bellingham, 2002.

(18) Landucci, L. E. Search for Lignin Condensation Reactions with Modern NMR Techniques. In *Adhesives from renewable resources: ACS symposium series 385*; Hemingway, R. W., Conner, A. H., Branham, S. J., Eds.; American Chemical Society: Washington DC, 1989; pp 27–42. https://doi.org/10.1021/bk-1989-0385.ch003.

(19) Furimsky, E.; Massoth, F. E. Deactivation of Hydroprocessing Catalysts. *Catal. Today* **1999**, *52* (4), 381–495. https://doi.org/10.1016/S0920-5861(99)00096-6.

(20) Zinovyev, G.; Sulaeva, I.; Podzimek, S.; Rössner, D.; Kilpeläinen, I.; Sumerskii, I.; Rosenau, T.; Potthast, A. Getting Closer to Absolute Molar Masses of Technical Lignins. *ChemSusChem* **2018**, *11* (18), 3259–3268. https://doi.org/10.1002/cssc.201801177.

(21) Gargulak, J. D.; Lebo, S. E.; McNally, T. J. Lignin. In *Kirk-Othmer Encyclopedia of Chemical Technology*; John Wiley & Sons, Inc.: Hoboken, NJ, USA, 2015; pp 1–26. https://doi.org/10.1002/0471238961.12090714120914.a01.pub3.

(22) Dessbesell, L.; Paleologou, M.; Leitch, M.; Pulkki, R.; Xu, C. (Charles). Global Lignin Supply Overview and Kraft Lignin Potential as an Alternative for Petroleum-Based Polymers. *Renew. Sustain. Energy Rev.* **2020**, *123*, 109768. https://doi.org/10.1016/j.rser.2020.109768.

(23) Kouisni, L.; Paleologou, M. Method for Separating Lignin from Black Liquor. U.S. Patent 9,091,023, 2015.

(24) Tomani, P.; Ohman, F.; Theliander, H.; Axegard, P. Separating Lignin from Black Liquor by Precipitation, Suspension and Separation. U.S. Patent 8,172,981, 2012.

(25) Kouisni, L.; Gagne, A.; Maki, K.; Holt-Hindle, P.; Paleologou, M. LignoForce System for the Recovery of Lignin from Black Liquor: Feedstock Options, Odor Profile, and Product Characterization. *ACS Sustain. Chem. Eng.* **2016**, *4* (10), 5152–5159. https://doi.org/10.1021/acssuschemeng.6b00907.

(26) Öhman, F.; Wallmo, H.; Theliander, H. Precipitation and Filtration of Lignin from Black Liquor of Different Origin. *Nord. Pulp Pap. Res. J.* **2007**, *22* (2), 188–193. https://doi.org/10.3183/npprj-2007-22-02-p188-193.

(27) Jardim, J. M.; Hart, P. W.; Lucia, L.; Jameel, H.; Chang, H-m. A Quantitative Comparison of the Precipitation Behavior of Lignin from Sweetgum and Pine Kraft Black Liquors. *BioResources* **2020**, *15* (3), 5464–5480. https://doi.org/10.15376/biores.15.3.5464-5480.

(28) Rabemanolontsoa, H.; Saka, S. Various Pretreatments of Lignocellulosics. *Bioresour. Technol.* **2016**, *199*, 83–91. https://doi.org/10.1016/j.biortech.2015.08.029.

(29) McDonough, T. J. *The Chemistry of Organosolv Delignification*; Technical Paper No. 455 for the Institute of Paper Science and Technology: Atlanta, October 1992.

(30) McMillan, J. D. Pretreatment of Lignocellulosic Biomass. In *Enzymatic Conversion of Biomass for Fuels Production*; Himmel, M. E., Baker, J. O., Overend, R. P., Eds.; American Chemical Society: Washington DC, 1994; pp 292–324. https://doi.org/10.1021/bk-1994-0566.ch015.

(31) Batalha, L. A. R.; Han, Q.; Jameel, H.; Chang, H-m.; Colodette, J. L.; Borges Gomes, F. J. Production of Fermentable Sugars from Sugarcane Bagasse by Enzymatic Hydrolysis after Autohydrolysis and Mechanical Refining. *Bioresour. Technol.* **2015**, *180*, 97–105. https://doi.org/10.1016/j.biortech.2014.12.060.

(32) Huang, C.; Jeuck, B.; Du, J.; Yong, Q.; Chang, H-m.; Jameel, H.; Phillips, R. Novel Process for the Coproduction of Xylo-Oligosaccharides, Fermentable Sugars, and Lignosulfonates from Hardwood. *Bioresour. Technol.* **2016**, *219*, 600–607. https://doi.org/10.1016/j.biortech.2016.08.051.

(33) Yang, J.-M.; Goring, D. A. I. The Phenolic Hydroxyl Content of Lignin in Spruce Wood. *Can. J. Chem.* **1980**, *58* (23), 2411–2414. https://doi.org/10.1139/v80-389.

(34) Lai, Y.-Z.; Guo, X.-P.; Situ, W. Estimation of Phenolic Hydroxyl Groups in Wood by a Periodate Oxidation Method. *J. Wood Chem. Technol.* **1990**, *10* (3), 365–377.

https://doi.org/10.1080/02773819008050245.

(35) Taneda, H.; Nakano, J.; Hosoya, S.; Chang, H-m. Stability of α-Ether Type Model Compounds during Chemical Pulping Processes. *J. Wood Chem. Technol.* **1987**, *7* (4), 485–497. https://doi.org/10.1080/02773818708085281.

(36) Holtman, K. M.; Chang, H-m.; Kadla, J. F. Solution-State Nuclear Magnetic Resonance Study of the Similarities between Milled Wood Lignin and Cellulolytic Enzyme Lignin. *J. Agric. Food Chem.* **2004**, *52* (4), 720–726. https://doi.org/10.1021/jf035084k.

(37) Crestini, C.; Lange, H.; Sette, M.; Argyropoulos, D. S. On the Structure of Softwood Kraft Lignin. *Green Chem.* **2017**, *19* (17), 4104–4121. https://doi.org/10.1039/c7gc01812f.

(38) Lancefield, C. S.; Wienk, H. L. J.; Boelens, R.; Weckhuysen, B. M.; Bruijnincx, P. C. A. Identification of a Diagnostic Structural Motif Reveals a New Reaction Intermediate and Condensation Pathway in Kraft Lignin Formation. *Chem. Sci.* **2018**, *9* (30), 6348–6360. https://doi.org/10.1039/C8SC02000K.

(39) Hu, Z.; Du, X.; Liu, J.; Chang, H-m.; Jameel, H. Structural Characterization of Pine Kraft Lignin: BioChoice Lignin vs Indulin AT. *J. Wood Chem. Technol.* **2016**, *36* (6), 432–446. https://doi.org/10.1080/02773813.2016.1214732.

(40) Capanema, E. A.; Balakshin, M. Y.; Kadla, J. F. A Comprehensive Approach for Quantitative Lignin Characterization by NMR Spectroscopy. *J. Agric. Food Chem.* **2004**, *52* (7), 1850–1860. https://doi.org/10.1021/jf035282b.

(41) Baumberger, S.; Abaecherli, A.; Fasching, M.; Gellerstedt, G.; Gosselink, R.; Hortling, B.; Li, J.; Saake, B.; de Jong, E. Molar Mass Determination of Lignins by Size-Exclusion Chromatography: Towards Standardisation of the Method. *Holzforschung* **2007**, *61* (4), 459–468. https://doi.org/10.1515/HF.2007.074.

(42) Asikkala, J.; Tamminen, T.; Argyropoulos, D. S. Accurate and Reproducible Determination of Lignin Molar Mass by Acetobromination. *J. Agric. Food Chem.* **2012**, *60* (36), 8968–8973. https://doi.org/10.1021/jf303003d.

(43) Chang, H-m.; Cowling, E. B.; Brown, W.; Adler, E.; Miksche, G. Comparative Studies on Cellulolytic Enzyme Lignin and Milled Wood Lignin of Sweetgum and Spruce. *Holzforschung* **1975**, *29* (5), 153–159.

(44) Kollman, M.; Jiang, X.; Thompson, S. J.; Mante, O.; Dayton, D. C.; Chang, H-m.; Jameel, H. Improved Understanding of Technical Lignin Functionalization through Comprehensive Structural Characterization of Fractionated Pine Kraft Lignins Modified by the Mannich Reaction. *Green Chem.* **2021**, *23* (18), 7122–7136. https://doi.org/10.1039/d1gc01842f.

(45) Kadla, J. F.; Kubo, S. Lignin-Based Polymer Blends: Analysis of Intermolecular Interactions in Lignin-Synthetic Polymer Blends. *Compos. Part A Appl. Sci. Manuf.* **2004**, *35* (3), 395–400. https://doi.org/10.1016/j.compositesa.2003.09.019.

(46) Holladay, J. E.; White, J. F.; Bozell, J. J.; Johnson, D. *Top Value-Added Chemicals from Biomass, Volume II: Results of Screening for Potential Candidates from Biorefinery Lignin*; Report No. PNNL-16983 for Department of Energy, October 2007.

(47) Cui, C.; Sun, R.; Argyropoulos, D. S. Fractional Precipitation of Softwood Kraft Lignin: Isolation of Narrow Fractions Common to a Variety of Lignins. *ACS Sustain. Chem. Eng.* **2014**, *2* (4), 959–968. https://doi.org/10.1021/sc400545d.

(48) Passoni, V.; Scarica, C.; Levi, M.; Turri, S.; Griffini, G. Fractionation of Industrial Softwood Kraft Lignin: Solvent Selection as a Tool for Tailored Material Properties. *ACS Sustain. Chem. Eng.* **2016**, *4* (4), 2232–2242.

https://doi.org/10.1021/acssuschemeng.5b01722.

(49) Jiang, X.; Savithri, D.; Du, X.; Pawar, S.; Jameel, H.; Chang, H-m.; Zhou, X. Fractionation and Characterization of Kraft Lignin by Sequential Precipitation with Various Organic Solvents. *ACS Sustain. Chem. Eng.* **2017**, *5* (1), 835–842. https://doi.org/10.1021/acssuschemeng.6b02174.

(50) Laurichesse, S.; Avérous, L. Chemical Modification of Lignins: Towards Biobased Polymers. *Prog. Polym. Sci.* **2014**, *39* (7), 1266–1290. https://doi.org/10.1016/j.progpolymsci.2013.11.004.

(51) Matsushita, Y. Conversion of Technical Lignins to Functional Materials with Retained Polymeric Properties. *J. Wood Sci.* **2015**, *61* (3), 230–250. https://doi.org/10.1007/s10086-015-1470-2.

(52) Naseem, A.; Tabasum, S.; Zia, K. M.; Zuber, M.; Ali, M.; Noreen, A. Lignin-Derivatives Based Polymers, Blends and Composites: A Review. *Int. J. Biol. Macromol.* **2016**, *93*. https://doi.org/10.1016/j.ijbiomac.2016.08.030.

(53) Bertella, S.; Luterbacher, J. S. Lignin Functionalization for the Production of Novel Materials. *Trends Chem.* **2020**, *2* (5), 440–453. https://doi.org/10.1016/j.trechm.2020.03.001.

(54) Wang, Y.-Y.; Meng, X.; Pu, Y.; Ragauskas, A. J. Recent Advances in the Application of Functionalized Lignin in Value-Added Polymeric Materials. *Polymers (Basel).* **2020**, *12* (10), 2277. https://doi.org/10.3390/polym12102277.

(55) Jiang, X.; Liu, J.; Du, X.; Hu, Z.; Chang, H-m.; Jameel, H. Phenolation to Improve Lignin Reactivity toward Thermosets Application. *ACS Sustain. Chem. Eng.* **2018**, *6* (4), 5504–5512. https://doi.org/10.1021/acssuschemeng.8b00369.

(56) Mahmood, N.; Yuan, Z.; Schmidt, J.; Xu, C. (Charles). Depolymerization of Lignins and Their Applications for the Preparation of Polyols and Rigid Polyurethane Foams: A Review. *Renew. Sustain. Energy Rev.* **2016**, *60*, 317–329. https://doi.org/10.1016/j.rser.2016.01.037.

(57) Pawar, S. N.; Venditti, R. A.; Jameel, H.; Chang, H-m.; Ayoub, A. Engineering Physical and Chemical Properties of Softwood Kraft Lignin by Fatty Acid Substitution. *Ind. Crops Prod.* **2016**, *89* (August), 128–134. https://doi.org/10.1016/j.indcrop.2016.04.070.

(58) Sadeghifar, H.; Cui, C.; Argyropoulos, D. S. Toward Thermoplastic Lignin Polymers. Part 1. Selective Masking of Phenolic Hydroxyl Groups in Kraft Lignins via Methylation and Oxypropylation Chemistries. *Ind. Eng. Chem. Res.* **2012**, *51*, 16713–16720. https://doi.org/10.1021/ie301848j.

(59) Zhang, M.; Ogale, A. A. Carbon Fibers from Dry-Spinning of Acetylated Softwood Kraft Lignin. *Carbon N. Y.* **2014**, *69*, 626–629. https://doi.org/10.1016/j.carbon.2013.12.015.

(60) Mendis, G. P.; Hua, I.; Youngblood, J. P.; Howarter, J. A. Enhanced Dispersion of Lignin in Epoxy Composites through Hydration and Mannich Functionalization. *J. Appl. Polym. Sci.* **2015**, *132* (1). https://doi.org/10.1002/app.41263.

(61) Li, J.; Wang, M.; She, D.; Zhao, Y. Structural Functionalization of Industrial Softwood Kraft Lignin for Simple Dip-Coating of Urea as Highly Efficient Nitrogen Fertilizer. *Ind. Crops Prod.* **2017**, *109* (May), 255–265. https://doi.org/10.1016/j.indcrop.2017.08.011.

(62) Phillips, R. B.; Brown, W.; Stannett, V. T. The Graft Copolymerization of Styrene and Lignin. II. Kraft Softwood Lignin. *J. Appl. Polym. Sci.* **1972**, *16* (1), 1–14. https://doi.org/10.1002/app.1972.070160101.

(63) Saidane, D.; Barbe, J.-C.; Birot, M.; Deleuze, H. Preparation of Functionalized Kraft

Lignin Beads. *J. Appl. Polym. Sci.* **2010**, *116*, 1184–1189. https://doi.org/10.1002/app.31659.

(64) Sen, S.; Sadeghifar, H.; Argyropoulos, D. S. Kraft Lignin Chain Extension Chemistry via Propargylation, Oxidative Coupling, and Claisen Rearrangement. *Biomacromolecules* **2013**, *14* (10), 3399–3408. https://doi.org/10.1021/bm4010172.

(65) Argyropoulos, D. S.; Sadeghifar, H.; Cui, C.; Sen, S. Synthesis and Characterization of Poly(Arylene Ether Sulfone) Kraft Lignin Heat Stable Copolymers. *ACS Sustain. Chem. Eng.* **2014**, *2* (2), 264–271. https://doi.org/10.1021/sc4002998.

(66) Wang, C.; Venditti, R. A. UV Cross-Linkable Lignin Thermoplastic Graft Copolymers. *ACS Sustain. Chem. Eng.* **2015**, *3* (8), 1839–1845. https://doi.org/10.1021/acssuschemeng.5b00416.

(67) Hao, C.; Liu, T.; Zhang, S.; Brown, L.; Li, R.; Xin, J.; Zhong, T.; Jiang, L.; Zhang, J. A High-Lignin-Content, Removable, and Glycol-Assisted Repairable Coating Based on Dynamic Covalent Bonds. *ChemSusChem* **2019**, *12* (5), 1049–1058. https://doi.org/10.1002/cssc.201802615.

(68) Baker, D. A.; Rials, T. G. Recent Advances in Low-Cost Carbon Fiber Manufacture from Lignin. *J. Appl. Polym. Sci.* **2013**, *130* (2), 713–728. https://doi.org/10.1002/app.39273.

(69) Ogale, A. A.; Zhang, M.; Jin, J. Recent Advances in Carbon Fibers Derived from Biobased Precursors. *J. Appl. Polym. Sci.* **2016**, *133* (45), 43794. https://doi.org/10.1002/app.43794.

(70) Frank, E.; Hermanutz, F.; Buchmeiser, M. R. Carbon Fibers: Precursors, Manufacturing, and Properties. *Macromol. Mater. Eng.* **2012**, *297* (6), 493–501. https://doi.org/10.1002/mame.201100406.

(71) Fang, W.; Yang, S.; Wang, X.-L.; Yuan, T.; Sun, R.-C. Manufacture and Application of Lignin-Based Carbon Fibers (LCFs) and Lignin-Based Carbon Nanofibers (LCNFs). *Green Chem.* **2017**, *19* (8), 1794–1827. https://doi.org/10.1039/C6GC03206K.

(72) Otani, S.; Fukuoka, Y.; Igarashi, B.; Sasaki, K. Method for Producing Carbonized Lignin Fiber. U.S. Patent 3,461,082, 1969.

(73) Sudo, K.; Shimizu, K. A New Carbon Fiber from Lignin. *J. Appl. Polym. Sci.* **1992**, *44* (1), 127–134. https://doi.org/10.1002/app.1992.070440113.

(74) Kadla, J. F.; Kubo, S.; Venditti, R. A.; Gilbert, R. D.; Compere, A. L.; Griffith, W. Lignin-Based Carbon Fibers for Composite Fiber Applications. *Carbon N. Y.* **2002**, *40* (15), 2913–2920. https://doi.org/10.1016/S0008-6223(02)00248-8.

(75) Chatterjee, S.; Saito, T. Lignin-Derived Advanced Carbon Materials. *ChemSusChem* **2015**, *8* (23), 3941–3958. https://doi.org/10.1002/cssc.201500692.

(76) Puziy, A. M.; Poddubnaya, O. I.; Sevastyanova, O. Carbon Materials from Technical Lignins: Recent Advances. *Top. Curr. Chem.* **2018**, *376* (4), 33. https://doi.org/10.1007/s41061-018-0210-7.

(77) Zhu, J.; Yan, C.; Zhang, X.; Yang, C.; Jiang, M.; Zhang, X. A Sustainable Platform of Lignin: From Bioresources to Materials and Their Applications in Rechargeable Batteries and Supercapacitors. *Prog. Energy Combust. Sci.* **2020**, *76*, 100788. https://doi.org/10.1016/j.pecs.2019.100788.

(78) Zakzeski, J.; Bruijnincx, P. C. A.; Jongerius, A. L.; Weckhuysen, B. M. The Catalytic Valorization of Lignin for the Production of Renewable Chemicals. *Chem. Rev.* **2010**, *110*, 3552–3599. https://doi.org/10.1021/cr900354u.

(79) Xu, C.; Arancon, R. A. D.; Labidi, J.; Luque, R. Lignin Depolymerisation Strategies:

Towards Valuable Chemicals and Fuels. *Chem. Soc. Rev.* **2014**, *43* (22), 7485–7500. https://doi.org/10.1039/c4cs00235k.

(80) Schutyser, W.; Renders, T.; Van den Bosch, S.; Koelewijn, S.-F.; Beckham, G. T.; Sels, B. F. Chemicals from Lignin: An Interplay of Lignocellulose Fractionation, Depolymerisation, and Upgrading. *Chem. Soc. Rev.* **2018**, *47*, 852–908. https://doi.org/10.1039/C7CS00566K.

(81) Cheng, F.; Brewer, C. E. Producing Jet Fuel from Biomass Lignin: Potential Pathways to Alkyl-Benzenes and Cycloalkanes. *Renew. Sustain. Energy Rev.* **2017**, *72*, 673–722. https://doi.org/10.1016/j.rser.2017.01.030.

(82) Huber, G. W.; Iborra, S.; Corma, A. Synthesis of Transportation Fuels from Biomass: Chemistry, Catalysts, and Engineering. *Chem. Rev.* **2006**, *106* (9), 4044–4098. https://doi.org/10.1021/cr068360d.

(83) Rinaldi, R.; Jastrzebski, R.; Clough, M. T.; Ralph, J.; Kennema, M.; Bruijnincx, P. C. A.; Weckhuysen, B. M. Paving the Way for Lignin Valorisation: Recent Advances in Bioengineering, Biorefining and Catalysis. *Angew. Chemie - Int. Ed.* **2016**, *55* (29), 8164–8215. https://doi.org/10.1002/anie.201510351.

(84) Ahvazi, B.; Cloutier, E.; Wojciechowicz, O.; Ngo, T. D. Lignin Profiling: A Guide for Selecting Appropriate Lignins as Precursors in Biomaterials Development. *ACS Sustain. Chem. Eng. Eng.* **2016**, *4* (10), 5090–5105. https://doi.org/10.1021/acssuschemeng.6b00873.

(85) Lupoi, J. S.; Singh, S.; Parthasarathi, R.; Simmons, B. A.; Henry, R. J. Recent Innovations in Analytical Methods for the Qualitative and Quantitative Assessment of Lignin. Renew. Sustain. Energy Rev. 2015, 49, 871–906. https://doi.org/10.1016/j.rser.2015.04.091.

CHAPTER 2: Melt Blending Lignin with Polyethylene terephthalate (PET)

Abstract

Pine kraft lignin was melt blended with polyethylene terephthalate to increase bio-based content and lower product cost. Lignin was fractionated into two molecular weight fractions. The high molecular weight fraction would not flow by heating, but original lignin was able to. Thus, it is possible that low molecular weight molecules acted as plasticizers to improve the free volume of the whole lignin sample and allow for melt processability. The lower molecular weight fraction, which also had lower dispersity appeared to be capable of blending with PET without phase separation. Both glass transition and degradation temperature of the low molecular weight fraction were reduced compared to whole lignin. There was evidence that crystallization of PET was disrupted by the inclusion of lignin as a miscible polymer. Lignin structure was altered during heating, likely through degradation and condensation reactions that resulted in increased glass transition and degradation points, but still exhibited thermoplastic behavior. The same structure and property changes occurred for whole lignin and high molecular lignin, but these were converted to thermosets. Structural changes during melt processing of the different fractions should be investigated further. Additionally, the suppression of crystallization and melting point reduction should be explored further to confirm the mechanism.

Introduction

Polyethylene terephthalate (PET) is a linear polyester with a repeat unit that is comprised of two monomers, terephthalic acid or a terephthalate and ethylene glycol (**Figure 2.1**). PET is used to make fibers, bottles, films, and to a lesser extent engineered plastic applications with 61% consumed for fiber production, 30% for packaging like bottles and containers.[1] Consumer

products include textiles and soda bottles, with industrial applications including carpet, car tire reinforcement, seat belts, and conveyor belts.[2] As a semicrystalline thermoplastic, it can be melt processed to a clear or opaque solid with high resistance to water and gas permeability or a strong, durable fiber. Polyester products are easier to recycle or reuse than some other plastics through ester hydrolysis, but collection of the used containers is required first. Furthermore, there is interest in replacing petroleum-based monomers with biomass-derived alternatives. Coca-Cola, Ford Motor, Heinz, and Procter & Gamble, as major consumers, created a consortium in 2012 to invest in bio-based PET chemistries and technologies.[3] Coca-Cola patented bio-based PET and processes for making terephthalic acid and ethylene glycol from different plant-derived sugars.[4] Refer to recent reviews that cover the current knowledge and ongoing efforts in the area of biomass-derived monomers for PET production for more information.[5,6]

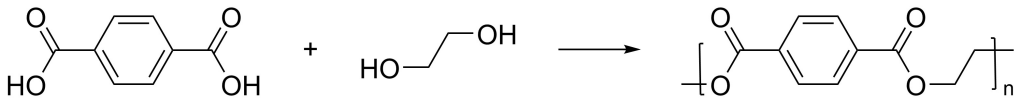

Figure 2.1. One route used in the production of PET.

Blending PET with a biopolymer may be an alternative to the multistep conversion of plant material to monomers while reducing total petroleum consumption. More biomaterials could be incorporated into the final product in one step which would likely be a cheaper process with higher carbon economy. Ideally, melt blending would be possible to avoid the use of hazardous solvents. Polymer blending would also ideally improve properties of the final product, besides reducing cost and improving life cycle sustainability. An example is the blending of one amorphous and one semi-crystalline polymer to take advantage of properties from each. Lignin may act as a radical scavenger or UV stabilizer to protect the polyester molecules and prolong

material life, though this needs to be tested. First, it should be verified that two polymers are miscible with each other, which is required for creating a stable blend.

Kadla and Kubo studied melt blending hardwood kraft lignin with PET through extrusion with the goal of creating a carbon fiber precursor.[7,8] A single glass transition temperature (T_g) indicated that the two polymers were miscible, and PET crystalline phase melting point decreased in the presence of lignin. Kraft and organosolv lignin were blended through compression molding in the only other example of melt mixing non-modified kraft lignin with PET.[9] Crosslinking or condensation was indicated for kraft lignin based on an increase in viscosity at low velocity. PET has a high softening temperature so it needs to be melt processed around 250 °C or above, which is high enough to cause degradation or crosslinking of kraft lignin molecules, though less should be expected for hardwood. In other studies, softwood kraft lignin was either esterified or etherified to improve thermal stability and lower T_g before melt kneading with PET at 170 °C.[10,11] T_g of the 50:50 w/w blend decreased below that of PET, which indicated that lignin acted as a plasticizer instead of miscible component in a blend. This effect was observed when using esterified lignin in a PET/low density polyethylene (LDPE) melt blend.[12] Esterified lignin was thought to improve compatibilization of the two normally incompatible synthetic polymers in addition to having a plasticizing effect. There was no discussion of the effect on crystalline phase melting point or dimensions. Whereas neat HW kraft lignin was found to decrease melting point by Kadla and Kubo, hydrolytic lignin was thought to improve crystallinity and unit dimensions in another study, though it is difficult to compare these with many factors being different.[13]

Relying on the available literature to draw conclusions about the interactions between softwood kraft lignin and PET is difficult due to differences in relative molecular weights of

lignin to PET, chemical modifications, or lack of, different blend compositions, and unreported data. The objective of this work was to study whether non-modified softwood kraft lignin could be successfully melt blended with PET, what effect lignin molecular weight has, and to determine the impact on crystallization and T_g.

Materials and Methods

Materials

Ethyl acetate was certified ACS quality and purchased from Fisher Chemical. Tetrahydrofuran (THF) was HPLC grade and purchased from Fisher Scientific. BioChoice® lignin (BCL) was produced at the Plymouth, North Carolina pulp mill and provided by Domtar, Inc. BCL is a pine, kraft lignin precipitated from black liquor using the Lignoboost® process. BCL was thoroughly washed with deionized water to remove any remaining ash and air-dried prior to use and is hereafter referred to as whole lignin. Whole lignin was subsequently fractionated into an insoluble and soluble portion through precipitation in ethyl acetate. PET was obtained from Scientific Polymer (Cat # 138, viscosity-average molecular weight (M_v): 20,000) and cryomilled to a powder and dried before use.

Melt blending

Melt blending of the polymers was performed in air using a furnace set to 260 °C, which was 10 °C above the melting point of PET. Lignin/PET mixtures of varying compositions (0:1, 1:3, 1:1, 3:1, 1:0 w/w) were heated for 30 minutes and stirred every 10 minutes. Samples cooled to room temperature and were ground to powder and stored in a desiccator.

Gel Permeation Chromatography

Molecular weight distributions of lignin samples were determined using gel permeation chromatography (GPC). Samples were first acetylated by dissolving 40 mg dried lignin in a 1 mL mixture of acetic anhydride and pyridine (1:1 v/v) and reacted at room temperature for 48 h in a sealed vial. The reaction mixture was added to 20 mL ice-cold water and shaken every few minutes to precipitate acetylated lignin and convert excess acetic anhydride. The suspension was filtered using a fine, glass-fritted filter and washed three times with cold, deionized water and the solids dried overnight in a vacuum oven at 45 °C over phosphorous pentoxide. Samples were dissolved in THF at a 1 mg/mL concentration and injected into a GPC system (Shimadzu) consisting of two columns in series (Styragel HR 1 7.8 x 300 mm and Styragel HR 5E 7.8 x 300 mm). The mobile phase used was THF at a flow rate of 0.7 mL/min and oven temperature was set to 35 °C. A UV detector measured absorbance at a wavelength of 280 nm. Monodisperse polystyrene standards were used for molecular weight calibration.

Thermal analyses

The specific heat capacity as a function of temperature was determined using a differential scanning calorimeter (DSC) (TA Instruments, Q2000). 5 mg to 10 mg dried sample was loaded into an aluminum pan and sealed. A similar empty pan was used as a reference. First the sample chamber was equilibrated to 40 °C under flowing nitrogen. Next, the temperature was increased to 200 °C to 300 °C depending on the experiment at a rate of 10 °C min^{-1} and the temperature held for 10 minutes. The temperature was reduced to 40 °C at a rate of 10 °C min^{-1}, held for 2 minutes and the cycle repeated. The isothermal stage at the upper temperature is performed so that each sample has a similar thermal history, which allows thermodynamic

transitions to be compared. DSC plots and data are given for the second temperature cycle unless otherwise noted.

Weight loss as a function of temperature was determined using a thermogravimetric analyzer (TGA) (TA Instruments, Q500). 5 mg to 10 mg dried sample was loaded onto a platinum pan and heated under nitrogen atmosphere. After holding at 105 °C for 10 minutes to remove any moisture, the sample was heated to 800 °C at a rate of 10 °C min^{-1}. DSC and TGA data were collected and analyzed using TA Universal Analysis software.

Results and Discussion

It is important to first review the thermal behaviors of neat PET and BCL under the processing temperatures used in this study. PET is a linear aromatic polymer and is semi-crystalline, meaning crystalline regions may form under certain conditions. PET can undergo up to three thermal events upon heating and one upon cooling depending on thermal history and rate of temperature change. DSC was used to measure these transitions. The first transition for PET used in this study occurred around 80 °C and was attributed to the glass-rubber transition of the polymer chain, or glass transition temperature, T_g (**Figure 2.2** and **Table A.1**). Next, PET underwent cold crystallization at 129 °C, which is the rearrangement of certain regions to a crystalline structure if crystallization was incomplete the last time the polymer sample was cooled. Finally, melting of the crystalline regions occurred from 237 °C to 252 °C depending on how melting point is defined and the thermal history, unlike a single crystal which has a well-defined and consistent melting point regardless of heating rate or sample history. Regardless, melt processing of PET usually occurs at temperatures greater than 250 °C to ensure complete deconstruction of crystalline regions. These regions will reform if cooling is performed slowly

enough, and crystallization occurred between 196 °C and 200 °C for the PET sample used in this study.

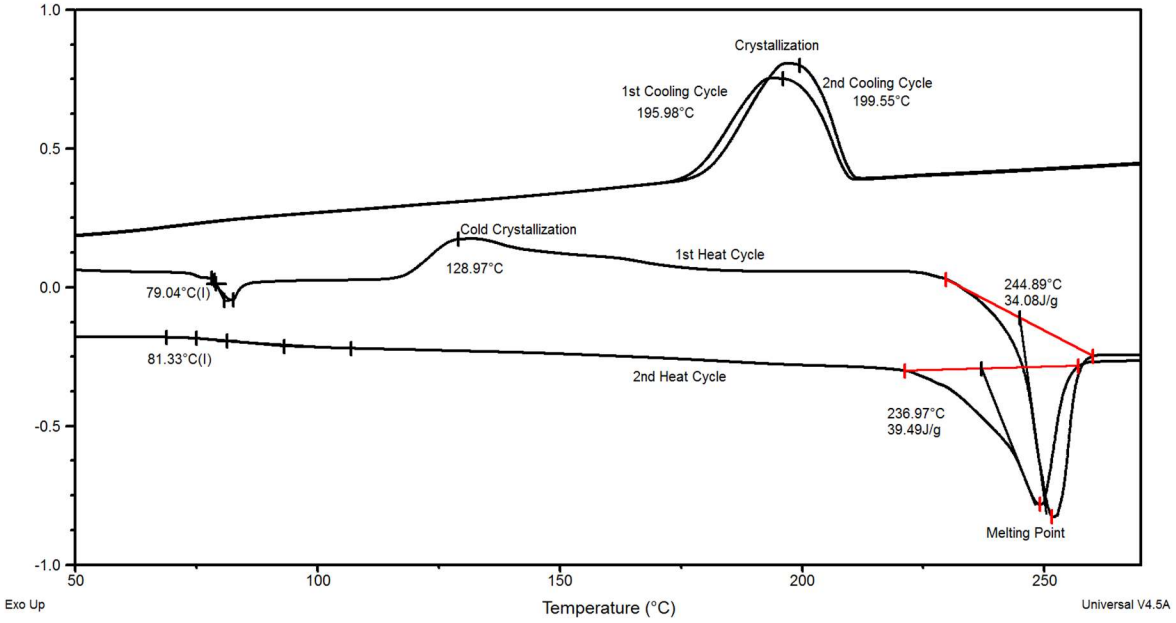

Figure 2.2. DSC thermogram (exo up) of PET sample.

As amorphous polymers, the main non-degradative response to thermal treatment of lignins is a relaxation of polymer chains observed as the T_g. Lignins are heterogeneous in chemical structure and molecular weight distribution, therefore they have relatively broad ranges over which the glass transition temperature is observed, as various components of the molecule begin to move at different temperatures.[14] Whole, dry BCL was found to exhibit a broad glass-rubber transition around 154 °C, which agreed with the observed transition temperature of other softwood kraft lignins from 147 °C to 157 °C (**Table A.1**).[15,16]

Melt blending whole lignin

PET and whole BCL was melt blended at 260 °C using 25%, 50%, and 75% lignin by weight. A sample of lignin with no PET was heated as a control. Thermograms are presented in **Figure 2.3**. Melt-processed lignin exhibited a possible glass-rubber transition at 225 °C, an increase of 71 °C above that of original whole BCL (**Table A.1** and **Figure A.1**). The transition was less defined than that of original lignin powder, indicative of a sample with lower mobility. Interunit, radical coupling is possible in softwood kraft lignin at the processing temperature of 260 °C, as is decomposition of the polymer network. Formaldehyde has been observed to evolve from softwood kraft lignin as low as 120 °C and an increase and broadening of the molecular weight distribution was observed above 130 °C.[17] The increase in molecular weight was attributed to interunit coupling a guaiacyl units to form either 5-5' or 4-O-5' condensed structures, which would decrease polymer mobility and increase transition temperatures.

Glass-rubber transitions of lignin-PET blends were difficult to identify by DSC. Almost imperceptible transitions were measured at 72.1°C and 73.6 °C for 25% and 50% blends, but the shift in heat capacity was too small to be attributed to a transition of the individual polymers or blend. A single rubber-glass transition is indicative of blend compatibility and lack of phase separation, although at high enough temperatures even compatible polymers may separate. Two distinct T_g temperatures would indicate immiscibility, but a lack of any defined transitions in the present case precludes a determination of compatibility. Small transitions were observed just above 100 °C that could be attributed to the evaporation of water, though samples were dried under vacuum prior to analysis.

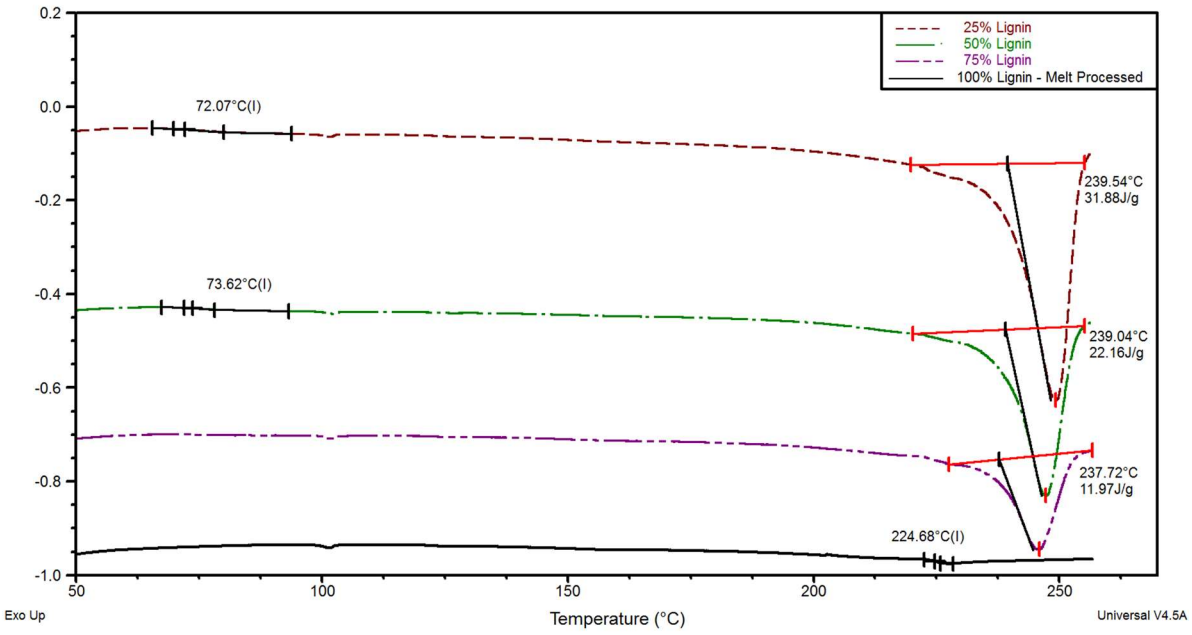

Figure 2.3. DSC thermogram (exo up) of whole lignin/PET melt blends.

The melting point decreased from 239.5 °C to 237.7 °C by increasing lignin content from 25% to 75%. More samples and measurements would be needed to determined significance of this change. The decrease in specific heat of melting was relatively greater (from 31.9 J g^{-1} to 12.0 J g^{-1}) when lignin content was increased by the same amount. A similar trend in both melting point and heat of melting was observed for melt blends of hardwood kraft and PET.[7] The decrease in melting point and heat of fusion is an indication of miscibility, as thermodynamics predicts this suppression when introducing a miscible diluent; however, polymer-polymer interactions are more complicated than solvent-polymer or solvent-solvent.[18] More points at various temperatures would need to be measured to gain a better understanding of miscibility.

Mixtures of lignin and PET were tested for thermal stability by TGA under nitrogen (**Figure 2.4**). Decomposition temperatures were defined as the temperature by which 5% of the sample weight was lost. Lignins have many more thermally labile functional groups than PET,

including aliphatic hydroxyl and hydroxymethyl and carboxylic acid groups, in addition to low molecular weight molecules. PET must undergo cleavage along the rigid aromatic backbone, though ester linkages have lower dissociation energies than carbon-carbon bonds, for example. The degradation temperature of PET was 122 °C higher than that of original, whole BCL. Heat treating BCL decreased this gap to 70 °C (**Figure 2.4**, **Table A.1**). The addition of lignin resulted in the initiation of degradation at a lower temperature and followed a linear mixing rule with lignin content. Overall weight loss due to thermal degradation decreased with increasing lignin content. Highly branched structure of kraft lignin with a tendency for radical coupling may have allowed for charring or the formation of a thermally stable polyaromatic structure, whereas the linear PET polymer chain degraded more completely with limited reactions towards a stronger material.

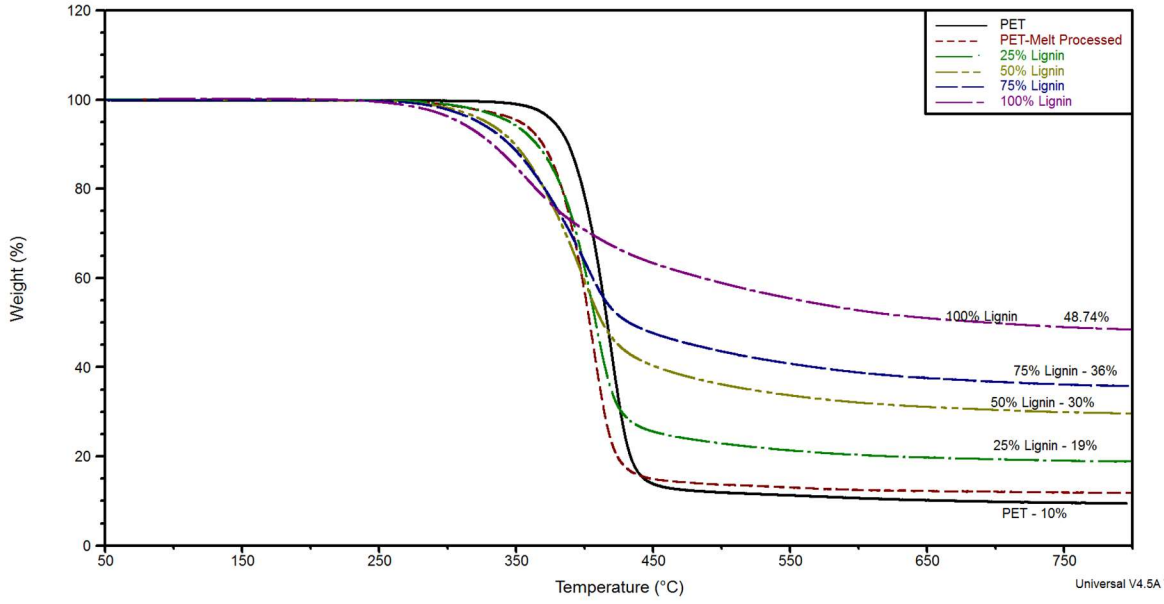

Figure 2.4. TGA weight loss profiles for lignin/PET melt blends.

Melt blending with fractionated lignin

Whole BCL was fractionated based on ethyl acetate solubility to explore the effects of lignin average molecular weight and dispersity when melt blended with PET. 85 percent by weight BCL was insoluble in ethyl acetate with a similar bimodal molecular weight distribution to whole BCL and similarly high dispersity (3.6 versus 4.1 for whole BCL) (**Figure 2.5** and **Table 2.1**). 15 percent original BCL was soluble in ethyl acetate and was more uniform in molecular weight. PET was not analyzed by GPC as it is insoluble in THF, but the vendor provided a viscosity-average molecular weight (M_v) of 20,000. It is not possible to directly compare M_v with GPC-determined relative MW values. Absolute weight-average molecular weight (M_w) values of monodisperse polymers are closely related to M_v, so it was assumed that all fractions of BCL were comprised of smaller polymer molecules than PET. It is important to consider relative molecular weights and relative physical structures (linear vs. branched) of two blended polymers, because this will inform understanding of rheological behaviors.

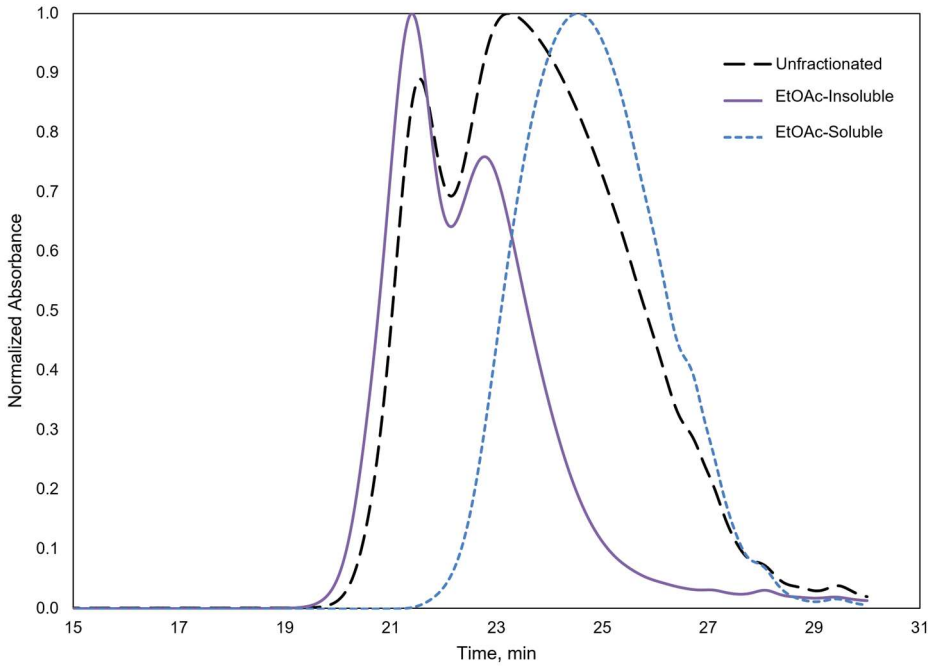

Figure 2.5. GPC chromatograms of whole, ethyl acetate insoluble and soluble fractions of BCL.

Table 2.1. Relative molecular weights for fractionated and whole BCL.

Sample	M_n (g mol^{-1})	M_w (g mol^{-1})	$Đ$	Yield (% wt)
Whole	1400	6000	4.1	100
EtOAc-Insoluble	3500	12400	3.6	85
EtOAc-Soluble	900	1600	1.7	15

Ethyl acetate insoluble lignin did not display any glass transition temperature so was incapable of melt processing and not used further. It is thought that low molecular weight molecules contained in whole BCL acted as plasticizers to reduce intermolecular friction and by extension allow for a glass-rubber transition.[19] Ethyl acetate soluble lignin had a T_g of 103 °C, while the heat-treated control sample had a T_g of 145 °C following the same behavior of unfractionated lignin (**Table A.1**, **Figure A.1**). Molecular size affects translational and rotational movement of macromolecules like lignins. Glass transition temperature increases with molecular weight because the energy barrier for initiating movement is higher. Limited spatial conformations exist as polymer chains are restricted from moving by neighboring molecules. For relatively low molecular weight polymer samples like lignins, glass transition temperature theoretically increases linearly with number-average molecular weight as described by the Flory-Fox equation:

$$T_g = T_{g,\infty} - \frac{K}{M_n} \qquad (2.1)$$

where T_g (K) is the glass transition temperature of the polymer, $T_{g,\infty}$ (K) is the limiting glass transition temperature of the polymer as molecular weight approaches infinity, above which T_g is independent of molecular weight, K is a constant related to free volume of the polymer, and M_n is number-average molecular weight (g mol^{-1}).[20] Though $T_{g,\infty}$ is unknown for BCL, the linear relationship between Mn and T_g is expected to still apply for monodisperse samples. As the

molecular weight dispersity increases, glass transition temperature of the lignin sample decreases and the temperature over which the transition occurs is broadened.[21]

Ethyl acetate soluble lignin was blended with PET at two lignin concentrations, 25% and 50% by weight. DSC thermograms indicated only one clear glass-rubber transition for both mixtures, indicating good compatibility of the two polymers (**Figure 2.6**). Similarly, melting points and heats of melting of the PET crystalline regions were lowered compared to the pure PET sample as another indication of miscibility.[18] The broad, low amplitude melting event observable for the 50-50 blend mixture and lowered T_g compared to lignin was indicative of significant disruption of the crystallization of PET caused by an intimate blend and increase of free volume. The Fox equation is valid for predicting the glass transition temperature of mixtures of two highly miscible polymers or a statistical copolymer:

$$\frac{1}{T_g} = \frac{w_1}{T_{g,1}} + \frac{w_2}{T_{g,2}}, \qquad (2.2)$$

where w_i and $T_{g,n}$ are the weight fraction and T_g of a pure polymer in the blend. The glass transition temperature for 1:3 and 1:1 blends were predicted to be 90.1 °C and 103 °C compared to measured values 97.5 °C and 98.3 °C. Predictions of the Fox equation not have to follow perfectly to indicate compatibility; the increase of T_g relative to pure PET and decrease relative to lignin supports that the two polymers were at least partially miscible.

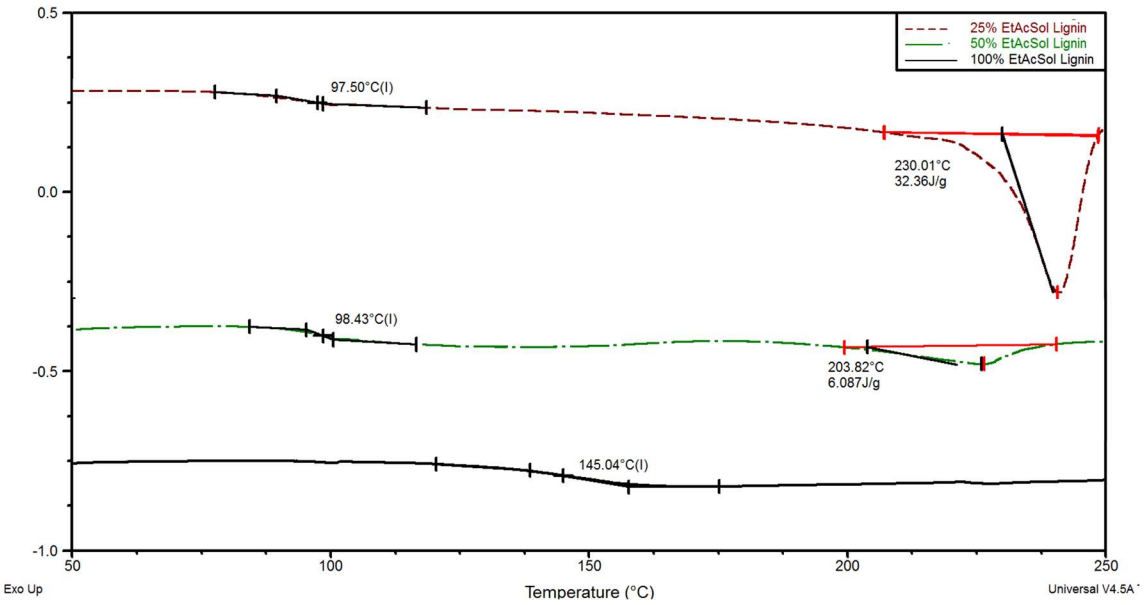

Figure 2.6. DSC thermogram (exo up) of ethyl acetate soluble lignin/PET melt blends.

Conclusion

Unfractionated and a low molecular weight, low dispersity fraction (ethyl acetate soluble) of pine kraft lignin was melt blended with PET. Ethyl acetate insoluble lignin did not exhibit a rubber-glass transition below the degradation temperature indicating a lack of thermoplastic behavior. Heat treatment of whole and ethyl acetate lignin increased glass transition temperatures, which was attributed to an increase in molecular weight, though chemical and other physical parameters like free volume reduction may have also contributed. Unfractionated lignin and PET did not exhibit any glass transition temperature according to DSC analyses, though there was some effect on reducing PET crystallinity.

DSC thermograms indicated better miscibility of ethyl acetate soluble fraction with PET compared to whole lignin. The single glass transition temperatures for both 1:3 and 1:1 blends were close to values predicted by ideal miscibility. A 1:1 PET-EtOAc-sol lignin blend demonstrated the highest miscibility as determined by the highest suppression of crystallization

as determined by DSC, though other characterization methods like XRD should be employed to confirm.

Even if ethyl acetate soluble BCL is miscible with PET, its low degradation temperature ($T_{d,5\%}$ = 219 °C) should be expected to cause defects in an extruded blend resulting in poor bulk strength properties and low yield. However, a porous material may have application as an adsorbent and these bulk properties would need to be tested and compared to industry standards. To avoid thermal degradation and heat-induced condensation, solvent blending was attempted. Trifluoracetic acid (TFA) was the only solvent capable of dissolving both PET and BCL. As TFA is expensive and highly hazardous, solvent blending of lignin and PET does not appear to be an attractive route. Previously heat-treated ethyl acetate soluble softwood kraft lignin that has a higher degradation temperature may be capable of imparting desirable properties to PET blends like crystallization disruption if amorphous PET is being produced, which usually requires additives or comonomers to be successful.[1]

REFERENCES

(1) Weissmann, D. PET Use in Blow Molded Rigid Packaging. In *Applied Plastics Engineering Handbook*; Kutz, M., Ed.; Elsevier: Oxford, UK, 2011; pp 603–623. https://doi.org/10.1016/C2010-0-67336-6.

(2) Polyethylene Terephthalate: Structure, Properties, and Uses. *Encyclopaedia Britannica* [Online]; Britannica Group, Inc., Posted May 20, 2020. https://www.britannica.com/science/polyethylene-terephthalate (accessed Sep 13, 2021).

(3) Coca-Cola's 100% Plant-Based Bottle. https://www.packaging-gateway.com/projects/coca-cola-plant-based-bottle/ (accessed Sep 13, 2021).

(4) Prakash, I.; Chaturvedula, V. S. P.; Kriegel, R. M.; Huang, X. Methods of Preparing Para-Xylene from Biomass. U.S. Patent 10,174,158, 2019.

(5) Maneffa, A.; Priecel, P.; Lopez-Sanchez, J. A. Biomass-Derived Renewable Aromatics: Selective Routes and Outlook for p-Xylene Commercialisation. *ChemSusChem* **2016**, *9* (19), 2736–2748. https://doi.org/10.1002/cssc.201600605.

(6) Pang, J.; Zheng, M.; Sun, R.; Wang, A.; Wang, X.; Zhang, T. Synthesis of Ethylene Glycol and Terephthalic Acid from Biomass for Producing PET. *Green Chem.* **2016**, *18* (2), 342–359. https://doi.org/10.1039/c5gc01771h.

(7) Kadla, J. F.; Kubo, S. Lignin-Based Polymer Blends: Analysis of Intermolecular Interactions in Lignin-Synthetic Polymer Blends. *Compos. Part A Appl. Sci. Manuf.* **2004**, *35* (3), 395–400. https://doi.org/10.1016/j.compositesa.2003.09.019.

(8) Kubo, S.; Kadla, J. F. Lignin-Based Carbon Fibers: Effect of Synthetic Polymer Blending on Fiber Properties. *J. Polym. Environ.* **2005**, *13* (2), 97–105. https://doi.org/10.1007/s10924-005-2941-0.

(9) Bush, J. D. Rheology of Lignin and Lignin / PET Blends. Master's Thesis, University of Tennessee, Knoxville, 2006.

(10) Jeong, H.; Park, J.; Kim, S.; Lee, J.; Cho, J. W. Use of Acetylated Softwood Kraft Lignin as Filler in Synthetic Polymers. *Fibers Polym.* **2012**, *13* (10), 1310–1318. https://doi.org/10.1007/s12221-012-1310-6.

(11) Kim, S.; Park, J.; Lee, J.; Roh, H. gyoo; Jeong, D.; Choi, S.; Oh, S. Potential of a Bio-Disintegrable Polymer Blend Using Alkyl-Chain-Modified Lignin. *Fibers Polym.* **2015**, *16* (4), 744–751. https://doi.org/10.1007/s12221-015-0744-z.

(12) Aradoaei, S.; Darie, R.; Constantinescu, G.; Olariu, M.; Ciobanu, R. Modified Lignin Effectiveness as Compatibilizer for PET/LDPE Blends Containing Secondary Materials. *J. Non. Cryst. Solids* **2010**, *356* (11–17), 768–771. https://doi.org/10.1016/j.jnoncrysol.2009.11.046.

(13) Canetti, M.; Bertini, F. Supermolecular Structure and Thermal Properties of Poly(Ethylene Terephthalate)/Lignin Composites. *Compos. Sci. Technol.* **2007**, *67* (15–16), 3151–3157. https://doi.org/10.1016/j.compscitech.2007.04.013.

(14) Hatakeyama, T.; Hatakeyama, H. Lignin. In *Thermal Properties of Green Polymers and Biocomposites*; Springer Netherlands, 2004; pp 171–215. https://doi.org/10.1007/1-4020-2354-5.

(15) Ahvazi, B.; Cloutier, E.; Wojciechowicz, O.; Ngo, T. D. Lignin Profiling: A Guide for Selecting Appropriate Lignins as Precursors in Biomaterials Development. *ACS Sustain. Chem. Eng. Eng.* **2016**, *4* (10), 5090–5105. https://doi.org/10.1021/acssuschemeng.6b00873.

(16) Jiang, X.; Savithri, D.; Du, X.; Pawar, S.; Jameel, H.; Chang, H-m.; Zhou, X.

Fractionation and Characterization of Kraft Lignin by Sequential Precipitation with Various Organic Solvents. *ACS Sustain. Chem. Eng.* **2017**, *5* (1), 835–842. https://doi.org/10.1021/acssuschemeng.6b02174.

(17) Cui, C.; Sadeghifar, H.; Sen, S.; Argyropoulos, D. S. Toward Thermoplastic Lignin Polymers; Part II: Thermal & Polymer Characteristics of Kraft Lignin & Derivatives. *BioResources* **2013**, *8* (1), 864–886.

(18) Rim, P. B.; Runt, J. P. Melting Point Depression in Crystalline/Compatible Polymer Blends. *Macromolecules* **1984**, *17* (8), 1520–1526. https://doi.org/10.1021/ma00138a017.

(19) Saito, T.; Perkins, J. H.; Vautard, F.; Meyer, H. M.; Messman, J. M.; Tolnai, B.; Naskar, A. K. Methanol Fractionation of Softwood Kraft Lignin: Impact on the Lignin Properties. *ChemSusChem* **2014**, *7* (1), 221–228. https://doi.org/10.1002/cssc.201300509.

(20) Young, R.; Lovell, P. The Amorphous State. In *Introduction to Polymers*; CRC Press: Boca Raton, 2011; pp 383–397.

(21) Yoshida, H.; Mörck, R.; Kringstad, K. P.; Hatakeyama, H. Fractionation of Kraft Lignin by Successive Extraction with Organic Solvents. II. Thermal Properties of Kraft Lignin Fractions. *Holzforschung* **1987**, *41* (3), 171–176. https://doi.org/10.1515/hfsg.1987.41.3.171.

CHAPTER 3: Pine Kraft Lignin Modified by the Mannich Reaction

This chapter is a slightly modified version of: Kollman, M *et al. Green Chem.* **2021**, *23* (18), 7122–7136.

Abstract

Amino alkylation of technical lignins via the Mannich reaction can be used as an analytical derivatization technique, but also in an applied manner to improve kraft lignin hydrophilicity or metal ion adsorptive capacity. Recent studies have indicated the potential for increased amination under acidic conditions, however, the effects of pH on the amination of kraft lignins remain poorly understood because indirect quantification methods are often used. A quantitative technique combining 2D HSQC NMR and ^{13}C NMR spectroscopy was used in this study to directly probe the structure of high and low molecular weight fractions of an industrial pine kraft lignin aminated in acidic or basic media with dimethylamine or diethylamine. The degree of amine substitution was two times higher for low molecular weight lignin compared to the high molecular weight fraction. Neither pH nor amine species had any significant effect. New evidence confirms that amine substitution of pine kraft lignin takes place selectively *ortho* to non-etherified phenolic hydroxyl groups and displaces carboxylic acid groups of benzoic- and cinnamic-type subunits. Other pathways were proposed and tested, but substitution did not occur at sterically hindered sites. Elemental analysis has been the most widely used indicator of Mannich condensation, but unfortunately overestimates amine substitution because nitrogen-containing side products and impurities can be included in the total nitrogen content. Multiple methods should always be employed when characterizing complex, heterogenous biopolymers like lignins to avoid misinterpretation of results.

Introduction

Most commercial lignin-based products are derived from lignosulfonates, byproducts of the sulfite wood pulping process. The sulfite pulping process introduces sulfonate groups at the benzylic carbon in lignin, producing water-soluble, anionic polyelectrolytes that are used in cement formulations, animal feed, road dust suppressant, oil drilling thinners, and controlled release fertilizer granules.[1] As the number of sulfite mills declines, replacing lignosulfonates with lignins from the kraft pulping process has received commercial attention. Chemical modifications, such as phenolation, esterification, epoxidation, and amination are required to improve the functionality of kraft lignins.[2] Amination uniquely introduces cationic groups in the lignin chemical structure. Lignin amines may find application as heavy metal and dye adsorbents[3–5] and flocculants[6]. Additionally, amine-modified lignins have been shown to improve interfacial energy for polymer blending[7], or as a macromonomer for direct incorporation into polymer networks[8,9]. Lignin amines are also ideal binders for nitrogen fertilizers.[10] Several methods are known for introducing amine groups into lignin including oxidative ammonolysis[11] and epoxidation of phenolic hydroxyl groups followed by ring opening with an amine[12,13], but the most common method is Mannich condensation[14]. As applied research of kraft lignin amines continues to increase, it is critical that chemical and structural effects induced by the Mannich reaction are understood for proper elucidation of structure-property relationships.

The Mannich reaction was originally used to derivatize thio (kraft) lignin to facilitate chemical and structural analysis under non-catalyzed, room temperature conditions.[14] A series of lignin model compound experiments revealed that one alkylamino group was selectively and quantitatively substituted *ortho* to non-etherified phenolic hydroxyl groups**.** It was suggested that total nitrogen content could be correlated to the number of non-condensed, non-etherified

positions *ortho* to phenolic hydroxyl groups. This technique has been prominently employed to characterize lignin reactivity as a phenol substitute in adhesive formulations.[15–17] Jiang and Argyropoulos presented a complimentary analytical technique for characterizing lignins that incorporated the Mannich reaction with phosphorus-31 NMR spectroscopy to effectively improve identification of catechol, guaiacol, and C6-substituted phenyl units.[18]

Analytical methods that incorporate the Mannich reaction have been traditionally carried out under neutral conditions and at room temperature. In contrast, most recent applied research studies use either acetic acid in conjunction with an organic solvent, like dioxane, or sodium hydroxide in aqueous media to adjust pH and higher temperatures to decrease reaction time. Unfortunately, the pH is rarely reported if it is not intentionally modified, but reaction media should be slightly alkaline because amines are weak bases. In this study, basic conditions were achieved by adjusting the pH above that created by the amine. It is generally recognized that Mannich condensation proceeds through at least two pH-dependent pathways with the rate-determining step being reaction of the nucleophilic species with the iminium ion (under acidic conditions) or alkylaminomethylol (alkaline conditions).[19] Du *et al*. proposed these pathways also applied to the amination of lignins and that both routes would yield the same product, but only performed reactions with the use of a small amount of acetic acid and did not report pH.[20]

To date, only one paper has been published that explored the effect of acidic and basic conditions on kraft lignin amination *via* the Mannich reaction.[21] Elemental analysis of the aminated products following reactions conducted under pH levels of 5, 7, and 9 unexpectedly indicated the number of amine groups per 100 free phenolic hydroxyl group with non-condensed C5 positions to be 190, 62, and 46 mol%, respectively. These results suggest that 1) additional reaction sites are activated under acidic conditions; 2) side products are formed that contribute to

the nitrogen analysis; or 3) the reaction is thermodynamically or kinetically unfavorable in basic media. The final point is least likely, as the presence of acetic acid (pH 4 to pH 5) was shown to retard the rate of reaction as compared to runs with no acid,[18] consistent with an earlier fundamental study that demonstrated the Mannich reaction rate increased with increasing pH[19]. The higher apparent substitution at low pH was explained by showing that vanillin underwent side chain displacement to form a di-substituted Mannich base.[21] However, C1/C5 di-substituted products from vanillyl alcohol and vanillic acid have also been identified under slightly alkaline conditions.[14,18] Alternatively, the authors suspected but did not confirm, that non-volatile, nitrogen-containing impurities may have been responsible for the higher apparent substitution. Another possibility is that under acidic conditions, C5, C2, and C6 positions of etherified aromatic units are all equally activated by electron-donating, *ortho-* and *para*-directing methoxyl and phenoxyl groups, whereas under alkaline conditions, the non-etherified phenoxyl group is much more likely to dominate as an *ortho-, para*-directing entity through resonance (**Figure 3.1**).

Du *et al.* reported amine substitution of softwood kraft lignin below that of Wang *et al.* (per free phenolic hydroxyl group with non-condensed C5).[20,21] Reagents and reaction conditions were identical, but dialysis was used by the former and not the latter suggesting that loss of a low molecular weight fraction of aminated pine kraft lignin during dialysis may have resulted in an underestimation of amine substitution if the lost portion provided more reaction sites. Lower molecular weight, non-woody alkali lignin yielded higher degrees of amine substitution due to a relatively higher abundance of *para*-hydroxyphenyl-type (H-type) aromatic units.[22]

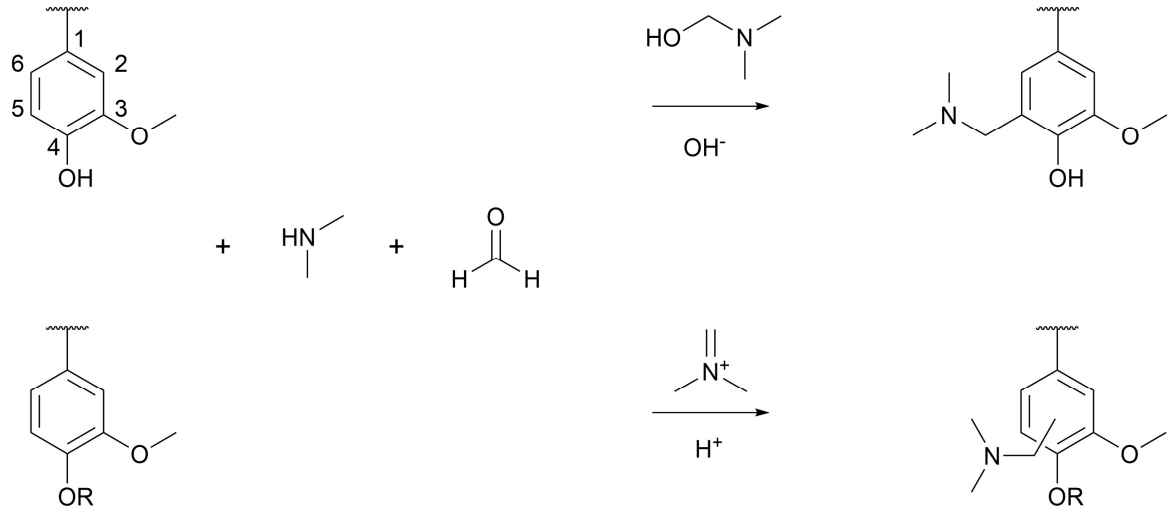

Figure 3.1. Proposed pH-dependent reaction pathways of Mannich condensation on the guaiacyl repeat unit. Note that the conjugate acid of dimethyl amine has a pKa = 10.73, so at pH = 11, roughly half the amine will exist as its conjugate acid. The free phenoxyl group of lignin has a similar pKa.

The objective of this study was to identify factors and reaction pathways that may result in greater than 1:1 amine/free phenolic hydroxyl group C5 substitution and offer mechanistic insight. Furthermore, structurally characterizing lignin amines prepared at elevated temperatures in the presence of acid/base catalysts can support evolving applied research efforts that were not possible using earlier methods developed for analytical studies. A secondary objective was to verify elemental analysis results, by far the most common method found in the literature to measure the extent of amination, against independent characterization techniques. Few publications related to lignin amines characterize or provide any detail of the lignin being used, and fewer provide satisfactory confirmation of lignin-amine bonding relative to potential reaction sites. ^{31}P NMR spectroscopy is a more direct method for quantifying amine substitution by tracking reduction of non-condensed, non-etherified positions *ortho* to the phenolic hydroxyl

group position (i.e., C5 position on guaiacyl-type (G-type) aromatic units). However, elemental analysis has underestimated substitution relative to ^{31}P NMR results.[21,23] Other condensation reactions may compete with Mannich condensation to complicate ^{31}P NMR analysis, especially when higher temperatures and acids or strong bases are used.[20–22,24–27] Quantitative carbon-13 NMR spectroscopy has been used to characterize various native and industrial lignins for many years.[28–34] A modified technique that combines this with two dimensional heteronuclear single quantum coherence (HSQC) NMR spectroscopy was developed to effectively improve the resolution of ^{13}C spectra and has been used to analyze technical and native lignins derived from softwood and hardwood species.[35–38] Like ^{31}P NMR spectroscopy, this method can characterize whole lignin samples and accuracy is not as dependent on purity as elemental analysis.

Herein, a comprehensive experimental design was executed to further understanding on the effects of amine species, pH, and lignin molecular weight fraction during the amination of commercially available, pine kraft lignin and clarify discrepancies found in the literature. Lignin chemical structure was characterized before and after modification by gel permeation chromatography (GPC), two dimensional ^{1}H-^{13}C HSQC, quantitative ^{13}C NMR, and ^{31}P NMR spectroscopy to validate proposed hypotheses and suggest the most suitable method for quantifying lignin amine substitution.

Materials and Methods

Materials

Ethyl acetate, petroleum ether, 1,4-dioxane, formaldehyde (37 wt% in water), acetic acid (glacial), and sodium hydroxide (0.5 N and 0.1 N) solutions were certified ACS and purchased from Fisher Chemical. Tetrahydrofuran (THF) was HPLC grade and purchased from Fisher

Scientific. Dimethylamine (40 wt% in water) (DMA), diethylamine (99.5%) (DEA), deuterated dimethyl sulfoxide (DMSO-d6), deuterated chloroform ($CDCl_3$), chromium(III) acetylacetonate, *N*-hydroxy-5-norbornene-2,3-dicarboxylic acid imide (97%) (NHND), and 2-chloro-4,4,5,5-tetramethyl-1,3,2-dioxaphospholane (TMDP) were purchased from Sigma-Aldrich. 1,3,5-trioxane was purchased from Acros Organics. All chemicals were used as received except for 1,4-dioxane, which was prepared by refluxing over sodium hydroxide and sodium borohydride for one hour, then distilled to dry the solvent, reduce any peroxides, and remove stabilizer. Note that 1,4-dioxane should never be completely evaporated to prevent concentration of peroxides, which are heat and shock sensitive.

BioChoice® lignin (BCL) was produced at the Plymouth, North Carolina pulp mill and provided by Domtar, Inc. BCL is a pine, kraft lignin precipitated from black liquor using the Lignoboost® process. BCL was thoroughly washed with deionized water to remove any remaining ash and air-dried prior to use and is hereafter referred to as whole lignin. Whole lignin was subsequently fractionated through solvent precipitation following a published protocol.[38] High molecular weight (HMW) lignin consisted of the fraction insoluble in ethyl acetate, and low molecular weight (LMW) consisted of the fraction which is soluble in a 1:1 v/v mixture of ethyl acetate: petroleum ether. A third fraction was produced consisting of 39 wt% of the starting lignin that was not used in this study, as the properties of HMW and LMW were most different. Key properties of relevance to the present study are provided in **Table 3.1**.

Table 3.1. Properties of pine kraft lignin fractions used in this study.

Lignin Fraction	Fraction, wt %[a]	M_w, g mol^{-1} ($Đ$)[b]	Abundance of key structures, mol/100 mol Ar units			
			ortho di-substituted Ph-OH[c]	*ortho* mono-substituted Ph-OH[c]	Carboxylic Acid OH[c]	Catechol[d]
Whole	100	6650 (4.0)	31.0	29.2	9.1	10.8
HMW	48	11190 (3.1)	27.8	24.0	7.6	4.4
LMW	13	650 (1.3)	23.7	54.9	16.9	20.3

a. A third fraction with 39% of starting lignin weight was also generated, but not used in this study.

b. Weight-average molecular weight and dispersity determined by gel permeation chromatography.

c. Phenolic hydroxyl and carboxylic acid groups determined by phosphorous-31 NMR.

d. As determined by UV-Vis spectroscopy absorbance at 560 nm.[38]

Preparation of lignin amines

Amination of lignin samples followed a previous procedure with a few modifications.[21] All lignin samples were dried in a vacuum oven at 40 °Cover phosphorus pentoxide prior to use. 100 mg of lignin were completely dissolved in 1 mL of 1,4-dioxane. 50 mmol dimethylamine or diethylamine per gram of lignin were then added followed by dropwise addition of 50 mmol formaldehyde per gram of lignin. This reagent amount corresponded to a molar excess of 3.75 mol/mol aromatic hydrogen assuming all free C2, C5, and C6 sites are active towards substitution. The pH was adjusted to 5 using acetic acid or to 11 using 0.1 N NaOH for DEA tests and 0.5 N NaOH for DMA tests to maintain similar volumes. The sealed mixture was heated in a water bath at 60 °C for 4 h, then placed in an ice bath. Excess reagents, volatile side products, and solvent were removed under vacuum (roughly 150 torr) at 40 °C through rotary evaporation. In preliminary tests, dialysis (1 kDa cutoff) was used to purify lignin amines

following rotary evaporation per literature,[20] but large product losses prevented the use of this technique for the main portion of this study (**Figure B.1**). Instead, successive rounds of freeze drying were performed following rotary evaporation until a powder was obtained, whereby each round consisted of the products being thoroughly mixed with water and freeze-dried. Lastly, all products were dried in a vacuum oven over phosphorous pentoxide before analyzing.

Synthesis and testing of 5-5' model compound

Biphenyl lignin substructure was hypothesized to provide for C2 or C6 substitution during the Mannich reaction. 3,3'-dimethoxy-5,5'-dimethylbiphenyl-2,2'-diol was used as the 5-5' model compound and was synthesized based on a previous report.[39] First, methyl guaiacol (2.0 mmol), [*meso*-tetra(4-methoxyphenyl) porphyrincobalt(II)] catalyst (0.004 mmol), and NaOH (2.0 mmol) were added to 10 mL of a methanol and water mixture (4:1 v/v). The reaction flask was evacuated and charged with oxygen (1 atm) and the mixture stirred for 16 hours at 60 °C. The mixture was cooled before being acidified with 2 N HCl, dissolved into ethyl acetate, passed through a plug of silica gel, and washed with ethyl acetate. Most of the remaining water in the filtrate was removed by drying over anhydrous sodium sulfate. Removal of solvent by rotary evaporation yielded the crude product. The desired product was isolated through silica gel column chromatography and purified by recrystallization from cyclohexane and ethyl acetate. NMR δ_H(500 MHz; DMSO-d6 = 2.50 ppm) 8.08 (s, 2H), 6.73 (s, 2H), 6.52 (s, 2H), 3.79 (s, 6H), 2.22 (s, 6H); mp 134.5 °C (from cyclohexane/ethyl acetate) (lit.,[39] 133 °C to 135 °C). The proton NMR spectrum can be found in Appendix B (**Figure B.2**).

Molecular weight determination

Molecular weight distributions of lignin and lignin amines were determined using gel permeation chromatography (GPC). Samples were first acetylated by dissolving 40 mg dried lignin in a 1 mL mixture of acetic anhydride and pyridine (1:1 v/v) and reacted at room temperature for 48 h in a sealed vial. The reaction mixture was added to 20 mL ice-cold water and shaken every few minutes to precipitate acetylated lignin and convert excess acetic anhydride. The suspension was filtered using a fine, glass-fritted filter and washed three times with cold, deionized water and the solids dried overnight in a vacuum oven at 45 °C over phosphorous pentoxide. For the aminated samples soluble in water, purification was performed through successive co-evaporations with toluene (three times), then with acetone/ethanol (1:1 v/v) to remove toluene. Samples were dissolved in THF at a 1 mg/mL concentration and injected into a GPC system (Shimadzu) consisting of two columns in series (Styragel HR 1 7.8 x 300 mm and Styragel HR 5E 7.8 x 300 mm). The mobile phase used was THF at a flow rate of 0.7 mL/min and oven temperature of 35 °C. A UV detector was set to measure absorbance at a wavelength of 280 nm. Polystyrene standards were used for molecular weight calibration. Chromatograms are reported in Appendix B (**Figure B.3**). Aminated samples did not easily dissolve in tetrahydrofuran, so comparing the chromatograms of aminated and parent lignin samples may not be useful due to differences in solvent-polymer interaction energy and possibly incomplete recovery. A sodium hydroxide mobile phase may be used to determine lignin amine molecular weight distribution, but a compatible system was not available.

Elemental analysis

Elemental analysis was performed using a Perkin Elmer 2400 CHNS Analyzer. Nitrogen-to-carbon ratios were used to calculate the number of amine groups per hundred aromatic units assuming all nitrogen was part of a covalently bonded tertiary amine group and that the parent lignins were comprised of 9.7 moles of carbon per unit, including methoxy groups.[38]

^{13}C and 2D HSQC spectroscopy

The NMR experimental methods have been described in detail in previous studies.[30,40] Lignin or lignin amines were dissolved in DMSO-d6 at a concentration of 200 mg/mL. HMW samples required several hours to completely dissolve. 2D HSQC experiments were performed using a 700 MHz Bruker Avance NEO magnet equipped with a 5 mm TCI helium-cooled probe. The following acquisition parameters were used: hsqcetgpsisp.2 adiabatic pulse program, spectral widths of 12 ppm for proton and 180 ppm for carbon centered at 5 ppm and 80 ppm, 2048 (proton) and 512 (carbon) digitized points for acquisition times of 125 ms and 8.1 ms, a D1 delay of 1.5 s, and 32 scans for a total experiment time of 7 h. Chromium(III) acetylacetonate, a relaxing agent, was added to the sample prior to 1D carbon-13 experiments to achieve a final concentration of 0.016 M. 1,3,5-trioxane was added as an internal standard (0.033 M). Quantitative ^{13}C NMR spectra were acquired on a 500 MHz Bruker Avance III magnet equipped with a 5 mm BBO room temperature probe with the following parameters: zgig decoupled, inverse-gated pulse program, spectral width of 220 ppm centered at 100 ppm, 83328 digitized points for an acquisition time of 1.5 s, a D1 delay of 2 s, and 19200 scans for a total experiment time of 19 h. To maximize sensitivity, the delay between pulses (D1) should be 4 to 5 times the

T1 relaxation time. A 2 s delay was ultimately used based on measured T1 relaxation times of various structures in lignin amine samples **(Figure B.4)**.

NMR spectral peak identification was facilitated by the recent work of Lancefield *et al.*, and assignments used for integration are given in **Table B.1**.[34] Integration of 2D spectra followed a method proposed by Zhang and Gellerstedt, whereby crosspeaks were referenced to "secondary internal standards" that represent regions containing structures with similar coupling constants and relaxation times.[41] This analysis was combined with ^{13}C NMR spectroscopy to provide quantitative measurements of specific lignin structures. ^{13}C NMR spectra were processed by applying an exponential multiplication (EM) window function to the free induction decay response (FID) with 2 Hz line broadening using Bruker TopSpin® 4 software. Phasing of Fourier-transformed spectra was corrected, and the baseline was zeroed in the regions of 205 to 200 ppm, 185 to 182 ppm, 97 to 94 ppm, and 5 to -10 ppm by a polynomial function according to literature.[31] Zero filling was employed to improve integration precision by setting the size of the real spectrum (SI) to be twice the number of points used (TD). Equation 3.1 demonstrates the NMR quantification calculation used:

$$\frac{\text{HSQC integral of x}}{\text{HSQC integral of secondary internal standard region}} \,{}^{13}\text{C integral of region}, \qquad (3.1)$$

where 'x' is the structure of interest. Carbon spectra were integrated by normalizing the aromatic region to 610 on average: 600 aromatic carbons plus 10 (on average) vinylic carbons per 100 aromatic units as estimated from HSQC spectra.

^{31}P NMR spectroscopy

Phosphorous-31 NMR spectroscopy was performed based on previously reported methodologies.[21,42] Aminated lignins were not soluble in the typical solvent mixture of $CDCl_3$

and pyridine (1:1.6 v/v), so the method detailed by Wang *et al.* was used.[21] Freeze- and vacuum-dried lignin or lignin-amine samples (20 mg to 30 mg) were swelled in 100 µL dimethylformamide and pyridine (1:1 v/v) at 35 °C until a homogenous mixture was achieved. Note that the high molecular weight fraction of lignin and corresponding aminated products required 300 µL solvent to remain dissolved throughout the analysis. Next, 100 µL of an internal standard (20 mg/mL NHND in pyridine), 100 µL of a relaxation agent (5 mg/mL chromium(III) acetylacetonate in pyridine), and 400 µL of $CDCl_3$ were successively added before immediately adding 100 µL of a phosphitylating agent, TMDP. Spectra were acquired within 30 minutes of sample preparation on a 500 MHz Bruker Avance III magnet equipped with a 5 mm BBO room temperature probe using the following parameters: zgig decoupled, inverse-gated pulse program, spectral width of 100 ppm centered at 140 ppm, 65536 digitized points for an acquisition time of 1.6 s, a D1 delay of 10 s, and 128 scans for a total experiment time of 25 minutes. Spectra were processed using automatic phasing and baseline corrections and calibrated to the phosphitylated water peak at 132.2 ppm.

Results and Discussion

Elemental analysis

A full factorial experimental design was developed to investigate the effects of pH adjustments and amine species when using the Mannich reaction to modify different molecular weight fractions of BCL pine kraft lignin. Three factors were included in the experimental design: pH at two levels (5 and 11), amine species at two levels (dimethylamine and diethylamine), and lignin fraction at three levels (whole, LMW, and HMW).

The extent of amination as revealed by elemental analysis ranged from 51.7 to 94.0 mol amine per 100 mol aromatic units across all tested conditions (**Table 3.2**). Samples at the extremes of this range were modified with DMA, with the lowest number of amine groups substituted in HMW lignin under alkaline conditions and the highest number in LMW under acidic conditions. Comparing the relative values of these extremes follows the pH trend observed by Wang *et al*.[21] It also supports the hypothesis that the LMW fraction should have a higher yield than the HMW fraction due to its higher content of mono-substituted phenolic hydroxyl groups (**Table 3.1**). On the other hand, the absolute values of the elemental analysis results did not follow expectations. Under alkaline conditions, only non-condensed, non-etherified C5 positions were expected to react with the methanolamine intermediate, so 30 mol% was expected as a maximum, not 51.7 mol%. Additionally, it was proposed that under acidic conditions, non-condensed C5 (etherified or non-etherified), C2, and C6 positions may all serve as reactive sites for a total of 2.7 sites per aromatic unit for LMW, or 270 mol%, which is much higher than the observed 94 mol%. Elemental analysis accuracy will be discussed further in the subsequent sections. As results from replicates were highly precise (less than 5% relative error under most conditions), it was concluded that statistical modelling could offer useful insights into the relative effects of different factors on amine substitution.

Table 3.2. Elemental analysis of lignin amine products varying pH, amine species, and starting lignin fraction.

Lignin	pH	Amine	wt% ± 90% CL[a]			mol% ± 90% CL[a]
			Mass Recovery[b]	Carbon	Nitrogen	Amine / Aromatic Unit
Whole	5	DEA	114.5 ± 10.9	65.57 ± 1.28	4.38 ± 0.03	68.2 ± 2.7
Whole	11	DEA	100.1 ± 8.0	64.69 ± 1.33	4.46 ± 0.38	68.7 ± 6.8
HMW	5	DEA	112.2 ± 16.8	65.36 ±0.27	4.39 ± 0.14	68.7 ± 3.7
HMW	11	DEA	96.93 ± 0.56	63.99 ± 0.28	4.09 ± 0.14	61.3 ± 3.4
LMW	5	DEA	104.3 ± 2.9	68.18 ± 0.26	5.32 ± 0.21	86.6 ± 5.7
LMW	11	DEA	108.2 ± 20.8	66.40 ± 0.40	5.38 ±0.27	88.7 ± 7.4
Whole	5	DMA	119.2 ± 2.5	60.77 ± 1.84	4.84 ± 0.18	73.0 ± 2.2
Whole	11	DMA	104.3 ± 1.0	58.17 ± 1.41	3.54 ± 0.11	57.5 ± 2.4
HMW	5	DMA	106.0 ± 3.4	62.84 ± 0.63	3.65 ± 0.08	52.9 ± 0.8
HMW	11	DMA	106.3 ± 5.6	60.24 ± 0.44	3.37 ± 0.22	51.7 ± 3.6
LMW	5	DMA	107.6 ± 12.7	64.08 ± 1.60	5.91 ± 0.33	94.0 ± 7.2
LMW	11	DMA	112.7 ± 0.9	61.68 ± 0.51	4.77 ± 0.21	77.1 ± 5.0

a. mol amine per 100 mol aromatic units. 90% confidence limit calculated from sample standard deviation using a student's t-distribution. Sample size varies between 2 and 5.

b. Mass recovery was calculated by dividing product weight by starting lignin weight. Product weight was first adjusted for the addition of amine groups based on nitrogen content and blanks (experiments with no lignin).

A standard least squares regression was chosen as the statistical model with an emphasis on effect screening and was generated using JMP® software. The model had an R-squared value of 0.83 and predicted that lignin fraction and pH-amine species two-factor interaction were significant based on a p-value of 0.05. Low molecular weight lignin had the highest amine substitution, with an average of 88.0 mol% on aromatic units regardless of pH or amine species, versus 65.0 mol% and 59 mol% for whole and HMW fractions, respectively (**Figure 3.2**). Whole

and HMW lignin fractions were not statistically different; 48 wt% of whole lignin is recovered as the HMW fraction so their composition is similar, whereas LMW lignin accounts for 13 wt% of the original lignin sample.

The model predicted an interaction between pH and amine species, but there was no significant difference in reactivity between acidic and alkaline environments for runs that used DEA (**Figure 3.3**). If DEA is sterically hindered, then it may not be able to access the additional sites activated under acidic conditions. pH had a larger impact on reactivity when using the smaller DMA amine. However, directly comparing pH=11 results in **Figure 3.3** suggests DMA is less reactive than DEA and does not support the steric hindrance argument. On the other hand, a systematic error may be induced by less volatile side products or impurities in DEA-derived lignin amine samples, thereby inflating DEA elemental analysis data. Even though reagent blank tests were performed to account for this type of error, the presence of lignin during main experiments may have contributed to the retention of unreacted intermediates during work-up.

Only evaporation and freeze drying were used to purify lignin amine products to minimize losses and ensure characterization of the full product. 100% mass recovery (adjusted for amine addition and sodium hydroxide in pH 11 runs) was expected for this work-up procedure. In fact, mass recoveries exceeded 100% for all but one sample, indicating the presence of impurities (**Table 3.2**). In general, acidic samples tended to be more viscous than alkaline samples after the first evaporation and freeze-drying cycle. Several rounds of freeze drying were required to achieve a dry powder for pH 5 samples, but not pH 11 samples. Amine groups in the aminated lignin are protonated (pKa ~11) and form salts with acetic acid that would remain after evaporation. Acetic acid was also expected to be present after freeze drying due to its low volatility. Acetate and acetic acid peaks were present in NMR spectra (δ_C = 174 to

172 ppm and δ_H = 22 to 21 ppm) in all aminated lignin samples regardless of the pH. Amides also resonate in the same region and may have formed from the reaction of dimethyl amine and carboxylic acid groups of lignin, which has been observed for cinnamic acid with amine catalysts.[43] This pathway should not contribute greatly, as direct amidation of carboxylic acids is unfavorable due to the lack of good leaving groups. Typically, carboxylic acid amidation requires the use of a dehydrating agent like *N,N′*-Dicyclohexylcarbodiimide. Instead, formation of a salt between the carboxylic acid and amine is more likely to contribute to N content. Additional experiments were performed along with NMR analyses to test this hypothesis and to check the accuracy of elemental analysis data.

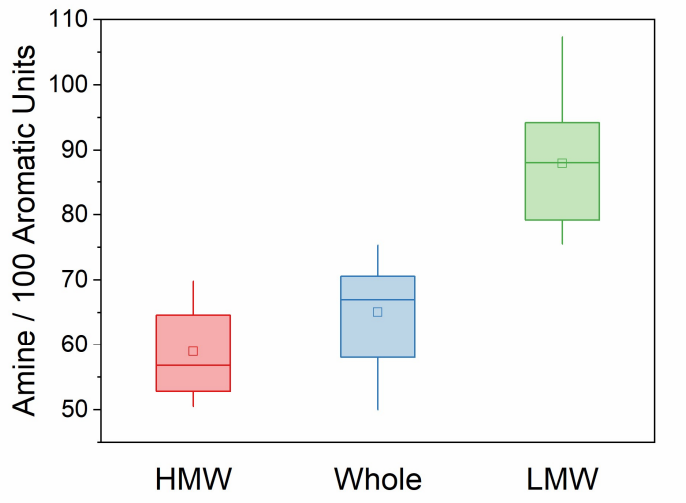

Figure 3.2. Effect of lignin fraction as a substrate for amination.

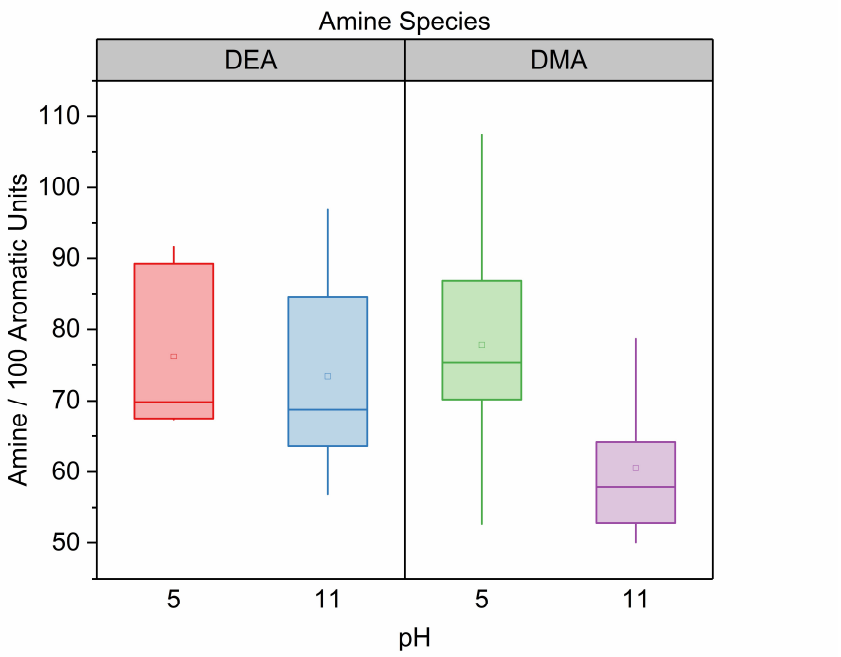

Figure 3.3. Interaction between pH and amine species.

^{13}C and ^{1}H-^{13}C HSQC NMR spectroscopy

Three parallel analyses were performed using HSQC and quantitative ^{13}C spectra to estimate the amount of amine groups substituted into the lignin structure. Each analysis was compared to determine the most appropriate one. ^{13}C NMR spectra integrations used in the current study were likely quantitative in terms of peak area being proportional to the number of carbon nuclei. However, lower than ideal signal-to-noise ratios were obtained while following the protocols of previous quantitative studies, which may limit accuracy. More detailed discussion can be found in Appendix B.

Software-predicted crosspeak assignments were verified using 2-methoxy-4-propylphenol (propyl guaiacol) as a model compound, which was selectively and quantitatively substituted at the C5 position when using either DMA or DEA (**Figure 3.4** and **Figure 3.5**). The first quantification method was to integrate the resonance signal of carbon nuclei in Ar-**CH_2**-N

structures. It is common to use the methylene bridge for DMA-modified lignin amines (δ_C/δ_H = 60.4 ppm / 3.50 ppm), because the only overlapping resonance is from gamma carbons in β-O-4' side chains, which have a relatively low abundance in kraft lignin and can be corrected for by quantifying β-O-4' alpha carbons.[20,21,44] Unfortunately, Ar-**CH_2**-N nuclei of the DEA-modified model compound resonated close to methoxy nuclei (55.2 ppm / 3.66 ppm vs. 55.3 ppm / 3.71 ppm) and were not distinguishable in spectra of lignin amines (**Figure 3.5**). The second method was to integrate the dimethyl crosspeak of DMA-modified (44.1 ppm / 2.21 ppm) or dimethylene crosspeak of DEA-modified lignin (45.5 ppm / 2.52 ppm). The third method was to quantify aryl carbon–hydrogen (Ar-H) bonds before and after amination and assume that the reduction in Ar-H signal corresponds to electrophilic substitution by the alkylamine.[22] Additional detail concerning the position of substitution is limited using 2D HSQC. While the number two guaiacyl carbon, G2-H, cluster is relatively isolated, signals of the remaining Ar-H structures (e.g., guaiacyl carbons C5 and C6, *p*-hydroxyphenyl carbons C3 and C5, and catechol carbons C2, C5, and C6) overlap with each other between 115 ppm and 125 ppm (**Figure 3.7**).

Samples were selected to provide a good representation of Mannich reaction variables. Results of the three methods are presented in **Table 3.3**. Elemental analysis overestimated amine substitution relative to NMR analyses for each sample, however the effect of lignin fraction was clear. Results from all methods agreed that that LMW samples were substituted to a higher degree. NMR analyses suggested that the bulkier DEA molecule may have limited yield in contrast with analysis of CHN data. pH did not appear to have an effect when using DMA, as was suggested in the previous section and previous findings.[21] Direct NMR analysis of aryl-amine linkages support that ionically bonded or other nonvolatile intermediates may have led to

an overestimation of lignin amine groups for pH=5 or DEA samples when using elemental analysis.

Table 3.3. Characterization of lignin amines by ^{13}C and HSQC NMR spectroscopy compared with elemental analysis (mol amine/100 mol aromatic units).

Fraction	Amine	pH	-OCH_3	CHN	^{13}C and 2D HSQC NMR		
					$(CH_3)_2$	(CH_2)	Total Ar-H Reduction
HMW	DMA	5	70.6	52.9	29.2	25.3	55.3
HMW	DEA	5	84.4[a]	68.7	23.9[b]	-[b]	43.4
LMW	DMA	5	72.8	94.0	47.9	45.1	63.9
LMW	DMA	11	69.1	77.1	50.6	41.7	62.1

a. Overlap with Ar-**CH_2**-N resonance signal may have inflated methoxyl group quantification, which is further complicated due to the difference in protons of the two moieties.

b. The aryl-amine methylene bridge signal could not be resolved from the methoxyl signal. Methylene groups Ar-CH_2-N-(**CH_2**$CH_3)_2$ were analyzed for DEA-modified lignin.

Comparing the first two methods, quantification of -N-**$(CH_3)_2$** nuclei overestimated substitution relative to Ar-**CH_2**-N nuclei of DMA-modified lignins. Overlap with the broad dimethyl sulfoxide solvent signal was a complicating factor, but the presence of unidentified side reaction products or contaminants seemed to be more problematic. A sharp peak upfield caused significant overlap and was assumed to be a small molecule impurity due to its narrow shape and reduced intensity upon increased purification (**Figure 3.4** and **Figure 3.6**). As a result, Ar-**CH_2**-N was deemed more reliable for analyzing DMA-modified lignin and -N-(**CH_2**-$CH_3)_2$ was preferred for DEA-modified lignin. The LMW/DMA/5 sample had the highest degree of amine substitution, in agreement with elemental analysis, at 45.1 mol per 100 aromatic units. LMW

lignin structures had almost twice the number of amine groups as the HMW fraction. While fractionation was used as an analytical method to investigate the effect of chemical structure, it may also direct future process development efforts. In this case, LMW lignin would be preferred in terms of maximizing amine substitution. Furthermore, fractionation (whether by pH precipitation, membrane filtration, or solvent dissolution) reduces chemical and physical heterogeneities characteristic of most lignins.[45] Any of these three processes may be used at commercial scale, but it is important to consider technical and economic viability.[46,47]

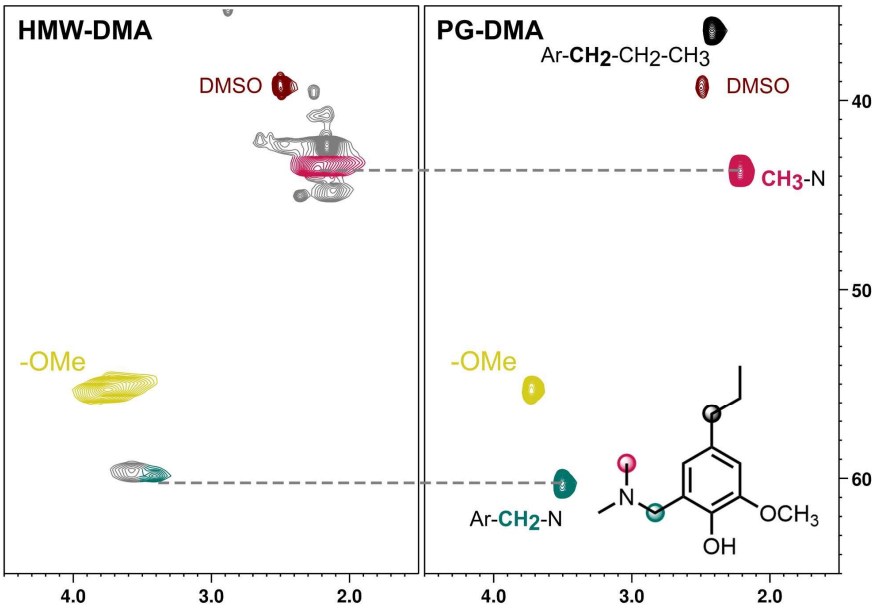

Figure 3.4. 2D HSQC NMR spectrum of HMW, DMA, pH 5 (dialyzed) aminated lignin (left side). Crosspeak assignment performed using aminated propyl guaiacol as model compound (right side).

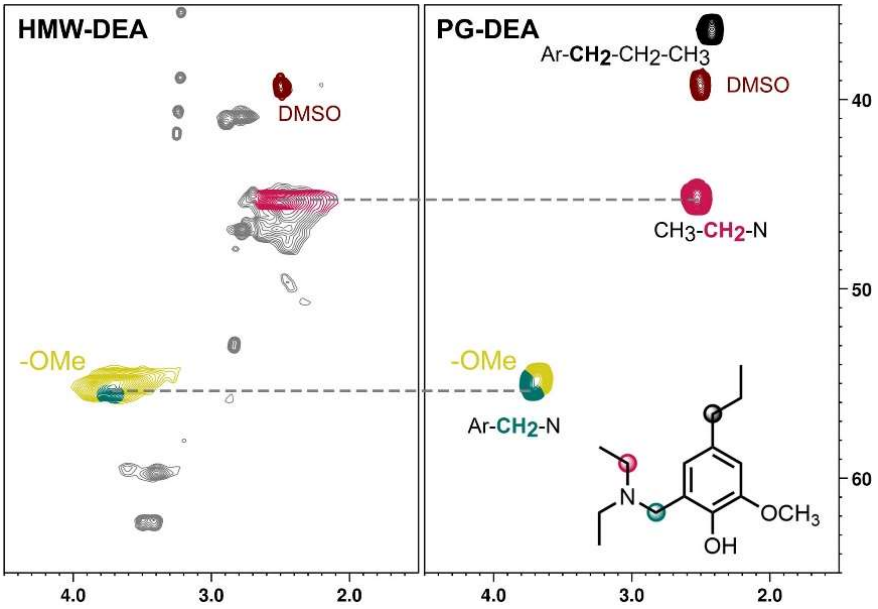

Figure 3.5. 2D HSQC NMR spectra of HMW, DEA, pH 5 aminated lignin (left side) and DEA-aminated propyl guaiacol model compound (right side).

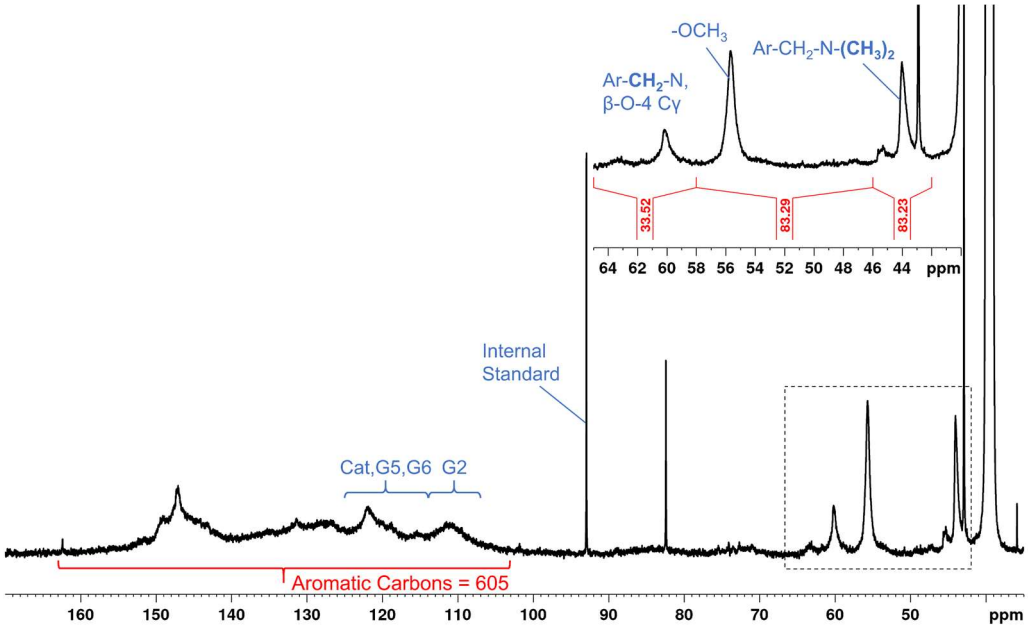

Figure 3.6. ^{13}C NMR spectrum of HMW, DMA, pH 5 aminated lignin. Integration regions labeled for total aromatic carbons (163 ppm > δ_C > 103 ppm), secondary internal standards G2-H (114 ppm > δ_C > 107 ppm), -CH_2 (65 ppm > δ_C > 58 ppm), -CH_3 (58 ppm > δ_C > 46 ppm), and primary internal standard trioxane at δ_C = 93 ppm.

Aromatic carbon-proton (Ar-H) signal reduction was the third method to quantify alkylamino substitution. The G2-H region (**Figure 3.7**) was selected as the secondary internal standard because 1) it is relatively isolated from other signals, 2) other Ar-H nuclei should have similar T2 relaxation times, and 3) the G2-H proton was not substituted in model compound studies using propyl guaiacol under the same reaction conditions. Higher amine substitution was estimated relative to direct quantification of aryl-alkylamine groups, 50% higher for LMW and two times for HMW lignin amines (**Table 3.3**). Available positions *ortho* to non-etherified phenolic hydroxyl groups were 57.6 and 33.3 mol/100 mol aromatic units for LMW and HMW fractions, respectively, as determined by ^{31}P NMR and assuming one substitution per aromatic unit. Ar-H reduction exceeded these values for all samples, which could serve as evidence for etherified C3/C5 or C2/C6 substitution if accurate.

On the other hand, Ar-H signal reduction may be unreliable if G2-H is not an appropriate secondary internal standard or if there are competing condensation reactions besides Mannich condensation. Secondary internal references must have a similar T2 relaxation to the structure being quantified.[41] The justification for using G2-H was that nuclei with similar chemical shifts should have similar T2 relaxation times, but this is not guaranteed. Other Ar-H groups possibly have longer T2 relaxation times than G2-H that would generate higher signal intensity. Additionally, G2-H abundance must remain constant before and after the reaction to be used as an internal standard. Although this was observed in model compound studies, G2-H signal did decrease relative to the methoxyl region in HSQC spectra, though this is a semi-quantitative observation. G2-H/-OCH_3 reduction indicates an overestimation of amine substitution assuming no demethylation (or demethoxylation) occurs during amination. Lastly, condensation of two

aromatic units by formaldehyde could have competed with the Mannich reaction, but diphenylmethane interunit linkages were not observed in HSQC spectra.

Ideally, Ar-H signals for the C2 and C6 carbons of catechol could be tracked to determine if these sites were substituted. Unfortunately, catechol crosspeaks were not resolved separately (**Figure 3.7**). It was hypothesized that catechol hydroxyl groups may activate C2, C5, and C6. If so, catechol abundances would contribute to differences in amine substitution yields of the two molecular weight fractions. LMW lignin has almost five times the number of catechol units compared to HMW (**Table 3.1**). Jiang and Argyropoulos demonstrated that methyl catechol reacted with piperidine and formaldehyde to produce multiple Mannich bases.[18] Though the exact structures were not identified, it was concluded that each product was only substituted once.

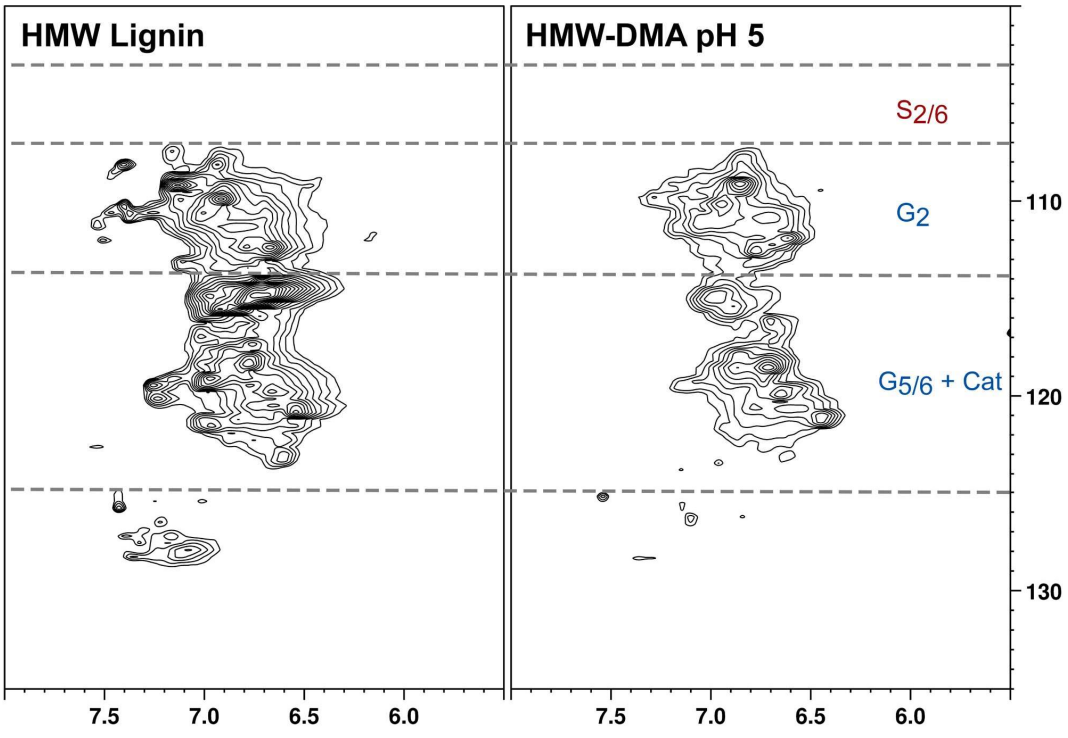

Figure 3.7. 2D HSQC spectra of the aromatic region for HMW lignin before and after Mannich reaction under acidic conditions using dimethylamine.

5-5’ biphenyl is another common softwood kraft lignin substructure that may promote electrophilic substitution at C2/C6 and has not previously been considered (**Figure 3.8**). The 5-5’ inter-unit linkage accounts for 23 to 27 mol per 100 mol C9 units in softwood milled wood lignin.[48] The degree of condensation for dissolved kraft softwood lignin was determined through quantification of quaternary carbons to only increase by 5 percent after kraft cooking; therefore, the quantity of 5-5’ linkages in dissolved softwood kraft lignin is assumed to be similar to softwood MWL.[28] At a pH of 11 or above, phenolate anion may activate C2/C6 carbons on the neighboring phenyl unit through resonance. To test whether C2/C6 substitution was possible, a 5-5’ model compound was reacted under similar conditions to those used in the lignin modification runs (see experimental section). Proton NMR analysis of the product was identical to the starting molecule. If the reaction did not proceed under favorable conditions when using a model compound, C2 or C6 activation of 5-5’ units is not expected during the amination of real lignins.

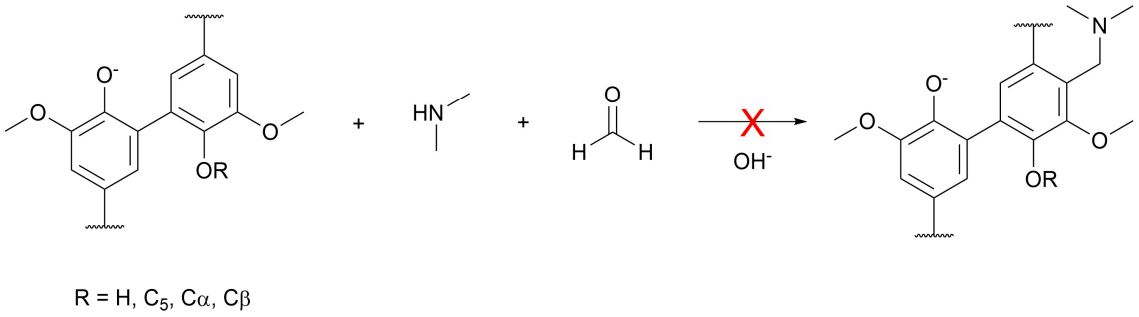

R = H, C_5, Cα, Cβ

Figure 3.8. Proposed biphenyl structure activation of C2 for substitution by alkylaminomethylol intermediate. This reaction did not proceed in model compounds tests (60 °C, 4 h, pH 12).

Although aromatic units with etherified phenolic hydroxyl groups were not directly studied here, alkylamino substitution has been shown to not proceed under room temperature, weakly basic conditions for these substructures.[14] Access may be limited at these sterically

hindered sites, similar to what was observed for C2/C6 carbons in propyl guaiacol and 5-5' biphenyl model compound tests. Analysis of the literature and 2D HSQC results of the current study support that the aromatic ring is selectively substituted mainly at C5 or C3 carbons of non-etherified, non-condensed units. Catechol subunits may be the only exception where substitution at the C2 and C6 carbon positions is possible.[18]

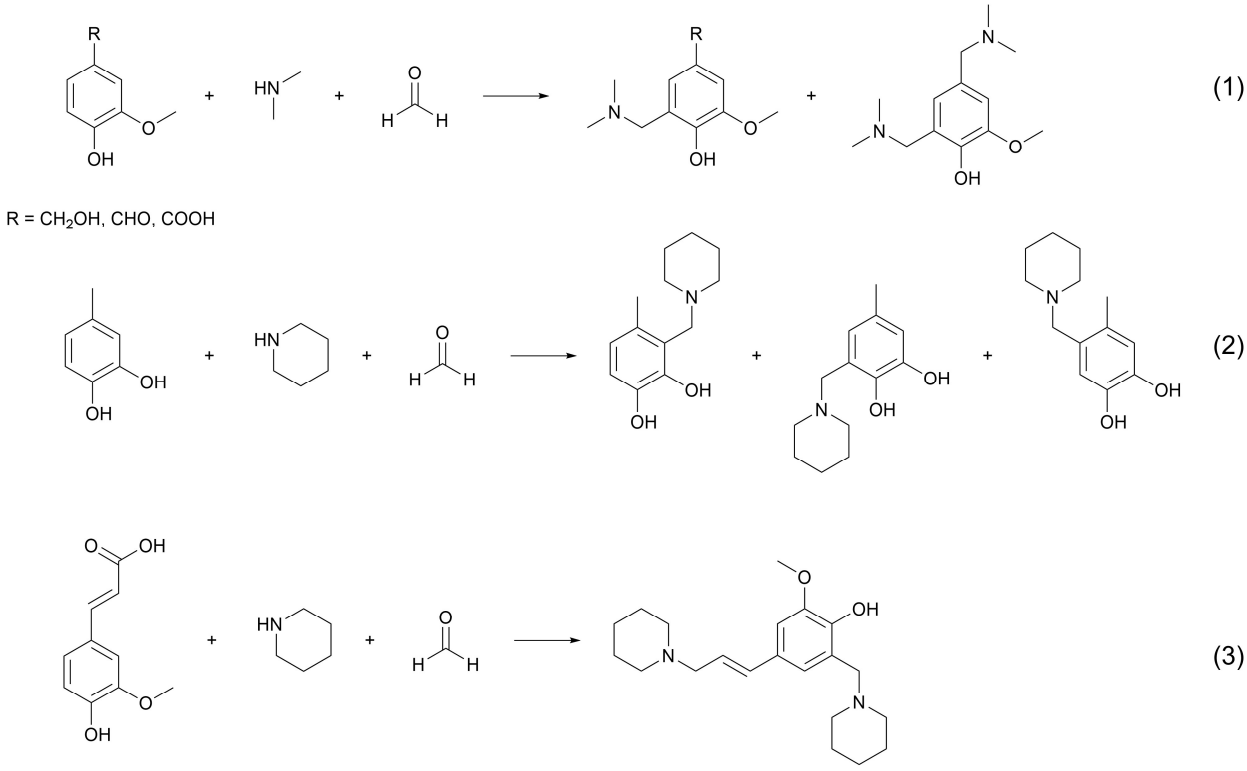

Figure 3.9. Products observed (1, 3) or proposed (2) by previous model compound studies.[14,18,21] Vanillin may or may not produce the di-substituted Mannich base, see discussion. Catechol yielded multiple products that were not fully characterized, though the most likely products are presented.

Side chain reactivity during Mannich reaction

Lignin side chains are not typically considered in the Mannich reaction but could skew free C5 quantification by elemental analysis if reactive. Sole HSQC analysis of the aromatic

region would underestimate amine substitution yield slightly by excluding reactions at the beta or gamma carbons. In past model compound studies, di-substituted Mannich bases were produced from vanillyl alcohol, vanillic acid, and possibly vanillin when using dimethylamine (**Figure 3.9**, reaction 1).[14,18,21] In each experiment, electrophilic substitution ortho to the phenoxyl group was preferred versus side chain replacement. Vanillic acid and vanillyl alcohol C5 positions were completely substituted and C1 partially replaced at room temperature in the absence of catalysts.[14,18] Vanillin did not yield a di-substituted product after one day at room temperature.[14] A more recent publication claimed di-substitution occurred after 4 h at 60 °C and a pH of 5.[21] Independent verification is required because products were analyzed using LC-MS and the supposed di-substituted Mannich base had a reported M+1 of 217, while M+1 for that compound should be 238 g mol^{-1}.

Reaction pathways accounting for the formation of di-substituted Mannich bases have not previously been discussed in detailed. Proposed mechanisms for empirically verified model compound reactions are presented in **Figure B.5**. Vanillic acid is proposed to undergo side chain displacement through substitution by the Mannich intermediate, resembling an Eschweiler-Clarke reaction (**Figure B.5**, reactions 1 and 2). The para-hydroxyl electron-donating group apparently reduces activation energy, as carboxyl group replacement of salicylic acid did not proceed under the same reaction conditions (room temperature, no catalyst).[18] Acid-catalyzed decarboxylation at elevated temperatures followed by electrophilic substitution may be an alternative mechanism. Kaeding showed that while salicylic acid underwent decarboxylation at 212 °C in the absence of catalyst, meta and para isomers did not.[49] The calculated activation energy of salicylic acid decarboxylation is 50% lower in aqueous media with acid, but this may not translate to lignin benzoic acid subunits.[50] Direct amidation by the amine at the benzylic

carbon followed by dehydration or reduction is yet another mechanism, though would require higher temperatures and better catalysts or a strong reducing agent. Vanillate salt in the presence of acetic acid and amine is a more likely byproduct (**Figure B.5**, reaction 3). Unlike vanillic acid, para-hydroxy cinnamic acids do readily decarboxylate to form a styrene across a wide pH range.[51] Electrophilic addition by the Mannich intermediate (iminium ion or alkylaminomethylol) would yield a Mannich base, as empirically observed with ferulic acid (**Figure 3.9**, reaction 3; **Figure B.5**, reaction 7).[18] Vanillyl alcohol may proceed by a similar route through a quinone methide intermediate (**Figure B.5**, reaction 6). Vanillin to vanillyl amine under typical Mannich reaction conditions is not likely nor has it been clearly demonstrated experimentally. Direct displacement by the Mannich intermediate is high energy (**Figure B.5**, reaction 5). Nucleophilic attack of the benzaldehyde by a secondary amine could create an iminium ion, which would then need to be reduced to yield an amine. Iminium salt with acetic acid is a more probable nitrogen-containing byproduct (**Figure B.5**, reaction 4). Changes to side chain interunit linkages were characterized by quantitative carbon-13 and HSQC NMR experiments to better understand side chain involvement during amination (**Table 3.4**).

Neither vanillyl alcohol nor vanillin crosspeaks were satisfactorily identified from HSQC spectra. Some lignin monomers may have been lost during freeze drying. Vanillic acid was detected in all lignin samples and decreased in abundance as expected, possibly through side chain displacement (**Figure B.5**, reaction 1 and 2). β-O-4' linkages remained unaffected, as expected from model compound studies.[18] Likewise, β-5' and β-β' abundances did not change. A more recent study that utilized the Mannich reaction to aminate a non-woody alkali lignin presented semi-quantitative HSQC data that suggested a decrease in the abundance of β-O-4', β-β', and β-5' linkages, contradicting model compound tests, but the authors did not discuss the

data to offer any explanation.[22] Beta-elimination of β-5' or β-β' linkages resulting in loss of formaldehyde is possible under acidic or basic media and would leave an unsaturated side chain conjugated with two phenyl groups that may then undergo electrophilic addition by the iminium ion. However, conditions used in this study were likely too mild to induce beta elimination. Stilbenes are already present in kraft lignin, having been formed through the same process during pulping. Stilbene abundance decreased by about half across all experiments, allowing for the possibility that these structures were substituted by alkylamines. This was not confirmed because the concentration was too low to use NMR analysis to identify the resulting Mannich base. Enol ethers were of relatively low abundance in starting lignin samples, suggesting that they did not contribute significantly to product yields or side reactions.

Table 3.4. Estimation of side chain structures before and after Mannich reaction using combined quantitative ^{13}C and ^{1}H-^{13}C HSQC NMR spectroscopy (mol/100 mol aromatic units).[a]

Fraction	HMW	HMW	HMW	LMW	LMW	LMW
Amine	-	DEA	DMA	-	DMA	DMA
pH	-	5	5	-	11	5
β-O-4'	3.5	3.5	3.5	ND[b]	0.1	ND[b]
β-5'	2.0	2.2	2.5	0.1	0.1	0.1
β-β'	3.2	3.2	3.6	0.6	0.5	0.5
Vanillic Acid	0.4	0.3	0.3	1.9	0.1	0.3
Enol Ethers	0.8	0.1	0.2	0.2	0.2	ND[b]
Stilbenes	2.7	1.5	1.4	6.7	3.9	3.4

a. HSQC experiment sensitivity may not be sufficient for confident integration of peaks less than 1 mol%.

b. ND = crosspeak was not detected.

Hydroxyl content analysis using ^{31}P NMR spectroscopy

Phosphorous-31 NMR was employed to confirm and quantify the substitution of amine groups onto the aromatic ring (**Figure B.6**). Any increase in C3 or C5 substitution was assumed to be a result of amine substitution and not another condensation reaction. Aliphatic hydroxyl and carboxylic groups were also quantified. Reduction in mono-substituted phenolic hydroxyl groups did not match the increase in di-substituted groups based on integration of the corresponding spectral regions (**Table B.2**). In other words, total phenolic hydroxyl group content differed before and after amination. Others have also reported a reduction following the Mannich reaction; unfortunately, that result was not discussed so no explanations are available by the authors.[21,22,52] To account for this reduction, data were normalized by total free aliphatic and phenolic hydroxyl group content assuming this is unchanged during the reaction (see Appendix B).

Normalized ^{31}P NMR data revealed a decrease (but not elimination) in free positions *ortho* to non-etherified phenolic hydroxyl groups following amination (**Table 3.5**). In previous studies, no signal was detected in the *ortho* mono-substituted region (140.4 ppm > δ_P > 138.5 ppm) following the Mannich reaction indicating complete substitution by the amine.[21,52] In the current study, signals in this region remained above the baseline. In fact, this should be expected as Jiang and Argyropoulos reported that one hydroxyl group of catechol units and the hydroxyl group of any C6-condensed guaiacyl unit would resonate in this region following the Mannich reaction.[18]

Table 3.5. Hydroxyl group characterization by ^{31}P NMR spectroscopy before and after Mannich reaction. Data normalized to total phenolic and aliphatic hydroxyl group content.

Lignin sample[b]	mol / 100 mol aromatic units ± 95% CL[a]					
	Aliphatic OH	Phenolic OH				Carboxylic OH[c]
		Di-substituted	Mono-substituted	Non-substituted	Total	
HMW	32	28	24	6.1	58	7.6
HMW /DMA/5	32.8 ± 0.1	47.2 ± 0.9	7.3 ± 0.2	2.4 ± 0.6	57 ± 0.1	3 ± 3
HMW /DEA/5	36.1 ± 0.4	43.9 ± 0.5	7.2 ± 0.3	2.4 ± 0.4	54 ± 0.4	2 ± 2
LMW	11	24	55	6.1	85	17
LMW/DMA/5	15 ± 1	74 ± 1	4.7 ± 0.4	1.9 ± 0.6	80 ± 1	15 ± 3
LMW/DMA/11	17 ± 1	71 ± 1	5.1 ± 0.7	2.7 ± 0.4	79 ± 1	12 ± 3

a. Where provided, the second value represents the 95% confidence limit calculated from an estimated standard deviation using student's t-distribution. Sample size is 3.

b. The sample designation is MW fraction of lignin / amine species / starting pH of reaction.

c. Values for aminated samples calculated by subtracting the large, overlapping acetic acid peak.

Aliphatic hydroxyl content increased in all samples, more so for LMW lignin amines, while total phenolic hydroxyl group content was slightly lower than the corresponding parent lignins, even after normalization. Recently it was reported that the number of aliphatic hydroxyl groups decreased following amination of a biorefinery lignin, but the authors utilized dialysis to purify products and product recovery yield was not provided so it is unclear if the entire product was characterized.[52] Catechols were suspected have a role, as LMW lignin is comprised of 20.3 mol catechol per 100 aromatic units, roughly 4.6 times that of HMW lignin (**Table 3.1**).[38] 4-methyl catechol was reacted with formaldehyde and dimethylamine under a pH of 11 for 4 h at 60 °C to investigate catechol content effects on analysis. ^{31}P NMR revealed that all phenolic hydroxyl groups of the product mixture resonated within the di-substituted or aliphatic integration regions (**Figure B.7**). Aliphatic and phenolic hydroxyl group contents may be

overestimated and underestimated, respectively, at least partly due to the presence of catechol subunits.

Carboxylic acid group quantification was complicated by the presence of an intense, sharp peak at δ_P = 134.7 ppm corresponding to acetic acid that remained following evaporation and lyophilization even though every effort was taken to remove it, including repeated co-evaporation of the samples with toluene. Oddly, this peak also appeared in the spectrum of sample produced under alkaline conditions. Deconvolution of spectra was attempted to remove the contribution of the overlapping peak, but accuracy of this method is questionable given the large relative difference in integration values. Qualitatively, the abundance of free COOH groups appeared to decrease following amination, which agrees with HSQC analysis (**Table 3.5**).

Comparison of yields determined by different analytical techniques

Mannich reaction yield was calculated using the theoretical number of reactive sites for each lignin fraction (**Table 3.6**). Two reaction pathways were considered to determine the theoretical yield based on above discussions of results found in literature and of current findings: 1) Electrophilic aromatic substitution *ortho* to mono- or non-substituted, non-etherified phenolic hydroxyl groups and 2) side chain displacement of vanillyl alcohol, vanillic acid, and cinnamic-type acids. Etherified units and C2/C6 carbons of non-etherified guaiacyl-type units were not considered to undergo aromatic substitution due to steric effects. Catechol units contribute two *ortho* mono-substituted positions, but only one amine was assumed to react per catechol; therefore, the abundance of catechol units was used to correct total free sites as determined by ^{31}P NMR. H-type units were similarly considered to provide one reactive site. Structural characterization results presented in **Table 3.1** and **Table 3.5** were used for theoretical reactive

site quantification. Actual yields were calculated from elemental (**Table 3.2**), combined ^{13}C/HSQC NMR (**Table 3.3** and **Table 3.4**), and ^{31}P NMR (**Table 3.5**) analyses.

Table 3.6. Mannich reaction yield determined by different analytical techniques.

Lignin Sample	Theoretical mol / 100 mol Ar units	Yield, %				
		CHN	^{13}C/HSQC NMR[a]	^{31}P NMR[b]	^{13}C/HSQC NMR, modified[c]	^{31}P NMR, modified[c]
HMW/DMA/5	33.3	159	76.3	87.1	98.8	94.7
HMW/DEA/5	33.3	206	72.1	88.1	94.6	95.1
LMW/DMA/5	57.6	163	80.9	106	108	131
LMW/DMA/11	57.6	134	75.3	107	102	128

a. Quantification of Ar-**CH_2**-N nucleus plus vanillic acid reduction as calculated by ^{13}C/HSQC spectra. Ar-CH_2-N-**CH_2-** nuclei were used for the DEA sample.

b. Reduction in *ortho* mono- and non-substituted phenolic hydroxyl group abundance was used to calculate actual aromatic substitution, plus reduction in COOH groups.

c. Assuming all COOH groups of original lignin were substituted.

Elemental analysis overestimated amine group abundance based on the theoretical number of reaction sites (**Table 3.6**). This was expected as elemental analysis is not a selective technique that accounts for all nitrogen including N-containing impurities and byproducts. Yield for LMW/DMA/11 was closest to 100% of theoretical supporting the observation that pH 11 samples were easier to purify through evaporation and freeze drying.

Combined ^{13}C/HSQC NMR analysis gave an average yield of 76% ± 3% (95 percent confidence limit) for HMW and LMW fractions (**Table 3.6**, left column). Phosphorus-31 NMR indicated that diffusion or steric hindrance may be limiting factors of the HMW fraction with 88% yield versus 106% for LMW lignin. Possible reasons for ^{13}C/HSQC yield below 100%: 1) theoretical yield is high (e.g., ^{31}P overestimated free phenolic OH groups); 2) HSQC analysis did

not capture total reduction of aliphatic carboxylic acid groups; 3) reaction was incomplete (some reactive sites were inaccessible or longer reaction time required); and 4) reproducible error in data collection/processing. Assuming the reactions proceeded to completion, yields were re-calculated to account for the second reason by considering complete alkylamino substitution of carboxylic acid groups (**Table 3.6**, right column). This gave an average yield of 101% ± 4%. Actual yield cannot be above 100 percent, but the slight overestimation is reasonable given that minor side products are inevitable and supports that no additional pathways contribute to yield. Neither the C5 carbon of etherified units nor C2 or C6 carbons of guaiacyl-type units are substituted by alkylamino groups in acidic or basic media.

^{31}P NMR yields were much greater than 100 percent when considering complete carboxylic acid group replacement for LMW samples. This is partly because the total phenolic hydroxyl group content decreased even after normalization (caused by catechol subunit resonance shift as described earlier). Additionally, ^{31}P NMR relies on subtracting integrated signals from spectra with very low signal-to-noise, possibly leading to inaccuracies. Finally, the assumption that data can be normalized to maintain total aliphatic and phenolic hydroxyl group abundance has not been validated.

Combined ^{13}C/HSQC NMR analysis was the most consistent technique across multiple samples and had the advantage of directly quantifying lignin amine bonds. Furthermore, ^{13}C/HSQC quantification aligned with previous characterizations of pine kraft lignin structure, whether the analysis was performed by room temperature, catalyst-free Mannich reactions (25 to 40 mol%)[14,16] or by nitrobenzene oxidation (25 to 33 mol%).[37,53] ^{31}P NMR does have the advantage of better tracking COOH groups, though this signal was obscured by residual acetic acid and may not be reliable.

One analytical technique should not be relied upon to characterize a complex macromolecule like lignin and findings should be confirmed with a second quantitative technique that directly characterizes the abundance of lignin-amine bonds. Past studies that employed multiple analytical techniques also encountered discrepancies that were not explained. When analyzing modified lignins it is important to report reaction yields and data from at least two independent characterization techniques in the same units for clear comparison. The authors have attempted to make the necessary conversions for previous studies (**Table B.3**).

Conclusion

In the only previous study that explored the effect of pH when using the Mannich reaction to modify technical lignins, a high degree of amination under acidic conditions indicated possible C1, C2, or C6 substitution. A comprehensive full factorial experimental design was executed to determine if this was possible and if pH, amine species, and lignin molecular weight fraction were factors in the amination of pine kraft lignin. Both NMR and elemental analysis results supported the hypothesis that lignin average molecular weight was the most significant factor in determining degree of substitution, likely due to the increased amount of available, non-condensed C5 positions and carboxylic acid groups. Neither pH nor amine species significantly affected yields according to NMR spectra, a result that was not obvious from elemental analysis alone. Elemental analysis was shown to regularly overestimate lignin amine yields compared to NMR analyses possibly due to N-containing byproducts and impurities. Dialysis would remove impurities but should be avoided to limit losses of low molecular weight lignin amines.

Quantitative ^{13}C NMR coupled with 2D HSQC spectroscopy was the most reliable method for degree of substitution determination, specifically when quantifying the methylene

group of the Ar-**CH_2**-N structure (60.4 ppm / 3.50 ppm) of DMA-modified samples or the N-(**CH_2**$CH_3)_2$ nuclei (45.5/2.52) of DEA-modified samples. While phosphorous-31 NMR spectroscopy has been used extensively to characterize lignin-amines, this technique does not directly quantify lignin-alkylamine bonds and could be prone to errors in quantification due to inaccurate mass balances or internal standard dosing. Further, catechol phenolic hydroxyl groups may have shifted downfield to overlap with aliphatic hydroxyl groups leading to inaccurate integrations. ^{13}C NMR coupled with 2D HSQC analysis relies only on the assumption that the number of aromatic carbons is unaffected during the mild reaction.

The possibility for pH to direct where Mannich condensation occurs on pine kraft lignin structures was explored for the first time, and steric effects were found to dominate. It was hypothesized that under acidic media, methoxyl and hydroxyl groups equally activate *ortho* and *para* positions for electrophilic substitution; and, under alkaline conditions C2/C6 carbons of 5-5' biphenyl are reactive. However, the C2/C6 protons on biphenyl or guaiacyl-type substructures were not substituted. Catechol subunits possibly react *meta* to free phenolic hydroxyl groups, but no direct evidence was found to support this.

For future applied research, amine-modification of low molecular weight kraft lignin is preferred due to greater number of reaction sites and water solubility. Omission of acid or base catalysts is preferred to simplify product purification, especially when used as a precursor in polymer synthesis or other downstream process. Application of heat is sufficient to increase the rate of lignin amination through the Mannich reaction if necessary.

The importance of reporting mass yields and employing multiple analytical tools when modifying a complex, heterogeneous substrate like lignin cannot be understated. Elemental analysis is an inconsistent method for accurately determining the amine degree of substitution

and likely the extent of other lignin modifications as well. The combination of 2D HSQC and quantitative ^{13}C NMR was demonstrated as a more direct alternate that can be applied to multiple types of lignins, modified or not. Additional studies validating the use of quantitative NMR spectroscopy (phosphorus-31 and carbon-13) to analyze multiple technical lignins will be invaluable to further chemical structure characterization of whole lignin samples. Additionally, an independent analytical method capable of direct qualification and quantification of Mannich-derived lignin structures should be developed to validate NMR analyses.

REFERENCES

(1) Gargulak, J. D.; Lebo, S. E.; McNally, T. J. Lignin. In *Kirk-Othmer Encyclopedia of Chemical Technology*; John Wiley & Sons, Inc.: Hoboken, NJ, USA, 2015; pp 1–26. https://doi.org/10.1002/0471238961.12090714120914.a01.pub3.

(2) Laurichesse, S.; Avérous, L. Chemical Modification of Lignins: Towards Biobased Polymers. *Prog. Polym. Sci.* **2014**, *39* (7), 1266–1290. https://doi.org/10.1016/j.progpolymsci.2013.11.004.

(3) Brežný, R.; Paszner, L.; Micko, M. M.; Uhrín, D. The Ion-Exchanging Lignin Derivatives Prepared by Mannich Reaction with Amino Acids. *Holzforschung* **1988**, *42* (6), 369–373. https://doi.org/10.1515/hfsg.1988.42.6.369.

(4) Brežný, R.; Schraml, J.; Cermak, J.; Micko, M. M.; Paszner, L. Specific Ion-Exchangers Based on Lignins and Their Characterization by 29Si-NMR Spectroscopy. *Tappi J.* **1990**, *June*, 199–204.

(5) Supanchaiyamat, N.; Jetsrisuparb, K.; Knijnenburg, J. T. N.; Tsang, D. C. W.; Hunt, A. J. Lignin Materials for Adsorption: Current Trends, Perspectives and Opportunities. *Bioresour. Technol.* **2019**, *272* (June 2018), 570–581. https://doi.org/10.1016/j.biortech.2018.09.139.

(6) Fang, R.; Cheng, X.; Xu, X. Synthesis of Lignin-Base Cationic Flocculant and Its Application in Removing Anionic Azo-Dyes from Simulated Wastewater. *Bioresour. Technol.* **2010**, *101* (19), 7323–7329. https://doi.org/10.1016/j.biortech.2010.04.094.

(7) Fang, C.; Liu, W.; Qiu, X. Preparation of Polyetheramine-Grafted Lignin and Its Application in UV-Resistant Polyurea Coatings. *Macromol. Mater. Eng.* **2019**, *304* (10), 1900257. https://doi.org/10.1002/mame.201900257.

(8) Abarro, G. J.; Podschun, J.; Diaz, L. J.; Ohashi, S.; Saake, B.; Lehnen, R.; Ishida, H. Benzoxazines with Enhanced Thermal Stability from Phenolated Organosolv Lignin. *RSC Adv.* **2016**, *6* (109), 107689–107698. https://doi.org/10.1039/C6RA22334F.

(9) Li, M.; Jiang, X.; Wang, D.; Xu, Z.; Yang, M. In Situ Reduction of Silver Nanoparticles in the Lignin Based Hydrogel for Enhanced Antibacterial Application. *Colloids Surfaces B Biointerfaces* **2019**, *177* (February), 370–376. https://doi.org/10.1016/j.colsurfb.2019.02.029.

(10) Chen, J.; Fan, X.; Zhang, L.; Chen, X.; Sun, S.; Sun, R. Research Progress in Lignin-Based Slow/Controlled Release Fertilizer. *ChemSusChem* **2020**, *13* (17), 4356–4366. https://doi.org/10.1002/cssc.202000455.

(11) Capanema, E. A.; Balakshin, M. Y.; Chen, C. L.; Gratzl, J. S.; Kirkman, A. G. Oxidative Ammonolysis of Technical Lignins Part 1. Kinetics of the Reaction under Isothermal Condition at 130°C. *Holzforschung* **2001**, *55*, 397–404.

(12) Liu, X.; Zhu, H.; Qin, C.; Zhou, J.; Zhao, J. R.; Wang, S. Adsorption of Heavy Metal Ion from Aqueous Single Metal Solution by Aminated Epoxy-Lignin. *BioResources* **2013**, *8* (2), 2257–2269.

(13) Pan, H.; Sun, G.; Zhao, T. Synthesis and Characterization of Aminated Lignin. *Int. J. Biol. Macromol.* **2013**, *59*, 221–226. https://doi.org/10.1016/j.ijbiomac.2013.04.049.

(14) Mikawa, H.; Sato, K.; Takasaki, C.; Ebisawa, K. Studies on the Cooking Mechanism of Wood. XV. Mannich Reaction on Lignin Model Compounds and the Estimation of the Amount of the Simple Guaiacyl Nucleus in Thiolignin. *Bull. Chem. Soc. Jpn.* **1956**, *29* (2), 259–265.

(15) Pan, X.-J.; Sano, Y. Atmospheric Acetic Acid Pulping of Rice Straw IV: Physico-

Chemical Characterization of Acetic Acid Lignins from Rice Straw and Woods. Part 2. Chemical Structures. *Holzforschung* **1999**, *53* (6), 590–596. https://doi.org/10.1515/HF.1999.098.

(16) El Mansouri, N.-E.; Salvadó, J. Structural Characterization of Technical Lignins for the Production of Adhesives: Application to Lignosulfonate, Kraft, Soda-Anthraquinone, Organosolv and Ethanol Process Lignins. *Ind. Crops Prod.* **2006**, *24*, 8–16. https://doi.org/10.1016/j.indcrop.2005.10.002.

(17) Ibrahim, M. N. M.; Zakaria, N.; Sipaut, C. S.; Sulaiman, O.; Hashim, R. Chemical and Thermal Properties of Lignins from Oil Palm Biomass as a Substitute for Phenol in a Phenol Formaldehyde Resin Production. *Carbohydr. Polym.* **2011**, *86*, 112–119. https://doi.org/10.1016/j.carbpol.2011.04.018.

(18) Jiang, Z.-H.; Argyropoulos, D. S. Coupling Phosphorus-31 NMR with the Mannich Reaction for the Quantitative Analysis of Lignin. *Can. J. Chem.* **1998**, *76* (5), 612–622. https://doi.org/10.1139/cjc-76-5-612.

(19) Cummings, T. F.; Shelton, J. R. Mannich Reaction Mechanisms. *J. Org. Chem.* **1960**, *25* (3), 419–423. https://doi.org/10.1021/jo01073a029.

(20) Du, X.; Li, J.; Lindstrom, M. E. Modification of Industrial Softwood Kraft Lignin Using Mannich Reaction with and without Phenolation Pretreatment. *Ind. Crops Prod.* **2014**, *52*, 729–735. https://doi.org/10.1016/j.indcrop.2013.11.035.

(21) Wang, M.; Sjoholm, E.; Li, J. Fast and Reliable Quantification of Lignin Reactivity via Reaction with Dimethylamine and Formaldehyde (Mannich Reaction). *Holzforschung* **2017**, *71* (1), 27–34. https://doi.org/10.1515/hf-2016-0054.

(22) Wang, B.; Chen, T.-Y.; Wang, H.-M.; Li, H.-Y.; Liu, C.-F.; Wen, J.-L. Amination of

Biorefinery Technical Lignins Using Mannich Reaction Synergy with Subcritical Ethanol Depolymerization. *Int. J. Biol. Macromol.* **2018**, *107*, 426–435. https://doi.org/10.1016/j.ijbiomac.2017.09.012.

(23) Li, J.; Wang, M.; She, D.; Zhao, Y. Structural Functionalization of Industrial Softwood Kraft Lignin for Simple Dip-Coating of Urea as Highly Efficient Nitrogen Fertilizer. *Ind. Crops Prod.* **2017**, *109* (May), 255–265. https://doi.org/10.1016/j.indcrop.2017.08.011.

(24) Yanhua, J.; Weihong, Q.; Zongshi, L.; Lubai, C. A Study on the Modified Lignosulfonate from Lignin. *Energy Sources* **2004**, *26* (4), 409–414. https://doi.org/10.1080/00908310490281528.

(25) Ding, N.; Wang, X.; Tian, Y.; Yang, L.; Chen, H.; Wang, Z. A Renewable Agricultural Waste Material for the Synthesis of the Novel Thermal Stability Epoxy Resins. *Polym. Eng. Sci.* **2014**, *54* (12), 2777–2784. https://doi.org/10.1002/pen.23838.

(26) Wang, X.; Zhang, Y.; Hao, C.; Dai, X.; Zhou, Z.; Si, N. Ultrasonic-Assisted Synthesis of Aminated Lignin by a Mannich Reaction and Its Decolorizing Properties for Anionic Azo-Dyes. *RSC Adv.* **2014**, *4* (53), 28156–28164. https://doi.org/10.1039/c4ra03133d.

(27) Ge, Y.; Song, Q.; Li, Z. A Mannich Base Biosorbent Derived from Alkaline Lignin for Lead Removal from Aqueous Solution. *J. Ind. Eng. Chem.* **2015**, *23*, 228–234. https://doi.org/10.1016/j.jiec.2014.08.021.

(28) Gellerstedt, G.; Robert, D. Quantitative 13C NMR Analysis of Kraft Lignins. *Acta Chem. Scand. B* **1987**, *41* (January), 541–546. https://doi.org/10.3891/acta.chem.scand.41b-0541.

(29) Landucci, L. L. Application of Modern Liquid-State NMR to Lignin Characterization: 2. 13C Signal Resolution and Useful Techniques. *Holzforschung* **1991**, *45* (6), 425–432. https://doi.org/10.1515/hfsg.1991.45.6.425.

(30) Capanema, E. A.; Balakshin, M. Y.; Kadla, J. F. A Comprehensive Approach for Quantitative Lignin Characterization by NMR Spectroscopy. *J. Agric. Food Chem.* **2004**, *52* (7), 1850–1860. https://doi.org/10.1021/jf035282b.

(31) Balakshin, M. Y.; Capanema, E. A. Comprehensive Structural Analysis of Biorefinery Lignins with a Quantitative 13C NMR Approach. *RSC Adv.* **2015**, *5* (106), 87187–87199. https://doi.org/10.1039/c5ra16649g.

(32) Balakshin, M. Y.; Capanema, E. A.; Santos, R. B.; Chang, H-m.; Jameel, H. Structural Analysis of Hardwood Native Lignins by Quantitative 13C NMR Spectroscopy. *Holzforschung* **2016**, *70* (2), 95–108. https://doi.org/10.1515/hf-2014-0328.

(33) Crestini, C.; Lange, H.; Sette, M.; Argyropoulos, D. S. On the Structure of Softwood Kraft Lignin. *Green Chem.* **2017**, *19* (17), 4104–4121. https://doi.org/10.1039/c7gc01812f.

(34) Lancefield, C. S.; Wienk, H. L. J.; Boelens, R.; Weckhuysen, B. M.; Bruijnincx, P. C. A. Identification of a Diagnostic Structural Motif Reveals a New Reaction Intermediate and Condensation Pathway in Kraft Lignin Formation. *Chem. Sci.* **2018**, *9* (30), 6348–6360. https://doi.org/10.1039/C8SC02000K.

(35) Balakshin, M.; Capanema, E.; Gracz, H.; Chang, H-m.; Jameel, H. Quantification of Lignin-Carbohydrate Linkages with High-Resolution NMR Spectroscopy. *Planta* **2011**, *233*, 1097–1110. https://doi.org/10.1007/s00425-011-1359-2.

(36) Berlin, A.; Balakshin, M. Industrial Lignins: Analysis, Properties, and Applications. In *Bioenergy Research: Advances and Applications*; Gupta, V. K., Tuohy, M. G., Kubicek, C. P., Saddler, J., Xu, F., Eds.; Elsevier: Oxford, UK, 2014; pp 315–336. https://doi.org/10.1016/B978-0-444-59561-4.00018-8.

(37) Hu, Z.; Du, X.; Liu, J.; Chang, H-m.; Jameel, H. Structural Characterization of Pine Kraft

Lignin: BioChoice Lignin vs Indulin AT. *J. Wood Chem. Technol.* **2016**, *36* (6), 432–446. https://doi.org/10.1080/02773813.2016.1214732.

(38) Jiang, X.; Savithri, D.; Du, X.; Pawar, S.; Jameel, H.; Chang, H-m.; Zhou, X. Fractionation and Characterization of Kraft Lignin by Sequential Precipitation with Various Organic Solvents. *ACS Sustain. Chem. Eng.* **2017**, *5* (1), 835–842. https://doi.org/10.1021/acssuschemeng.6b02174.

(39) Jiang, Q.; Sheng, W.; Tian, M.; Tang, J.; Guo, C. Cobalt(II)-Porphyrin-Catalyzed Aerobic Oxidation: Oxidative Coupling of Phenols. *European J. Org. Chem.* **2013**, *2013* (10), 1861–1866. https://doi.org/10.1002/ejoc.201201595.

(40) Mansfield, S. D.; Kim, H.; Lu, F.; Ralph, J. Whole Plant Cell Wall Characterization Using Solution-State 2D NMR. *Nat. Protoc.* **2012**, *7* (9), 1579–1589. https://doi.org/10.1038/nprot.2012.064.

(41) Zhang, L.; Gellerstedt, G. Quantitative 2D HSQC NMR Determination of Polymer Structures by Selecting Suitable Internal Standard References. *Magn. Reson. Chem.* **2007**, *45*, 37–45. https://doi.org/10.1002/mrc.1914.

(42) Meng, X.; Crestini, C.; Ben, H.; Hao, N.; Pu, Y.; Ragauskas, A. J.; Argyropoulos, D. S. Determination of Hydroxyl Groups in Biorefinery Resources via Quantitative ^{31}P NMR Spectroscopy. *Nat. Protoc.* **2019**, *14* (9), 2627–2647. https://doi.org/10.1038/s41596-019-0191-1.

(43) Nomura, E.; Hosoda, A.; Mori, H.; Taniguchi, H. Rapid Base-Catalyzed Decarboxylation and Amide-Forming Reaction of Substituted Cinnamic Acids via Microwave Heating. *Green Chem.* **2005**, *7* (12), 863–866. https://doi.org/10.1039/b510626e.

(44) Dimmel, D.; Gellerstedt, G. Chemistry of Alkaline Pulping. In *Lignin and Lignans:*

Advances in Chemistry; Heitner, C., Dimmel, D., Schmidt, J., Eds.; CRC Press: Boca Raton, 2010; pp 349–392.

(45) Gillet, S.; Aguedo, M.; Petitjean, L.; Morais, A. R. C.; da Costa Lopes, A. M.; Łukasik, R. M.; Anastas, P. T. Lignin Transformations for High Value Applications: Towards Targeted Modifications Using Green Chemistry. *Green Chem.* **2017**, *19* (18), 4200–4233. https://doi.org/10.1039/c7gc01479a.

(46) Ajao, O.; Jeaidi, J.; Benali, M.; Abdelaziz, O. Y.; Hulteberg, C. P. Green Solvents-Based Fractionation Process for Kraft Lignin with Controlled Dispersity and Molecular Weight. *Bioresour. Technol.* **2019**, *291* (July), 121799. https://doi.org/10.1016/j.biortech.2019.121799.

(47) Jiang, X.; Abbati De Assis, C.; Kollman, M.; Sun, R.; Jameel, H.; Chang, H-m.; Gonzalez, R. Lignin Fractionation from Laboratory to Commercialization: Chemistry, Scalability and Techno-Economic Analysis. *Green Chem.* **2020**, *22* (21), 7448–7459. https://doi.org/10.1039/d0gc02960b.

(48) Chang, H-m.; Jiang, X. Biphenyl Structure and Its Impact on the Macromolecular Structure of Lignin: A Critical Review. *J. Wood Chem. Technol.* **2020**, *40* (2), 81–90. https://doi.org/10.1080/02773813.2019.1697297.

(49) Kaeding, W. W. Oxidation of Aromatic Acids. IV. Decarboxylation of Salicylic Acids. *J. Org. Chem.* **1964**, *29* (9), 2556–2559. https://doi.org/10.1021/jo01032a016.

(50) Hu, Y.; Gao, L.; Dai, Z.; Sun, G.; Zhang, T.; Jia, S.; Dai, Y.; Zhang, X. DFT Investigation on the Decarboxylation Mechanism of Ortho Hydroxy Benzoic Acids with Acid Catalysis. *J. Mol. Model.* **2016**, *22* (3), 56. https://doi.org/10.1007/s00894-016-2923-2.

(51) Cohen, L. A.; Jones, W. M. A Study of pH Dependence in the Decarboxylation of p-

Hydroxycinnamic Acid. *J. Am. Chem. Soc.* **1960**, *82* (8), 1907–1911. https://doi.org/10.1021/ja01493a019.

(52) Meng, X.; Scheidemantle, B.; Li, M.; Wang, Y. yan; Zhao, X.; Toro-González, M.; Singh, P.; Pu, Y.; Wyman, C. E.; Ozcan, S.; Cai, C. M.; Ragauskas, A. J. Synthesis, Characterization, and Utilization of a Lignin-Based Adsorbent for Effective Removal of Azo Dye from Aqueous Solution. *ACS Omega* **2020**, *5* (6), 2865–2877. https://doi.org/10.1021/acsomega.9b03717.

(53) Marton, J. Reactions in Alkaline Pulping. In *Lignins: Occurrence, Formation, Structure and Reactions*; Sarkanen, K. V., Ludwig, C. H., Eds.; Wiley Interscience: New York, 1971; pp 639–694.

CHAPTER 4: Catalytic Hydrogenolysis of Multiple Technical Lignins

Abstract

Catalytic hydrogenolysis flexible technology platform that can improve lignin valorization through the production of fuel additives or as precursors to advanced biofuels, chemicals, and polymers. One-pot conversion of technical lignins to jet fuel has resulted in low yields. A two-stage process involving a first stage of converting technical lignins to oligomeric products by hydrogenolysis followed by a second stage that converts oligomeric molecules to hydrocarbons may result in a much higher yield by optimizing each individually. The objective of this work was to focus on the first stage. Time, temperature, and pressure effects on the hydrogenolysis of pine kraft and hardwood biorefinery lignins were investigated using one catalyst system. Then, three lignin types (adding hardwood kraft lignin) were depolymerized with three catalyst systems at a midpoint process condition with detailed product analysis to identify feedstock-catalyst-product relationships. HWAER depolymerization was most extensive using DAB-Ru. 25% starting lignin was converted to monomers and dimers and almost 30% to volatile products. Yield of volatiles remained high across all time and temperature conditions tested. Using a zeolite-supported cobalt-zinc catalyst resulted in the lowest extent of depolymerization for all lignins was accomplished. Replacement of cobalt with ruthenium reduced solid residue losses, likely due to increased hydrogenation and hydrogenolysis activity that prevented recondensation and promoted depolymerization. Hardwood kraft lignin hydroprocessed with ruthenium on carbon combined with zinc acetate catalyst produced a liquid product that was most suitable as a feedstock to jet fuel production.

Introduction

Lignins represent the largest source of renewable aromatic molecules and have a higher carbon-to-oxygen ratio than other abundant natural polymers like cellulose and starch. Their chemical structure is characterized by phenyl propane units linked through carbon-carbon single bonds and ether bonds, both aryl and aliphatic. Lignins are removed from woody biomass feedstocks during the production of pulp and paper and proposed second-generation biofuels processes. The pulp and paper industry recovers 2% of solubilized lignin, and lignin is expected to be produced by biorefineries in excess beyond electricity and steam demand.[1] It has been shown that the biorefinery concept is only economically justified by selling value-added lignin-derived products.[1,2] Depolymerization of lignins into monomeric and dimeric compounds for use as fuel additives or as precursors to advanced biofuels, chemicals, and polymers is one strategy to promote valorization.[1,3]

Many industrially relevant artificial flavor and aroma compounds like guaiacol, eugenol, vanillin, syringol, and pyrogallol can be derived from lignins. In fact, vanillin was once commercially produced using lignin isolated from the acid sulfite pulping of wood and accounted for 60% of the global supply in the early 1980's.[4] These flavor and aroma compounds are valuable but only in their pure form. The heterogenous phenolic mixtures created by depolymerization are comprised of many compounds with similar heats of evaporation, which makes separation by distillation difficult. Conversion of lignin to liquid transportation fuels results in a mixture of aromatics and hydrocarbons that may be used as is or fed to conventional distillation operations at petrochemical refineries. Sustainable aviation fuels (SAFs) are of particular interest to government agencies and airline companies, having funded several research initiatives to reduce aircraft greenhouse gas emissions.[5] Lignin has been identified as a suitable

feedstock for producing SAFs because of the aforementioned relatively high carbon-to-oxygen ratio. In addition, aromatic compounds generated during lignin depolymerization may eliminate the need to add aromatics downstream or to blend with conventional fuel.[6]

Several whole biomass and lignin catalytic conversion processes have been evaluated for the generation of liquefied products, each with their own advantages and disadvantages.[7] Fast catalytic pyrolysis is one of the more common technologies.[8] In general, pyrolysis products are divided into four fractions: vapor, aqueous and organic liquid phases, and char. The organic liquid phase, termed bio-oil, is of most interest in the production of hydrocarbons for fuel, although they still contain a high number of unsaturated and oxygenated compounds, which lead to poor stability and low heating value.[9] Bio-oil will react in storage, even at low temperatures.[6]

Aqueous-phase oxidation routes utilize heterogenous catalysts like metal oxides, organometallics, and heteropolyacids among others under air or oxygen atmospheres to fragment the lignin polymer network.[7,10–12] These processes are effective at C-O and C-C bond cleavage at relatively mild conditions compared to other thermochemical routes like pyrolysis.[12] Cleavage of ether interunit linkages in the β-O-4' structure is thought to be facilitated by the oxidation of α-OH to a carbonyl, which was calculated to reduce the bond dissociation energy of C_β-O from 69.2 to 55.9 kcal/mol.[13] However, this pathway is only relevant for lignins with high ether linkage abundances like native or organosolv and not kraft. Cao and co-workers performed microwave-assisted depolymerization of three lignin types using CuO/BCN catalyst and found that the kraft lignin had 50% to 60% lower bio-oil yields than organosolv or bio-enzymatic lignin.[14] Photocatalysts are attractive for their high activity at ambient conditions, but process scalability is limited. Oxidation pathways are favorable for small-scale production of high-value oxygenated compounds like vanillin, vanillic acid, and succinic acid. Like pyrolysis bio-oils, the oxygenated mixtures are unstable for long-

term storage and are likely not suitable for downstream conversion to liquid fuels given the high oxygen content.

Reductive processes are effective for depolymerization and stabilization of lignins through hydrogenolysis and hydrogenation. Redox catalysts (platinum group metals like Pt, Pd, Ru, and base metals like Ni, Fe, Co) have been used to fragment lignins and whole biomass to a stable liquid product but are generally thought to be incapable of C-C bond activation.[15] Hydrogen can be supplied by hydrogen-donating solvents and/or external hydrogen gas, though solvents are advantageous in terms of promoting solvolysis and eliminating the gas-liquid transport barrier for hydrogen gas.[16] The more accessible hydrogen is, the faster hydrogenation can proceed to reduce unstable unsaturated bonds and carbocations, thereby avoiding polymerization and condensation reactions towards recalcitrant C-C bonds and coke formation. Hydrogenolysis process conditions are milder (≤ 320 °C) than other thermochemical routes like pyrolysis, which results in lower volatile formation in addition to the minimization of char formation. High selectivity towards a stabilized liquid product makes the reductive route attractive for conversion towards diesel or jet fuel-range hydrocarbons. Bifunctional catalysts that incorporate a combination of acid or base and redox sites have been developed to improve the yield and selectivity of aromatic and saturated hydrocarbon products.[17] The objective of these catalyst systems is to balance activities of hydrogenolysis, hydrodeoxygenation, dehydration, and hydrogenation to optimize yield and selectivity.

Over the past five to ten years, several one-pot or single-stage processes capable of converting lignins to cycloalkanes and alkylated aromatics have been described.[18,19,28,20–27] However, lignin-to-liquid fuel processes using pyrolysis and hydrogenolysis have been investigated for many years and earlier work has been summarized by Chum and Johnson.[29] Of

recent reports, hydrogenolysis and hydrodeoxygenation of birch organosolv catalyzed by Ru/Nb_2O_5 gave the best hydrocarbon yield of 30%.[23] The two highest yields for hydrocarbons from kraft lignins were 14%[27] and 17%[28]. The process conditions for both examples were relatively severe with the former having a reaction time of 40 h at 310 °C and the latter requiring 10 MPa hydrogen pressure at room temperature and 425 °C. Further, the U.S. Department of Energy has recommended carbon yields (C in fuel / C in feedstock) be greater than 50% for biomass-to-fuel processes. Many different multi-stage process have been suggested over the years as a way to increase overall yield, selectivity, and carbon economy.[30–32] A 1999 patent submitted by Shabtai *et al*. described a three stage process beginning with base-catalyzed depolymerization using sodium hydroxide and followed by two stages of hydroprocessing catalyzed by sulfided transition metals supported by alumina or aluminosilicates.[30] The patent reported that a 73% reformulated gasoline yield (on dry feedstock) was achieved when starting with kraft lignin. The conversion of the lignin polymer network to monomer, dimer, and trimer cycloalkanes is composed on many reactions. Using multiple stages allows for control and optimization of each set of reactions. Severe treatment of isolated lignins would likely favor recondensation but is necessary for cleavage of high energy aryl-aryl bonds and dehydration of phenolic compounds. The three-stage process was likely successful because the lignin structure was first fragmented and stabilized to prevent recondensation before the high temperature hydrocracking and hydrogenation stage. Most research has focused on the hydrodeoxygenation or hydrotreatment of lignin model compounds or pyrolysis bio-oil, but not enough attention has been paid to the initial depolymerization step, especially for the hydrogenolysis of technical lignins.

Recent lignin hydrogenolysis efforts have been summarized by extensive reviews, but it is difficult to draw conclusions when comparing studies that all use different lignin types, different evaluation methods, and/or insufficient characterization of feedstocks and product mixtures.[33] Comprehensive, systematic studies that include multiple technical lignins, catalyst systems, and detailed structural analyses are key to elucidating lignin-catalyst-product relationships. Furthermore, it is important for applied lignin research to focus on kraft lignins as the number of sulfite mills declines and the availability of isolated kraft lignins increases.[34] A few studies have recently been published that compare multiple lignins, including kraft, with good characterization of feedstock and product characterization.[35–38] However, in each case catalyst development and process condition optimization were performed for depolymerization of a model compound or a non-kraft lignin, and the optimum catalyst and conditions were applied to multiple lignins. Oasmaa *et al*. executed a proper screening experimental design that evaluated multiple kraft lignins, catalysts, and process conditions but chemical structural analyses were limited to monomeric products.[39]

Many studies on one-pot conversion of technical lignins to jet fuel resulted in low yield.[18,19,28,20–27] A two-stage process involving a first stage of converting technical lignins to oligomeric products by hydrogenolysis followed by a second stage of converting the oligomeric lignin products to hydrocarbons by hydrodeoxygenation may result in a much higher yield than the one-pot processes. In the current study, the first stage was explored by investigating the hydrogenolysis of three different technical lignin samples (pine kraft, hardwood kraft, and hardwood biorefinery) using three different catalyst systems with comprehensive structural characterization of feedstocks and products. Two of the catalysts were specifically designed for softwood kraft lignin depolymerization previously.[40,41] First, time, temperature, and pressure

effects on the hydrogenolysis of pine kraft and hardwood biorefinery lignins were investigated using one catalyst system. Second, all three lignin types were depolymerized with three catalyst systems at a midpoint process condition with in-depth product analysis to identify feedstock-catalyst-product relationships. Oligomeric products were evaluated for the potential as precursors for jet fuel-range hydrocarbons following subsequent hydroprocessing.

Materials and Methods

Purchased chemicals

Ethyl acetate, petroleum ether, 1,4-dioxane, methanol, and nitric acid were certified ACS and purchased from Fisher Chemical. Ruthenium on activated charcoal (5% Ru/C), deuterated dimethyl sulfoxide (DMSO-d6), deuterated chloroform, chromium(III) acetylacetonate, *N*-hydroxy-5-norbornene-2,3-dicarboxylic acid imide (97%) (NHND), and chloro-4,4,5,5-tetramethyl-1,3,2-dioxaphospholane (TMDP) were purchased from Sigma-Aldrich. Ammonium beta zeolite (SiO_2/Al_2O_3 = 25:1) and zinc acetate dihydrate (for ACS analysis) were purchased from Alfa Aesar. All chemicals were used as received except for 1,4-dioxane, which was prepared freshly prior to each use by refluxing over sodium hydroxide and sodium borohydride for one hour, then distilled to dry the solvent, reduce any peroxides, and remove stabilizer. Note that 1,4-dioxane should never be completely evaporated to prevent concentration of peroxides, which are heat and shock sensitive.

Lignin feedstocks

BioChoice® lignin (BCL) was produced at the Plymouth, North Carolina pulp mill and provided by Domtar, Inc. BCL is a pine, kraft lignin precipitated from black liquor using the

Lignoboost® process. BCL was thoroughly washed with deionized water to remove any remaining ash and air-dried prior to use. Mixed hardwood kraft lignin (HWK) was isolated using a pilot scale Lignoboost® process in Plymouth, NC from black liquor collected at a pulp mill in Hawesville, Kentucky. HWK was washed with deionized water upon receipt. Biorefinery lignin (HWAER) was generated at the Department of Forest Biomaterials at NC State University (Raleigh, NC) from the hydrothermal and enzymatic treatments of sweetgum wood chips.[42,43]

Catalyst preparation and characterization

Primarily three catalyst systems were used in this study: 1) a solid dual acid-base, $S_2O_8^{2-}$, K_2O/TiO_2, fed with 5% Ru/C (3:1 w/w); 2) cobalt and zinc (1:3 mol/mol) supported on a dealuminated beta zeolite (CoZn/DeAl H-beta); and 3) 5% Ru/C fed with zinc acetate. A fourth, Zn/DeAl H-beta, was prepared and tested to compare homogeneous and supported zinc catalysts. The dual acid-base catalyst and CoZn catalysts were provided by the Laboratory of Basic Research in Biomass Conversion and Utilization (University of Science and Technology of China, Hefei). Their preparation and characterization are extensively discussed elsewhere.[40,41,44] Briefly, the dual acid-base catalyst was prepared by wet impregnation of ammonium persulfate and potassium oxide precursors onto titanium dioxide followed by drying and calcining in air. The cobalt-zinc catalyst was prepared by solid-state mixing of acetate precursors with a dealuminated beta zeolite followed by calcining in air. Zn/DeAl H-beta was prepared similarly to CoZn/DeAl H-beta except cobalt acetate precursor was omitted. Zinc-to-zeolite (mol/g) ratio was unchanged. In brief, ammonium beta zeolite was converted to H-beta zeolite by calcining in air at 640 °C for 8 h. Dealumination was accomplished by treating the zeolite with 13 M nitric acid (20 mL g^{-1} zeolite) at 100 °C for 20 h. Dealuminated zeolite was washed with 40 mL nitric acid

followed by repeated washing with water and dried overnight at 120 °C. Zinc acetate dihydrate (138.94 mg g^{-1} zeolite) was ground with DeAl H-beta using a mortar and pestle to achieve a zinc loading of 0.633 mmol g^{-1} zeolite. Finally, the zinc acetate/zeolite mixture was heated in air to 550 °C at a rate of 5 °C min^{-1}, calcined for 5 h, and stored in a desiccator prior to use.

Hydrogenolysis of lignins

Hydrogenolysis experiments were carried out using a 300 mL 316 stainless steel batch reactor (Parr Instrument Company). Catalysts (0.4 g/g catalyst on lignin) were added to the reactor followed by 60 mL of solvent (1,4-dioxane and methanol mixture, 5:1 v/v). Prior to use, catalysts were dried in a vacuum oven at 80 °C overnight. They were not pre-reduced. The solvent system was selected to fully dissolve kraft lignins and provide *in situ* generation of hydrogen from methanol.[45] Methanol may serve an added function by helping to stabilize carbocation intermediates as observed during acid-catalyzed extraction of organosolv lignin from wood.[46] On the other hand, methanol has also been shown to inhibit hydrogenation at least when using Raney nickel in model compound experiments.[47] Air-dried lignin (0.9 oven-dried g, average moisture content of 5%) was finally added. After sealing the reactor, the headspace was purged three times with 2 bar of nitrogen followed by 10 bar of hydrogen three times and vessel pressure was increased to 20 bar or 40 bar after the third time. A heating mantle was used to increase the temperature to the desired setpoint under 300 RPM agitation with ramp times of 20 to 30 minutes. Reaction times were defined as the time spent at the temperature setpoint. To stop the reaction, the vessel temperature was reduced first by air cooling, submerged in hot water, and then ice-cold water. By this procedure, the temperature could be safely reduced from 280 °C to 100 °C in 10 minutes. The vessel was slowly vented once below room temperature after an

additional 50 minutes in the ice bath. A temperature and pressure profile of a typical run can be found in Appendix C (**Figure C.1**). For safety, it is important to perform regular leak tests with nitrogen, have installed an appropriately rated rupture disk or relief valve, and only open the reactor once the pressure is at 0 bar(g). Ruthenium on carbon will absorb a high amount of hydrogen and readily oxidize upon exposure to air so care should be taken when filtering and drying the catalysts, especially in the presence of flammable solvents.

Product work-up

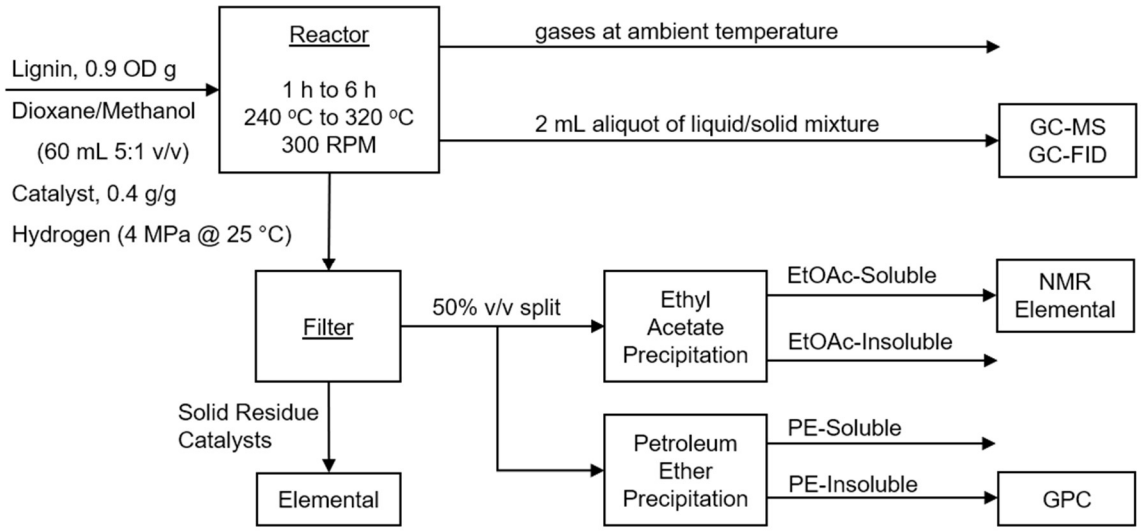

Figure 4.1. Process diagram for product work-up and analysis.

A schematic of the product work-up and analysis is presented in **Figure 4.1**. After gases were vented to atmosphere an internal standard was added and a 2 mL aliquot of the reaction mixture was taken and stored for GC analyses. The remaining reaction mixture was filtered using a fine glass-fritted filter and rinsed with the dioxane-methanol mixture. The resulting insoluble material (denoted as "solid residue") was dried overnight at 105 °C and weighed. The weight of

catalyst added to the reactor was subtracted assuming no catalyst leaching. Filtrate was adjusted to 200 mL and divided into two equal fractions. Solvent was removed from each fraction at 45 °C under 25 inHg vacuum using rotary evaporation. One fraction was redissolved into acetone and precipitated into 100 mL ethyl acetate, while other fraction was precipitated into 100 mL or more of petroleum ether. In many cases, more solvent was needed to achieve solid precipitation and avoid the formation of two liquid phases. Both suspensions were filtered and rinsed with their respective solvents and solids dried in a vacuum oven at 45 °C over phosphorous pentoxide prior to weighing. Solvent was removed by rotary evaporation to obtain dried ethyl acetate-soluble and petroleum ether soluble products and weighed. Methanol was used to co-evaporate ethyl acetate followed by dichloromethane to assist in evaporation of the methanol. Ethyl acetate soluble product is referred to as liquid product. The small amount of ethyl acetate-insoluble product was not characterized on its own. Instead, the petroleum ether-insoluble product, which contains any ethyl acetate-insoluble product, was characterized and defined as "oligomers". Petroleum ether soluble product was considered to represent monomeric and dimeric products (M_w < 500 g/mol). Mass balance calculations are in supplementary information, equations C.1 through C.5. Volatiles were not measured directly and estimated by subtraction; therefore, these values include mass balance errors in addition to the mass of volatiles generated.

Elemental and methoxyl analyses

Carbon and nitrogen contents of lignin, liquid product, and solid residue samples were measured using a Leco CN928 Analyzer. Sulfur compositions of acid-digested lignin samples were determined by ICP-OES (Perkin Elmer Corporation, model 8000). The samples were digested with heat, HNO_3, H_2O_2, and HCl.

The method for determination of methoxyl group content followed previous literature.[48] 20 mg oven-dried lignin was treated with 5 mL of 57% hydroiodic acid (HI) at 130 °C for 30 minutes in a sealed vial. Vials were cooled in hot water, then an ice bath to prevent shocking the glass and 100 µL of internal standard solution (97 mg mL^{-1} ethyl iodide in pentane) was added. The mixture was extracted with 10 mL pentane and the pentane phase was sampled and injected into a GC-FID (Agilent, 6890N) with a CP-Sil 13 CB column (25 m × 0.32 mm i.d. x 1.2 µm film). Helium at a flow rate of 1.1 mL min^{-1} was used as carrier gas. Inlet temperature was 110 °C and oven temperature was held at 40 °C for 2 min and then increased to 80 °C at 8 °C min^{-1}. Hydrogen and air with flow rates were 40 and 300 mL min^{-1}, respectively with a detector temperature of 150 °C.

Nitrobenzene oxidation

Syringyl to vanillyl group ratio was estimated by nitrobenzene oxidation (NBO) according to Min *et al*.[49] 50 mg lignin was placed into a stainless-steel bomb reactor along with 7.0 mL NaOH and 0.4 mL nitrobenzene. The bomb was heated at 170 °C for 2.5 h and shaken every half hour. Cold water was used to quench the reaction. 1.0 mL of internal standard (16 mg mL^{-1} 5-iodovanillin in 1,4-dioxane) was added, and the mixture was extracted with 30 mL dichloromethane three times collecting the aqueous phase. After acidifying the solution to a pH of 2, dichloromethane extraction was performed again. The organic phase was collected and dried using anhydrous sodium sulfate. The isolated products were silylated and analyzed using GC-FID (Agilent, 6890N) with an HP-1 column (30 m x 0.32 mm x 0.25 µm). Helium at a flow rate of 2.0 mL min^{-1} was used as carrier gas. Inlet temperature was 200 °C and oven temperature was held at 120 °C for 3 min, increased to 200 °C at 5 °C min^{-1}, and finally increased to 260 °C

and held for 5 minutes. Hydrogen and air with flow rates were 40 and 300 mL min^{-1}, respectively with a detector temperature of 270 °C.

Molecular weight distribution

Relative molecular weight distributions of lignins and depolymerized products were obtained using a gel permeation chromatography (GPC) instrument (Shimadzu). Samples were first acetylated to improve solubility by dissolving 100 mg dried sample in a 1 mL mixture of acetic anhydride and pyridine (1:1 v/v) and reacted at room temperature for 48 h in a sealed vial under nitrogen.[50] The reaction mixture was added to 20 mL ice-cold dilute hydrochloric acid (0.1 N) and shaken every few minutes to precipitate acetylated lignin and convert excess acetic anhydride. The suspension was filtered using a fine, glass-fritted filter and washed three times with cold, 0.1 N HCl, followed by cold, deionized water to remove acetic acid and pyridine.[51] The solids were dried overnight in a vacuum oven at 45 °C over phosphorous pentoxide, dissolved in tetrahydrofuran at a 1 mg/mL concentration, and separated by GPC using two columns in series (Styragel HR 1 7.8 x 300 mm and Styragel HR 5E 7.8 x 300 mm) at a flow rate of 0.7 mL/min and oven temperature of 35 °C. The UV detector was set to measure absorbance at a wavelength of 280 nm. Monodisperse polystyrene standards were used for calibration.

Monomer and dimer characterization

An aliquot of the reaction mixture was filtered and silylated prior to injection into a GC-MS instrument (Agilent 7820-5977) equipped with a HP-5 MS column. (30 m × 0.25 mm i.d. x 0.25 μm). Helium at a flow rate of 1.0 mL min^{-1} was used as carrier gas. Inlet temperature was

270 °C and oven temperature was held at 40 °C for 3 min and then increased to 260 °C at 10 °C min^{-1} and held for 10 minutes. The MS source and quad temperatures were 230 °C and 106 °C.

Nuclear Magnetic Resonance (NMR) analyses

The methods for collecting two-dimensional heteronuclear single quantum coherence (HSQC) and one dimensional quantitative ^{13}C NMR spectra of lignin samples are described in Chapter 3.[52] 2D HSQC experiments of liquid products were performed using the same procedure. Phosphorous-31 NMR spectroscopy was performed based on a published protocol and spectra were collected using a 500 MHz Bruker Avance III magnet equipped with a 5 mm BBO room temperature probe.[53]

Results and Discussion

Lignin feedstock properties

BCL and HWAER were characterized previously and HWK lignin was characterized for this study using the above methods (**Tables 4.1 to 4.3**).[42,43,54–56] Only 30% by weight of HWAER could be dissolved and analyzed for solution-state methods (GPC, NMR) given the high average molecular weight, while 100% of kraft lignin samples were analyzed. AER-soluble (AER-S) is used to denote data that corresponds to the soluble portion.

BCL and HWK are both dissolved kraft lignins that were isolated from black liquor at an industrial scale using CO_2 precipitation. HWAER was produced at laboratory-scale and represents lignin typical of a biorefinery process using hot water or autohydrolysis biomass pretreatment. HWAER contained more carbohydrates than either BCL or HWK, which had high lignin contents of 96.5% by dry weight each (**Table 4.1**). Syringyl-type and guaiacyl-type

monomer ratio were similar between sweetgum and HWAER, as compared to the difference observed between the two kraft lignins and their wood source (**Table 4.2**). HWAER retained more carbohydrates and had similar repeat units to the corresponding wood because hot water pretreatment is less severe than the kraft process. NBO yield and phosphorus-31 NMR results also support this conclusion. Decreased NBO monomer yields indicate that the kraft lignins are more condensed than in wood (**Table 4.2**). Higher total phenolic hydroxyl group contents of kraft lignins than HWAER can be attributed to the higher degree of aryl-ether interunit linkage cleavage (**Table 4.3**). It may be possible to depolymerize HWAER to a greater extent or under less severe conditions given the lower bond dissociation energy of ether linkages compared to aryl-aryl carbon-carbon bonds.

Kraft lignin molecules have a lower average molecular weight because of the fragmentation that occurred during the pulping process, which allows for higher solubility in organic solvents like dioxane, dimethyl sulfoxide, and ethyl acetate. Only 3% of HWAER was soluble in ethyl acetate compared to 15% of BCL and 50% of HWK, which is comprised of smaller molecules than BCL on average. It was predicted that HWAER molecules would have restricted access to active sites on the catalyst surface because of solubility and mass transfer limitations.

The low ash contents of the two hardwood lignins is most likely a desirable property for efficient biomass conversion by heterogenous catalysis (**Table 4.1**). For the kraft lignins this is advantageous as ash is partly comprised of sulfate salts, which will be reduced to sulfides that will readily deactivate platinum group metal catalysts, even in small concentrations.[57,58] Similarly, organic sulfur in the form of thiol groups contained within the kraft lignin structure may lead to catalyst deactivation through poisoning. HWAER did not have a measurable ash

content. No inorganics were used during pretreatment to react or bond with sweetgum lignin, and any ash contribution from the wood was probably removed during filtration and washing.

Table 4.1. Compositions of isolated lignins and corresponding extractive-free wood (w/w %).

Component	Sweetgum		Mixed Southern US Hardwoods[a]		Southern Pine[a]	
	Wood[59]	HWAER[42]	Wood[59]	HWK	Wood[60]	BCL[54]
Carbohydrates	75.6	12.2	74.0	0.6	66-69	2.0
Lignin[b]	24.1	81.9	25.5	96.5	27-30	96.5
Ash	0.3	< 0.1	0.4	0.4	< 0.5	1.4
Others[c]	-	5.9	-	2.5	2-4	0.1
Lignin Yield[d]	-	83	-	37	-	66

a. Mixed southern hardwood percentages are based on an approximation of eastern Tennessee species. HWK is from black liquor produced at a Kentucky mill. Loblolly pine (*Pinus taeda*) figures are used to represent typical pulpwood for the Plymouth, NC mill where BCL is produced.

b. Defined as the sum of acid-insoluble (Klason) and acid-soluble lignin.

c. Mass contribution of other groups or constituents like uronic anhydrides, acetyls, and pectin.

d. Based on lignin in wood. BCL and HWK assumes 97% lignin in wood goes to black liquor and a previous lignin precipitation study was used to estimate subsequent recovery of kraft lignin from black liquor precipitated at pH 9.5.[61]

Table 4.2. Abundances of substructures and inter-unit linkages of wood or MWL[a] and isolated lignins.

Component	Sweetgum		Mixed Southern US Hardwoods		Southern Pine[54]	
	Wood	AER-S	Wood[e]	HWK	Wood	BCL
S/V[b]	2.86[55]	2.62[55,c]	2.86	1.75	ND	ND
S+V yield, mmol/g	3.10[55]	2.76[55,c]	3.10	0.743	3.08	1.34

Table 4.2 (continued).

Methoxyl / C_9	1.55	not avail.	1.55	1.11	0.95	0.74
β-O-4’	49.1[55]	16.3	49.1	2.1	41	2.2
β-5’	3.6[55]	2.7	3.6	0.1	9	1.6
β-β’	7.7[55]	9.6	7.7	1.2	4	6.0
Stilbenes	-	1.8	-	1.9	-	7.3
Lignin yield[d], %	-	83	-	37	-	66

a. Wood was used to find S and V values, but the remaining data were collected by solution-state methods so milled wood lignin (MWL) samples were used.

b. As determined by nitrobenzene oxidation; S = Syringaldehyde + Syringic Acid; V = Vanillin + Vanillic acid.

c. Solid residue following hydrothermal pretreatment. Solids recovered after enzymatic hydrolysis (HWAER) were not analyzed by NBO.

d. Based on lignin in wood. BCL and HWK assumes 97% lignin in wood goes to black liquor and a previous lignin precipitation study was used to estimate subsequent recovery of kraft lignin from black liquor precipitated at pH 9.5.[61]

e. Values assumed to be like sweetgum, as that is one of the main southern US hardwood species.

Table 4.3. Hydroxyl contents of lignin samples (mol per 100 mol aromatic unit).[a]

Sample	Aliphatic	Phenolic				
		Di-substituted	Mono-Substituted	Non-Substituted	Total	Catechol
BCL[56]	36.7	35.3	39.5	3.0	77.8	10.4
HWK	25.2	55.2	21.6	ND	76.8	19.3
AER-S[56]	86.2	37.2	10.8	0.6	48.6	ND[b]

a. All data obtained by phosphorus-31 NMR spectroscopy except catechol, which was determined by a colorimetric method.[54]

b. ND = Not determined. Expected to be very low, if any, considering the absence of a good nucleophile during hot water treatment and enzymatic hydrolysis treatments.

Catalyst properties

The preparation and characterization of the $S_2O_8^{2-}$-K_2O/TiO_2[40,44] and CoZn/DeAl H-beta[41] catalysts were described in previous publications and their properties are summarized here along with Zn/DeAl H-beta that was prepared for this study (**Table 4.4**). Both catalysts were designed for optimized depolymerization of a softwood kraft lignin (Indulin® AT) to phenolic monomers through hydrogenolysis. Note that BCL and Indulin AT have similar properties.[54] $S_2O_8^{2-}$-K_2O/TiO_2 was designed to take advantage of acid- and base-catalyzed routes in the fragmentation of the lignin structure combined with an effective hydrogenation catalyst (Ru/C) in a reductive environment to limit competing recondensation reactions. Dual acid-base to Ru/C ratio was kept at 3:1 w/w. This system is hereafter abbreviated as DAB-Ru. For the second system, CoZn/DeAl H-beta was used as the sole catalyst having both reductive (Co) and acidic (Zn) active sites supported by a dealuminated beta zeolite (abbreviated CoZn hereafter). Full dealumination followed by incorporation of zinc into the zeolite framework was performed to reduce support acidity in a controlled manner. A Co:Zn molar ratio of 1:3 mol mol^{-1} was experimentally determined to be the most effective in terms of lignin conversion to monomers and dimers and was also used in this study. Thirdly, Ru/C was combined with zinc acetate (ZnAc) to screen the effect of ruthenium versus cobalt and compare a stronger acid, persulfate, with zinc (RuZnAc system, Ru:Zn = 1:3 mol mol^{-1}). Ru/C and ZnAc were used as received for these tests. Finally, two tests using Zn/DeAl H-beta and Ru/C were conducted to observe any differences between the homogeneous and heterogeneous zinc catalysts. The zinc loading on zeolite was unchanged from the CoZn system and Ru/C was charged to the reactor to maintain a 1:3 molar ratio of Ru to Zn.

Table 4.4. Catalyst concentration, active site estimation, and surface area.

Catalyst	Species	Conc. (mmol/g)	Acidic Sites[a] (mmol/g)	Basic Sites[a] (mmol/g)	Reductive Sites[a] (mmol/g)	Surface Area[b] (m^2/g)
$S_2O_8^{2-}$-K_2O/TiO_2[40,44]	$S_2O_8^{2-}$	0.48	2.31[c]	1.19[c]	-	50
	K_2O	1.70				
CoZn/DeAl H-beta[41]	Co	0.211	0.49	-	1.05	520
	Zn	0.633				
Zn/DeAl H-beta	Zn	0.633	1.0	-	-	513
Ru/C	Ru	0.412	-	-	6.7	687

a. As determined by temperature programmed desorption (TPD) using NH_3, CO_2, and H_2 for acid, base, and reductive site quantification, respectively.

b. As determined by nitrogen adsorption and Brunauer-Emmett-Teller (BET) theory.

c. The catalyst loadings used in reference (*40*) are used in the current study, but NH_3-TPD was not performed. Instead, catalysts with a range of loadings were analyzed in reference (*44*) and the results were interpolated to match the loadings used.

$S_2O_8^{2-}$-K_2O/TiO_2 total acidity was 4.7 times that of CoZn with 65% more active sites for a higher acid density as well. Assuming a monolayer and that 2 mol NH_3 were adsorbed per mol persulfate, potassium oxide is calculated to adsorb 1.4 mol ammonia per mol. The adsorption of ammonia on zinc was about 2 mol ammonia per mol for Zn/DeAl H-beta catalyst, which was quite a bit higher than reported for CoZn catalyst. Two independent tests confirmed this. It is possible that dealumination was incomplete or that physiosorbed ammonia gas was not completely removed prior to TPD. Potassium oxide was the only basic species tested in this study and had 1:1 adsorption with CO_2. Only CoZn and Ru/C catalysts should have reductive activity and Ru/C has a much higher capacity, though TPR indicated much higher than

stoichiometric chemisorption for both catalysts. Hydrogenation catalysts are well known to have high hydrogen sorption capacities due to the spillover effect.[62]

Acids and bases are both capable of lignin interunit-unit cleavage as well as promotion of recondensation and solid catalyst coking, which has motivated many efforts to maximize the former and minimize the latter.[63–68] Catalyst deactivation through coking is recognized as one of the main technological challenges hindering the development of biomass conversion processes.[9] Mechanisms of coke formation and the design of coke-resistant catalysts have been the subject of numerous studies.[9,69–71] The role of acids is particularly interesting and not straightforward. Both Lewis and Brønsted acids can lead to coke formation through carbocation intermediates, but many reactions necessary for the depolymerization of lignins are acid-catalyzed (transalkylation, dehydration, and hydrogenolysis).[6,9] Centeno and co-workers concluded that Lewis acid sites catalyzed the re-condensation of guaiacol leading to deactivation.[69] In another case, Lewis acid sites were thought to be responsible for coke prevention.[72] Most likely acid site density, strength, type, and process conditions all have an impact on the role of acids in catalyst deactivation. Beta zeolite acidity was moderated by dealumination followed by incorporation of zinc into the framework, resulting in a lower total acidity.[41] Complete removal of acid sites limited depolymerization and some zinc was needed to improve monomer and dimer yields. Model compound studies demonstrated that zinc likely serves as a Lewis to catalyze the hydrogenolysis of aryl-ether inter-unit linkages by adsorption of hydroxyl groups.[73,74] It is hypothesized that this route will be especially applicable to HWAER lignin, which has a higher abundance of β-O-4' bonds (**Table 4.2**). Co or Ru redox metals were included in the catalyst systems to suppress recondensation pathways towards coke and char through the reduction of unsaturated moieties and carbocation intermediates.

All catalyst samples showed a typical N_2 adsorption-desorption isotherm (**Figures C.2** and **C.3**). Under the pressure $P/P_0 = 0.6$ to 1.0, the amount of N_2 adsorbed increased, indicating the successful formation of holes in all samples. BET surface area of Zn/DeAl H-beta increased after the incorporation of Zn, implying that Zn is well dispersed in the lattice vacancies of H-beta (**Table C.1**). At the same time, the overall pore size distribution has not changed significantly after the introduce of Zn, and Zn/DeAl H-beta maintains the original structure.

Accessibility of the active sites is challenge in biomass conversion given the large molecules involved, therefore, catalyst textural properties are important to consider. High surface area may not be as important as large pore size or quantity of sites on the external instead of the internal surface area of a catalyst. Titanium dioxide did not have a high surface area relative to the other supports investigated in this study (**Table 4.4**). Activated charcoal had the highest surface area and smallest average pore size with dealuminated beta zeolite falling in between. Zeolites are of interest in biomass conversion for their water resistance and tunability in terms of acidity and pore size. Yu and coworkers demonstrated the shape selectivity of zeolites in pyrolysis different woods.[75] ZSM-5 was unable to convert some bulkier, syringyl-type lignin fragments (e.g. syringol and pyrogallol), while H-beta, with the highest ratio of external to internal surface area and second highest total surface area of the zeolites studied, was ideal for converting bulkier substrates unable to diffuse into the pores.

Effect of process conditions on lignin hydrogenolysis

BCL and HWAER were treated using the DAB-Ru catalyst system at various times, temperatures, and hydrogen loadings to determine impact on hydrogenolysis of these two different lignin feedstocks (**Table 4.5**). Hydrogen loading is given as the initial pressure of pure

hydrogen in the batch reactor at room temperature. The midpoint conditions of 280 °C and 3 h was run in duplicate to check for replicability for both BCL (2 MPa H_2 and 4 MPa H_2) and HWAER (4 MPa H_2).

Time and temperature were varied to simulate different process severities like the H-factor used in wood pulping.[76] In that case, a first order reaction is assumed to sufficiently model the many reactions involved during the pulping process. A similar methodology was considered in the present study but was not successful in modeling the conversion of lignin (**Figure C.4** and **Figure C.5**).[77] Instead, multiplying time and temperature was used to create a simplified severity factor for data visualization and was not intended to signify any fundamental kinetic or thermodynamic properties of the depolymerization reaction network. Nevertheless, this simplified severity factor was used to extract useful information and could be used to plan future experiments.

Table 4.5. Hydrogenolysis process conditions exploring time, temperature, and pressure effects.[a]

Lignin	Times, h	Temperatures, °C	H_2 Pressure, MPa
BCL	1	260, 300, 320	2, 4
	3	280	2, 4
	6	260, 300, 320	2, 4
HWAER	1	260, 300	4
	3	280	4
	6	260, 300	4

a. Lignin: 0.9 OD g; catalyst loading: 0.4 g/g; solvent: 60 mL dioxane/methanol (5:1 v/v); impeller: 300 RPM.

Doubling hydrogen charge used in the hydrogenolysis of BCL decreased solid residue formation for all time-temperature combinations by an average of 60% (**Figure 4.2**). Solid

residues were thought to be comprised of high molecular weight condensed lignin fragments and polyaromatic hydrocarbons (coke) based on insolubility, color, though detailed characterization was not performed. Almost all solid residues were black in color with high carbon contents, indicative of a coke-like structure (**Table C.3**). The degree to which solid residue decreased was directly related to temperature. In other words, an interaction existed between hydrogen loading and temperature whereby the same increase in hydrogen loading was more effective at higher temperatures in the prevention of coke formation. This interaction effect was more apparent when analyzing the yields of monomers and dimers.

Below 300 °C a change in hydrogen loading had no impact on the weight of monomers and dimers generated for severity factors of 260, 840, and 1560 (**Figure 4.2**). The reduction activity of ruthenium, and other transition metals, is directly related to temperature and a minimum temperature must be reached for reduction to occur. Note that catalysts used in this study were not pre-reduced prior to using and the liquid-gas reaction system added an additional barrier to ruthenium oxide reduction through mass transport limitations. Increased temperatures may have lowered barriers to mass transport and reduction, thereby increasing the number of adsorbed and dissociated hydrogen atoms available for hydrogenation of unsaturated side chains and phenolic carbocations. This is only one explanation for the observed trends given the complexity of this reaction system and other phenomena are likely involved. Whereas in this study hydrogen pressure had little effect on monomer/dimer yield across numerous time-temperature conditions, that is effect is not a given. Li *et al.* observed a reduction in petroleum ether soluble products with increased hydrogen charge, which was explained by the stabilization of molecules against further degradation as well as further recondensation.[78] It cannot be assumed that a greater hydrogen charge is needed or will have the intended effects. A pressure of

4 MPa hydrogen was selected in the present study as it did not have a negative impact on monomer/dimer yield and had a positive role in reducing solid residue.

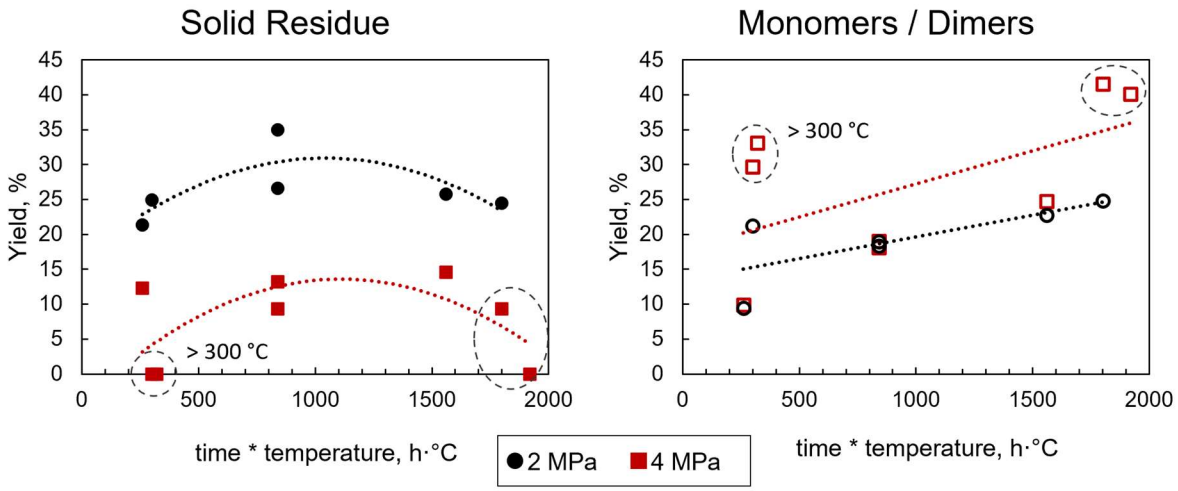

Figure 4.2. Effect of charged hydrogen pressure on solid residue and monomer / dimer yields. Note that at 840, there are two data points for 2 MPa and two data points for 4 MPa, indicating a high level of reproducibility.

Next, HWAER was subjected to treatment under 4 MPa H_2 at multiple time-temperature points to compare the effects of varying process conditions against those observed for BCL. Solid residue yields ranged from 3% to 8% for HWAER and 0% to 15% for BCL as percent weight of initial dry lignin (**Figure 4.3**). The lowest yields for HWAER were observed when reaction temperatures were greater than or equal to 300 °C. This relationship with temperature was not as strong as that observed for BCL. BCL was converted to a negligible amount of residue at 300 °C after 1 h of reaction time and to 12.3% at 260 °C after 1 h; conversely, HWAER was converted to 4.3% and 4.8% at these two conditions, respectively. HWAER is partially comprised of syringyl-type units that are less prone to recondensation reactions than the

guaiacyl-type units that make up BCL. Fewer opportunities for deactivation pathways may have limited the impact that temperature could have on activating ruthenium towards already stable HWAER molecules.

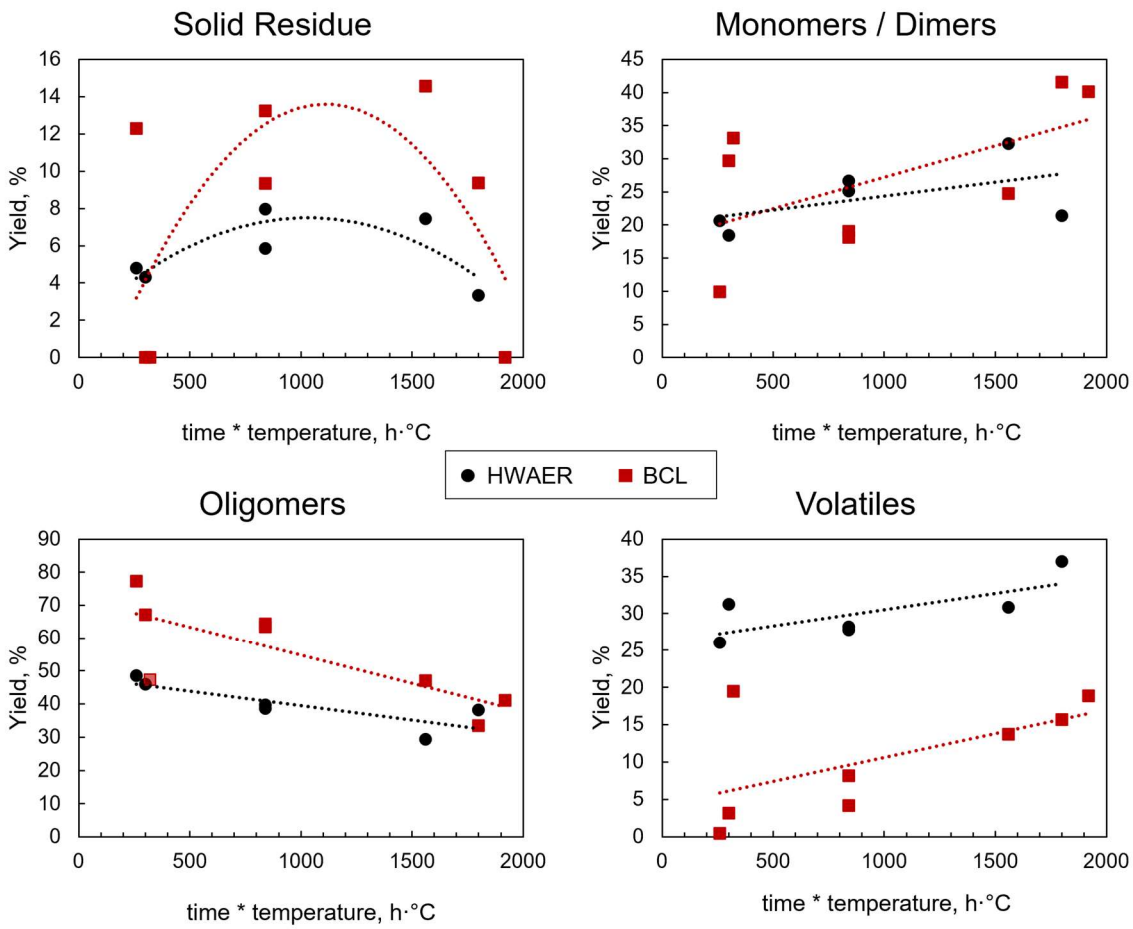

Figure 4.3. Effect of time and temperature on product yields (wt %) for HWAER (black circle) and BCL (red square). Time * Temperature is used as a simplified severity factor for displaying data. Trend lines are solely for clarity and do not imply any mechanistic behavior.

The yields of low weight compounds like monomers, dimers, and volatiles generally increased with increasing severity while oligomers decreased for both HWAER and BCL lignins

(**Figure 4.3**). The distinction in mono/dimer yield at or above 300 °C observed for BCL was not observed for HWAER. The higher monomer yield at or above 300 °C for BCL was explained by an increase in ruthenium activity in a previous section, but this should also apply to HWAER. Chemical structure difference between the two types of lignin may offer an explanation. BCL interunit linkages are predominantly carbon-carbon bonds, while HWAER has a higher proportion of ether linkages that have a relatively lower bond dissociation energy. It was necessary to provide sufficient energy to the reaction system for BCL C-C bonds to be cleaved and produce additional low molecular weight molecules. The low temperature of 260°C was sufficient for depolymerization of the HWAER structure. In fact, at the highest severity of 1800 (300 °C, 6 h) the production of monomers and dimers from HWAER decreased.

This yield reduction was curiously accompanied by an increase in both oligomers and volatiles and a decrease in solid residue. If conditions were so harsh as to degrade monomeric compounds to volatiles through ring opening and cracking reactions, then only volatile yield should have gone up. If recondensation was favored, then an increase in solid residue should have been observed. Primary monomeric and dimeric products apparently proceeded to secondary products by two different major pathways: one to volatiles and one of partial recondensation to oligomers and not recalcitrant polycyclic aromatics. These data provide evidence of the many competing reactions that occur during hydrogenolysis of lignins.

Monomer/dimer product distribution

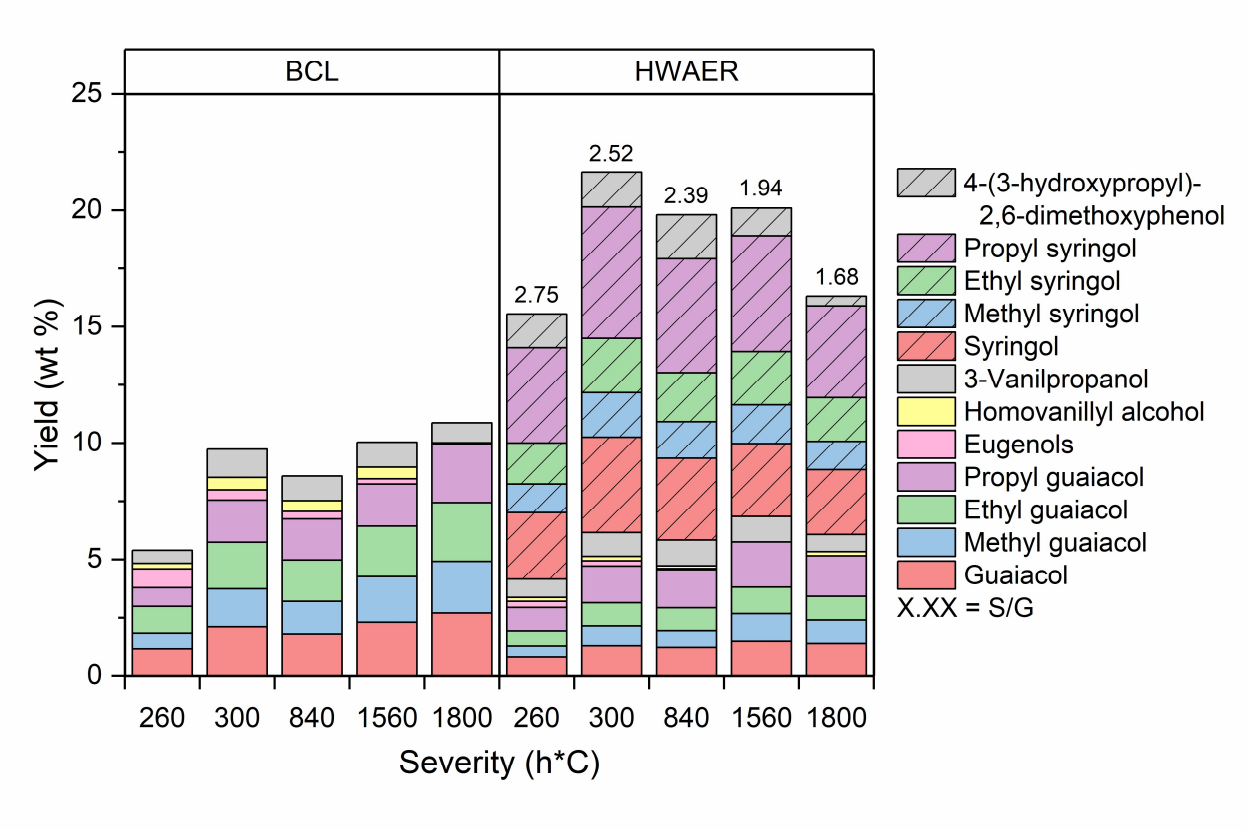

Figure 4.4. Major monomeric products using the DAB-Ru catalyst system as a function of hydrogenolysis severity at 40 bar H_2. Yields were determined semi-quantitatively based on weight of starting lignin.

Major monomeric products shown in **Figure 4.4** accounted for 90% ± 5% of the GC peak area. Primarily, the compounds obtained from both types of lignin were alkylated phenols, guaiacols (BCL and HWAER) and syringols (HWAER). Full results can be found in Appendix C (**Table C.2**). Monomer yield increased with increasing severity for BCL and increased except for the most severe condition for HWAER following the trend observed for petroleum ether soluble yield. Increased severity was selective towards alkylated phenols as the portion of compounds with aliphatic alcohol and unsaturated (eugenols) side chains decreased likely due to

hydrogenation and dehydration reactions. For HWAER, the total amount of syringyl moieties decreased steadily as the severity of the reaction increased from 300 to 1800, whereas the total amount of guaiacyl moieties remained relatively constant. Furthermore, the yield of volatile compounds increased with increasing severity. These results suggest that monomeric and dimeric syringyl moieties are more prone to degradation (most likely to volatile compounds) than those of the guaiacyl moieties. The low number of different species generated would facilitate downstream separations efforts. Additionally, these data suggest that the liquid product may have a higher energy density and storage stability given the low quantities of monomers containing primary or secondary alcohols or unsaturated side chains, which is ideal for conversion to liquid transportation fuels.

Interactions of multiple catalyst systems and lignin structures

Wood species, isolation method, and catalyst were selected to explore interactions amongst these three variables. Specifically, three lignin-rich feedstocks (BCL, HWK, and HWAER) were subjected to hydrogenolysis at 280 °C for 3 h with 40 bar H_2 using three catalytic systems (DAB-Ru, CoZn, and RuZnAc). The objective was to identify effects of lignin chemical structure on depolymerization routes and products and identify interactions between feedstock structure and catalyst properties. The DAB-Ru and CoZn catalyst systems were previously designed and optimized for the degradation of a softwood kraft lignin to monomers or dimers in a similar experimental set-up and it was of interest to see how their performance was affected by different starting materials. A third system, RuZnAc, was included to compare cobalt and ruthenium as redox catalysts in the hydrogenolysis of different lignin types. Reaction conditions were selected as a midpoint in the range typical for reductive liquefaction processes and were

relatively mild in terms of other thermochemical conversion processes (e.g. pyrolysis and gasification). Each reaction mixture was fractionated and classified into three product groups of solid residue, oligomers, and monomer/dimers with the balance defined as volatile products like the previous section (**Figure 4.5**). Yields were calculated in terms of total dry feedstock material, not only lignin.

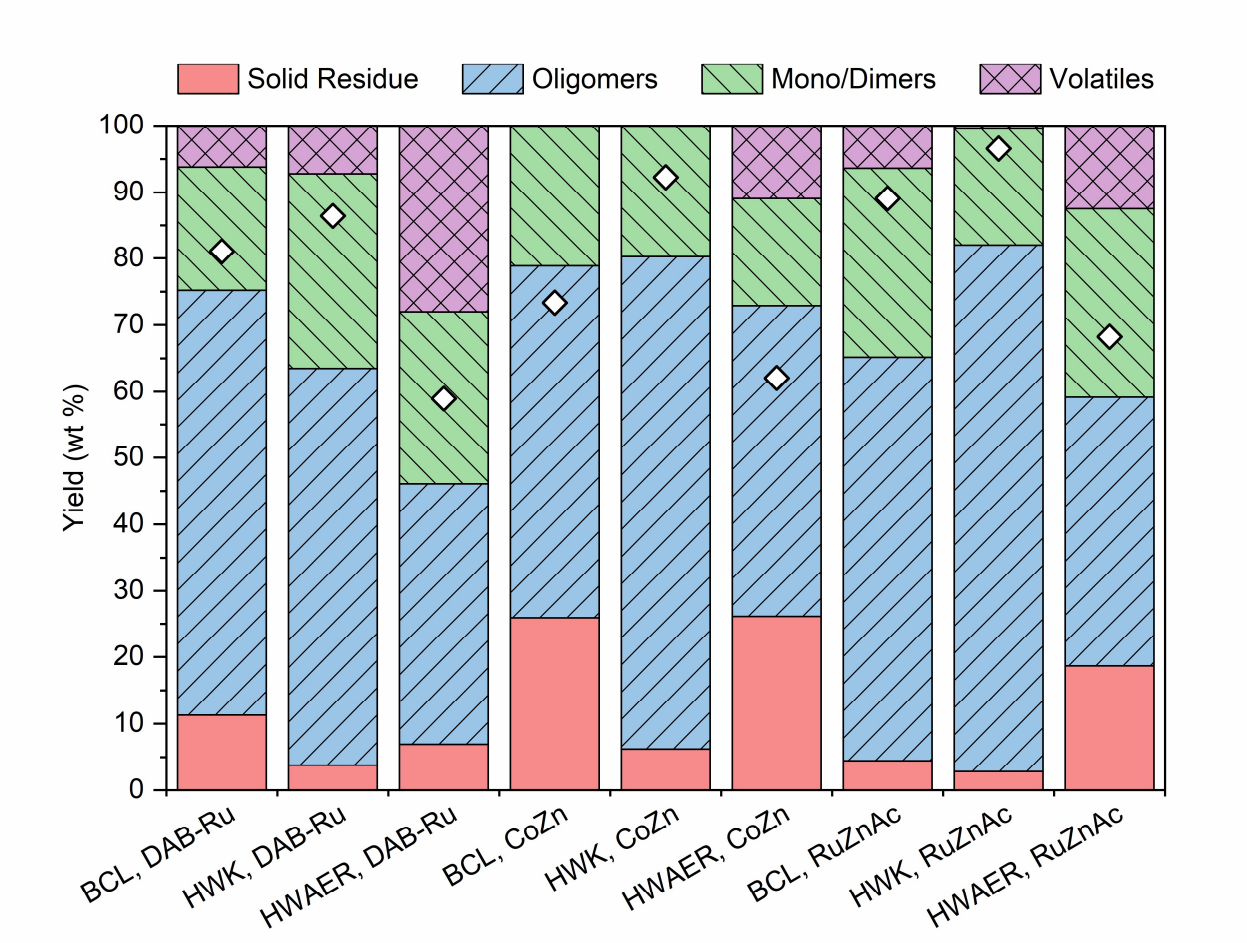

Figure 4.5. Product distribution for three lignin feedstocks depolymerized by three different catalyst systems at 280 °C for 3 h. Yields are given as weight percentages on the starting material. DAB-Ru = dual acid-base catalyst, $S_2O_8^{2-}$-K_2O/TiO_2, combined with 5% Ru/C; CoZn = CoZn/DeAl H-beta; RuZnAc = 5% Ru/C mixed with zinc acetate. Diamond symbol: ethyl acetate soluble product.

Distribution of bulk products

After filtering out solid residue, solvent was evaporated from the filtrate. The resulting oil was precipitated into ethyl acetate as a quick screening test for extent of depolymerization. Original BCL, HWK, and HWAER feedstocks were 18%, 54%, and 4% soluble in ethyl acetate, respectively. These solubilities increased to an average of 81%, 92%, and 63% for BCL, HWK, and HWAER following hydrogenolysis across all runs. The median amount of liquid product insoluble in ethyl acetate was 0.8%, so the balance was mainly comprised of solid residue and volatile compounds. The two kraft lignins had similar liquid product yields when using DAB-Ru or RuZnAc catalysts but not CoZn. Ruthenium can be reduced to metal at temperatures used in this study (250 °C), whereas cobalt is only reduced to the zero valent state above 800 °C.[79] The increased rate of hydrogenation was needed to stabilize carbocation intermediates formed through hydrogenolysis of guaiacyl-type fragments of BCL before recondensation occurred. Conversion of BCL to solid residue in the absence of a strong hydrogenation catalyst limited liquid product production. HWK was largely unaffected by changes to the catalyst system at the condition tested with high liquid, low solids, and low volatile yields throughout. This type of lignin was already highly soluble in ethyl acetate (corresponding to a lower average molecular weight) and syringyl-type units probably prevented recondensation allowing hydrogenolysis pathways to be favored.

Greater than half the mass of HWAER was converted to monomers, dimers, and volatiles when treated with DAB-Ru catalyst. The catalyst system was effective at depolymerization of the biorefinery lignin to the point of limiting liquid product production. CoZn and RuZnAc yielded fewer volatile products and more than 2.5 times the amount of solid residue, indicating these catalysts were relatively ineffective at HWAER depolymerization at the condition tested.

Acid and base sites of DAB-Ru appeared to be essential to deconstruct the HWAER polymer network. Solid residue yield from HWAER did not decrease when using ruthenium versus cobalt as it did for BCL. Residue might not have formed by condensation and dehydration to coke but may have instead been due to limited depolymerization of lignin, which would explain the lighter brown color compared to the black color of kraft lignin-derived solids. Reaction time was increased from 3 h to 6 h using RuZnAc to see if HWAER solid residue could be converted to a liquid product. In fact, residue increased slightly to a yield of 19.5% by weight of starting lignin. Total oil production remained unchanged as oligomer yield decreased from 41% to 30% with a corresponding increase of monomers and dimers to 40.4%. This indicated that while the residue of HWAER following hydrogenolysis over RuZnAc catalyst may be rather recalcitrant, the lighter fractions may be subjected to further depolymerization in subsequent processing stages, for example, hydrotreatment.

DAB-Ru was effective at limiting solid residue formation and promoting interunit cleavage of HWAER lignin, while CoZn and RuZnAc were less effective. Hydrogenolysis of HWAER using DAB-Ru would be the preferred process for high production of aromatic monomers among the catalyst-lignin combinations tested. Furthermore, it was previously shown that this yield could be optimized by a lower temperature and longer reaction time (**Figure 4.3**). The use of CoZn did not generate any volatile losses from kraft lignins and did not produce much residue from HWK, but RuZnAc was effective at depolymerization with limited recondensation of both types. HWK and RuZnAc would be the best system to use in a two-step scheme of lignin to jet fuel of the nine combinations tested for the high total yield of oligomeric products and high liquid product carbon yield (around 100% due to low solids and volatile yields) (**Table C.3**). In such a system, oligomeric products could be separated from lightweight

compounds for further processing, because it is expected that additional hydrogenolysis would take place in a hydrotreating step. The oligomeric fractions from each lignin-catalyst combination were characterized to predict potential for downstream conversion to jet fuel-range hydrocarbons. In addition, a deeper characterization of the whole liquid product should reveal chemical structural changes not derivable from monomer characterization alone.

Oligomeric product characterization

Oligomeric fractions of reaction mixtures were analyzed by GPC to better determine the extent to which each lignin type was depolymerized by different catalysts at the midpoint conditions of 280 °C and 3 h. (**Figure 4.6**). Overall, oligomeric products had a rather consistent weight-average molecular weight of 1500 g-mol^{-1} with relatively low dispersities (M_w/M_n) compared to feedstocks. Most molecules were comprised of less than 8 aromatic units assuming 180 g-mol^{-1} for one aromatic unit, though the actual value is probably less following demethylation, demethoxylation, and side chain displacement. GPC analyses verified that oligomeric products were significantly degraded compared to the corresponding starting lignins. The large reductions in weight-average molecular weights suggest that interunit cleavage occurred throughout the lignin structure and not only through loss of monomers from polymer end units. It would be useful to estimate the number and location of bonds cleaved as is possible with synthetic, linear polymers, but the nature of lignin structures precludes such an estimation. Regardless, any of the oligomeric fractions analyzed would serve as good feedstocks for hydrotreatment to diesel- or jet fuel-range hydrocarbons (C_8 to C_{16}) assuming further interunit cleavage and side chain losses at the more severe conditions given the starting average molecular weights. The other important factor to consider is oligomer yield.

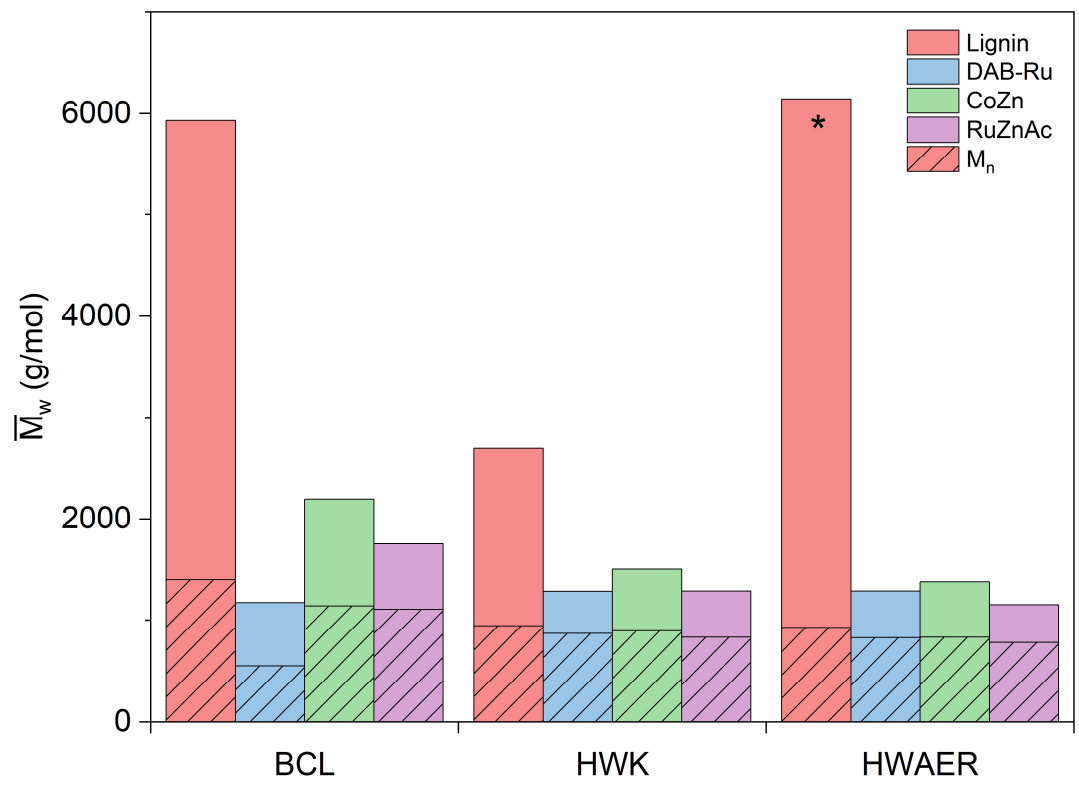

Figure 4.6. Molecular weight distribution for starting lignins and oligomeric products following hydrogenolysis for DAB-Ru, CoZn, and RuZnAc catalysts given in weight-average (total column) and number-average (shaded portion) molecular weights. *HWAER is only 20% soluble in THF, even after acetylation, so the actual average molecular weight is much higher.

Oligomers derived from HWK when processed with CoZn or RuZnAc would be the most suitable for further processing given the high yield (74% and 79%) and weight-average molecular weights (1510 g-mol^{-1} and 1290 g-mol^{-1}). HWAER underwent the highest degree of depolymerization, although the conversion to oligomers was low with high solid residue formation as described previously. BCL did not appear to be suitable after processing at 280 °C for 3 h, but the yields at 300 C for 1 h did seem ideal with high conversion to oligomers, non-detectable solids, and less than 5% volatiles. Process conditions may also be optimized for

HWAER, though the evidence presented so far suggests that monomer and dimer production is the best use of this feedstock. The biorefinery hardwood lignin monomer and dimer yields were limited when using DAB-Ru and CoZn catalysts because of high volatile losses or solid residue losses, respectively. Replacement of cobalt with ruthenium reduced solid residue losses, likely due to increased hydrogenation and hydrogenolysis activity that prevented recondensation and promoted depolymerization. Besides yield and physical properties, chemical structure of the liquid products should also be considered.

Two-dimensional HSQC NMR spectra were analyzed to characterize the structure of liquid product samples and original lignin feedstocks. Common substructures and interunit linkages were integrated and normalized by hundred aromatic units (**Table 4.6**). It should be noted that the analysis was semi-quantitative, because HSQC resonance signals were not necessarily proportional to the number of nuclei they represented. Furthermore, the proportionality between signal and number of nuclei may be different for different substructures due to variations in relaxation times. Structural changes that occurred during catalytic hydrogenolysis can be inferred and inform possible reaction pathways despite these limitations. Specifically, compositional differences between liquid products of a given substructure should be accurate given similar chemical shifts of the nuclei and average molecular weights of the mixture.

All liquid product samples had lower methoxyl group contents than starting lignins. This could be partially attributed to differences in molecular weight dependent T1 relaxation times, but there were also variations among liquid product samples. Products generated by DAB-Ru and RuZnAc catalysts contained lower methoxyl contents than those derived using CoZn, regardless of lignin feedstock. These results suggest that some deoxygenation and

demethoxylation may have occurred during hydrogenolysis as Ru is more active towards hydrogenolysis and hydrodeoxygenation than Co. The suggestion is also supported by the fact that reactions involved Ru as a catalyst gave higher volatile products than Co (**Figure 4.5**).

A small decrease in S/G ratios observed for HWK and HWAER product mixtures versus corresponding lignins. Although, it is probably not possible to compare S/G ratio of 1.8 for parent HWAER lignin to the products, because only 30% of the total feedstock was dissolved for NMR analyses. S/G ratios for HWAER products were directly related to methoxyl content as expected. The same relationship was not observed for HWK products. S/G ratio was corrected for catechol content (see Appendix C) and the correction is sensitive to assumptions about the catechol content and distribution between S-type and G-type. It was assumed that catechol content did not change from the feedstock, and this was supported by GC-MS data (**Table C.2**). Additionally, catechols have been shown to concentrate in low molecular weight fraction of BCL, so they are likely to volatilize during hydrogenolysis.[48] Demethylation was still a possible reaction at 280 °C, so the catechol content of liquid products was not lowered.

Side chain interunit linkages of each starting lignin were previously discussed in the section on feedstock properties. All linkages presented in **Table 4.6** were less abundant in liquid products compared to their respective starting lignins, which provided evidence of multiple reaction pathways that led to molecular weight reduction. β-O-4' bonds were most relevant to HWAER due to the relatively high abundance of this structure in the starting material. DAB-Ru was most effective at catalyzing the hydrogenolysis of these linkages, which helps to explain why HWAER processed with DAB-Ru had the highest yield of volatiles, monomers, and dimers (**Figure 4.5**). Kraft lignin-derived liquid product also had lower amounts of β-O-4' side chain interunit bonds regardless of the catalyst used. Similarly, enol ether contents of the liquid product

were lower than the corresponding kraft lignins. This is not a structure commonly found in native lignins and none were detected in HWAER. However, HSQC spectra of liquid product generated by DAB-Ru and CoZn did indicate the presence of this linkage. Enol ethers are formed during kraft pulping from β-O-4' structures through γ-elimination of formaldehyde. The same reaction may have occurred during the depolymerization of HWAER by these catalysts.

All catalysts demonstrated carbon-carbon activation capability as demonstrated by a reduced β-β' and β-5' abundance per aromatic unit following hydrogenolysis. There was no evidence that one catalyst was particularly effective over another, and model compound work should be performed to investigate this further. Stilbene content was lower in kraft lignin-derived liquid product but not those generated from HWAER. Stilbenes, like enol ethers, are created during the kraft pulping process and constitute a limited proportion, if any, of native interunit linkages. They are generated during the hydrolysis of β-5' and β-1' structures, which may explain the higher stilbene content for HWAER liquid products. This is not guaranteed as the NMR analysis for HWAER only accounted for 30% of the total, so any increase could be from the original insoluble portion. Stilbene decreases seen for both kraft lignins were likely not caused by C-C cleavage; instead, reduction of the unsaturated carbons by hydrogenation was more probable. In fact, stilbene contents were lower when the stronger hydrogenation catalyst, ruthenium, was present.

Table 4.6. Semi-quantitative substructure and interunit linkage abundances of lignins and liquid products as determined by ^{1}H-^{13}C HSQC NMR (mol / 100 mol Ar).[a]

Structure	BCL				HWK				HWAER[b]			
	-	DAB-Ru	CoZn	RuZnAc	-	DAB-Ru	CoZn	RuZnAc	-	DAB-Ru	CoZn	RuZnAc
Methoxyl	67	52	61	54	111	96	106	86	116	75	108	86
S/G	0.02	0.03	0.04	0.03	1.75	1.46	1.30	1.45	1.8	0.89	2.1	1.5
H	1.8	1.7	0.79	3.0	0.35	0.86	1.4	0.75	1.0	3.4	0.28	0.50
β-O-4'	3.8	0.12	0.44	0.26	4.9	1.0	0.4	0.13	14	0.07	3.2	1.0
Enol ethers	1.9	0.02	0.55	0.00	0.15	0.03	0.09	0.00	0.00	0.00	0.06	0.00
β-5'	1.1	0.02	0.53	0.27	0.52	0.23	0.22	0.18	2.3	0.65	0.97	0.18
β-β'	1.7	0.10	0.91	0.36	2.5	1.3	1.5	0.56	4.0	0.06	2.5	0.71
Stilbenes	8.8	2.8	6.3	3.1	3.9	2.3	3.8	2.4	0.80	1.3	1.8	0.47

a. All experiments conducted at 280 °C and 3 h. Values normalized by the number of aromatic units using the expression: $(\frac{1}{2}*S_{2/6} + \frac{1}{2}*H_{2/6} + G_2)$, where each term is the HSQC integration volume of the corresponding aromatic methine nuclei. Corrected for catechol content based on discussion in Appendix C.

b. The original HWAER lignin was 30% soluble in the NMR solvent, DMSO-d6, while the hydrogenolysis liquid products were completely soluble.

Aryl-aryl bonding or degrees of condensation were not directly measured. Indeed, the generation of coke is evidence of recondensation reactions. The extent to which those pathways affected bio-oil molecular structure is not that clear from HSQC analysis. Integration of the G_5-H region for BCL-derived liquid products revealed a reduction of this free aryl-hydrogen by 10% to 20%, indicating that condensation at the G_5 position did have some impact on bio-oil chemical structure but the proportion of non-condensed subunits was not so different from the starting lignin. Some degree of aryl-aryl linkages, which have a high BDE, would be desired in a precursor of jet fuel-range hydrocarbons to achieve the C_8 to C_{16} carbon numbers that are typical of that fuel.

Homogeneous vs. solid acid zinc

The RuZnAc catalyst system appeared to be the most versatile and effective catalyst at the condition tested, because it was able to depolymerize all three lignin types while minimizing conversion to solid residue and volatiles and maximizing conversion to oligomeric products. Lignins that underwent hydrogenolysis using DAB-Ru may have been more completely depolymerized and stabilized as indicated by methoxyl content, side chain bonding, and stilbene content; however, RuZnAc was still effective in those areas, especially compared to CoZn. Comparing zinc that was incorporated into a zeolite framework (CoZn) with zinc acetate in solution (RuZnAc) may have been complicated by differences in the physical state of the catalyst. Zinc supported by dealuminated H-beta zeolite was synthesized and physically mixed with Ru/C to generate new results to provide fairer comparisons with CoZn and DAB-Ru systems. Furthermore, the solid Zn/H-beta catalyst would be more suitable for future process

development efforts. **Table 4.7** contains bulk product yield data comparing RuZnAc with Ru/C, Zn/DeAl H-beta in the depolymerization of BCL and HWAER.

Table 4.7. Bulk product yields using ruthenium on carbon with homogeneous or zeolite-supported zinc.[a]

Lignin	Catalyst	Solid Residue	Oligomers	Monomer/ Dimers	Volatiles	EtOAc-Sol
BCL	Ru/C, ZnAc	4.5	60.7	28.5	6.4	89.1
BCL	Ru/C, Zn/DeAl H-beta	4.9	73.4	17.5	4.2	90.5
HWAER	Ru/C, ZnAc	18.7	40.5	28.4	12.5	68.3
HWAER	Ru/C, Zn/DeAl H-beta	16.3	39.5	34.1	10.1	73.0

a. Yields given as weight percentages on starting whole feedstock. Reaction conditions: 280 °C, 3 h, 0.321 mmol Ru+Zn per gram lignin which is the same as previous tests, 300 RPM.

Using zeolite-supported zinc as opposed to homogeneous Lewis acid reduced the fragmentation of BCL molecules to monomers, dimers, and volatiles with a slight increase in the amount of solid residue formed. The solid acid was capable of depolymerization of BCL to oligomers, but these bulk product yields suggest that the fragmentation was less extensive than when using ZnAc. It was hypothesized that mass transfer effects would be more relevant when using supported zinc assuming a portion of active sites would be located within pores that provided limited access to bulky lignin molecules.[80] However, the same decrease in monomer and dimer yield was not observed for HWAER, which was less soluble and comprised of larger molecules. The hydrogenolysis of HWAER was less affected than in the case of BCL when

switching from ZnAc to Zn/DeAl H-beta. A lower conversion to solids and volatiles corresponded to a slight increase in monomer/dimer yield. The yield of oligomeric products was almost unchanged by switching between the two catalysts. These small differences support the assumption that RuZnAc results could be reliably compared with DAB-Ru and CoZn experimental results, at least to screen catalyst effects during early-stage development. BCL and HWAER were both converted to more suitable product mixtures for hydrotreatment to jet fuel-range hydrocarbons when using zeolite-supported zinc based on this preliminary data. Oligomeric product yield was the same or higher, solid residue was kept low, and volatile losses were reduced, which should have improved carbon economy. Further investigation of a dealuminated H-beta zeolite-supported Ru and Zn catalyst is warranted to determine the effect of active site proximity on depolymerization and hydrogenation of lignin molecules.

Conclusion

Reductive depolymerization of three technical lignins was demonstrated using three catalysts that were effective at maximizing liquid product yield for downstream conversion to phenolic monomer/dimer mixtures or further hydrotreatment to liquid transportation fuels. HWAER depolymerization was most extensive using DAB-Ru. 25% starting lignin was converted to monomers and dimers and almost 30% to volatile products. Yield of volatiles remained high across all time and temperature conditions tested. Using a zeolite-supported cobalt-zinc catalyst resulted in the lowest extent of depolymerization for all lignins was accomplished. Replacement of cobalt with ruthenium reduced solid residue losses, likely due to increased hydrogenation and hydrogenolysis activity that prevented recondensation and promoted depolymerization.

HWK lignin hydroprocessed with RuZnAc catalyst produced a liquid product that was most suitable as a feedstock to jet fuel production. Oligomers were produced in the highest yield and had a weight-average molecular weight of 1500 g mol^{-1} with low dispersity. The milder treatment by CoZn catalyst was beneficial in terms of carbon economy and minimizing losses to volatiles, but the tradeoff was higher solid residue Optimization of carbon yield and depolymerization is key to developing a successful hydrotreating scheme.

Reductive cleavage of lignin carbon-carbon bonds is not well researched, as opposed to oxidative cleavage that has received some attention through model compound studies. This study provided evidence of carbon-carbon cleavage, which is especially relevant to the fragmentation of the kraft lignin polymer network and should be explored further.

REFERENCES

(1) Ragauskas, A. J.; Beckham, G. T.; Biddy, M. J.; Chandra, R.; Chen, F.; Davis, M. F.; Davison, B. H.; Dixon, R. A.; Gilna, P.; Keller, M.; Langan, P.; Naskar, A. K.; Saddler, J. N.; Tschaplinski, T. J.; Tuskan, G. A.; Wyman, C. E. Lignin Valorization: Improving Lignin Processing in the Biorefinery. *Science* **2014**, *344* (6185), 1246843. https://doi.org/10.1126/science.1246843.

(2) Treasure, T.; Gonzalez, R.; Jameel, H.; Phillips, R. B.; Park, S.; Kelley, S. Integrated Conversion, Financial, and Risk Modeling of Cellulosic Ethanol from Woody and Non-Woody Biomass via Dilute Acid Pre-Treatment. *Biofuels, Bioprod. Biorefining* **2014**, *8* (6), 755–769. https://doi.org/10.1002/bbb.1494.

(3) Zakzeski, J.; Bruijnincx, P. C. A.; Jongerius, A. L.; Weckhuysen, B. M. The Catalytic Valorization of Lignin for the Production of Renewable Chemicals. *Chem. Rev.* **2010**, *110*, 3552–3599. https://doi.org/10.1021/cr900354u.

(4) Hocking, M. B. Vanillin: Synthetic Flavoring from Spent Sulfite Liquor. *J. Chem. Educ.* **1997**, *74* (9), 1055–1059. https://doi.org/10.1021/ed074p1055.

(5) ICAO. U.S. Aviation Greenhouse Gas Emissions Reduction Plan. *U.S. Aviat. Greenh. Gas Emiss. Reduct. Plan* **2015**, 1–42.

(6) Cheng, F.; Brewer, C. E. Producing Jet Fuel from Biomass Lignin: Potential Pathways to Alkyl-Benzenes and Cycloalkanes. *Renewable and Sustainable Energy Reviews*. 2017, pp 673–722. https://doi.org/10.1016/j.rser.2017.01.030.

(7) Key, R. E.; Bozell, J. J. Progress toward Lignin Valorization via Selective Catalytic Technologies and the Tailoring of Biosynthetic Pathways. *ACS Sustain. Chem. Eng.* **2016**, *4* (10), 5123–5135. https://doi.org/10.1021/acssuschemeng.6b01319.

(8) Huber, G. W.; Iborra, S.; Corma, A. Synthesis of Transportation Fuels from Biomass: Chemistry, Catalysts, and Engineering. *Chem. Rev.* **2006**, *106* (9), 4044–4098. https://doi.org/10.1021/cr068360d.

(9) He, Z.; Wang, X. Hydrodeoxygenation of Model Compounds and Catalytic Systems for Pyrolysis Bio-Oils Upgrading. *Catal. Sustain. Energy* **2012**, *1*, 28–52. https://doi.org/10.2478/cse-2012-0004.

(10) Lange, H.; Decina, S.; Crestini, C. Oxidative Upgrade of Lignin - Recent Routes Reviewed. *Eur. Polym. J.* **2013**, *49* (6), 1151–1173. https://doi.org/10.1016/j.eurpolymj.2013.03.002.

(11) Behling, R.; Valange, S.; Chatel, G. Heterogeneous Catalytic Oxidation for Lignin Valorization into Valuable Chemicals: What Results? What Limitations? What Trends? *Green Chem.* **2016**, *18* (7), 1839–1854. https://doi.org/10.1039/C5GC03061G.

(12) Gazi, S. Valorization of Wood Biomass-Lignin via Selective Bond Scission: A Minireview. *Appl. Catal. B Environ.* **2019**, *257* (March), 117936. https://doi.org/10.1016/j.apcatb.2019.117936.

(13) Kim, S.; Chmely, S. C.; Nimlos, M. R.; Bomble, Y. J.; Foust, T. D.; Paton, R. S.; Beckham, G. T. Computational Study of Bond Dissociation Enthalpies for a Large Range of Native and Modified Lignins. *J. Phys. Chem. Lett.* **2011**, *2* (22), 2846–2852. https://doi.org/10.1021/jz201182w.

(14) Cao, Y.; Chen, S. S.; Tsang, D. C. W.; Clark, J. H.; Budarin, V. L.; Hu, C.; Wu, K. C. W.; Zhang, S. Microwave-Assisted Depolymerization of Various Types of Waste Lignins over Two-Dimensional CuO/BCN Catalysts. *Green Chem.* **2020**, *22* (3), 725–736. https://doi.org/10.1039/c9gc03553b.

(15) Van den Bosch, S.; Koelewijn, S.-F.; Renders, T.; Van den Bossche, G.; Vangeel, T.; Schutyser, W.; Sels, B. F. Catalytic Strategies Towards Lignin-Derived Chemicals. *Top. Curr. Chem.* **2018**, *376* (5), 36. https://doi.org/10.1007/s41061-018-0214-3.

(16) Cheng, C.; Shen, D.; Gu, S.; Luo, K. H. State-of-the-Art Catalytic Hydrogenolysis of Lignin for the Production of Aromatic Chemicals. *Catal. Sci. Technol.* **2018**, *8* (24), 6275–6296. https://doi.org/10.1039/c8cy00845k.

(17) Schutyser, W.; Renders, T.; Van den Bosch, S.; Koelewijn, S.-F.; Beckham, G. T.; Sels, B. F. Chemicals from Lignin: An Interplay of Lignocellulose Fractionation, Depolymerisation, and Upgrading. *Chem. Soc. Rev.* **2018**, *47*, 852–908. https://doi.org/10.1039/C7CS00566K.

(18) Huang, X.; Korányi, T. I.; Boot, M. D.; Hensen, E. J. M. Ethanol as Capping Agent and Formaldehyde Scavenger for Efficient Depolymerization of Lignin to Aromatics. *Green Chem.* **2015**, *17* (11), 4941–4950. https://doi.org/10.1039/c5gc01120e.

(19) Kasakov, S.; Shi, H.; Camaioni, D. M.; Zhao, C.; Baráth, E.; Jentys, A.; Lercher, J. A. Reductive Deconstruction of Organosolv Lignin Catalyzed by Zeolite Supported Nickel Nanoparticles. *Green Chem.* **2015**, *17* (11), 5079–5090. https://doi.org/10.1039/C5GC02160J.

(20) Kumar, C. R.; Anand, N.; Kloekhorst, A.; Cannilla, C.; Bonura, G.; Frusteri, F.; Barta, K.; Heeres, H. J. Solvent Free Depolymerization of Kraft Lignin to Alkyl-Phenolics Using Supported NiMo and CoMo Catalysts. *Green Chem.* **2015**, *17* (11), 4921–4930. https://doi.org/10.1039/c5gc01641j.

(21) Wang, H.; Ruan, H.; Pei, H.; Wang, H.; Chen, X.; Tucker, M. P.; Cort, J. R.; Yang, B. Biomass-Derived Lignin to Jet Fuel Range Hydrocarbons via Aqueous Phase

Hydrodeoxygenation. *Green Chem.* **2015**, *17* (12), 5131–5135. https://doi.org/10.1039/c5gc01534k.

(22) Wang, X.; Rinaldi, R. Bifunctional Ni Catalysts for the One-Pot Conversion of Organosolv Lignin into Cycloalkanes. *Catal. Today* **2016**, *269*, 48–55. https://doi.org/10.1016/j.cattod.2015.11.047.

(23) Shao, Y.; Xia, Q.; Dong, L.; Liu, X.; Han, X.; Parker, S. F.; Cheng, Y.; Daemen, L. L.; Ramirez-Cuesta, A. J.; Yang, S.; Wang, Y. Selective Production of Arenes via Direct Lignin Upgrading over a Niobium-Based Catalyst. *Nat. Commun.* **2017**, *8*, 16104. https://doi.org/10.1038/ncomms16104.

(24) Wang, H.; Ben, H.; Ruan, H.; Zhang, L.; Pu, Y.; Feng, M.; Ragauskas, A. J.; Yang, B. Effects of Lignin Structure on Hydrodeoxygenation Reactivity of Pine Wood Lignin to Valuable Chemicals. *ACS Sustain. Chem. Eng.* **2017**, *5* (2), 1824–1830. https://doi.org/10.1021/acssuschemeng.6b02563.

(25) Wang, H.; Ruan, H.; Feng, M.; Qin, Y.; Job, H.; Luo, L.; Wang, C.; Engelhard, M. H.; Kuhn, E.; Chen, X.; Tucker, M. P.; Yang, B. One-Pot Process for Hydrodeoxygenation of Lignin to Alkanes Using Ru-Based Bimetallic and Bifunctional Catalysts Supported on Zeolite Y. *ChemSusChem* **2017**, *10* (8), 1846–1856. https://doi.org/10.1002/cssc.201700160.

(26) Dong, L.; Shao, Y.; Han, X.; Liu, X.; Xia, Q.; Parker, S. F.; Cheng, Y.; Daemen, L. L.; Ramirez-Cuesta, A. J.; Wang, Y.; Yang, S. Comparison of Two Multifunctional Catalysts [M/Nb2O5 (M = Pd, Pt)] for One-Pot Hydrodeoxygenation of Lignin. *Catal. Sci. Technol.* **2018**, *8* (23), 6129–6136. https://doi.org/10.1039/c8cy01459k.

(27) Dong, L.; Lin, L.; Han, X.; Si, X.; Liu, X.; Guo, Y.; Lu, F.; Rudić, S.; Parker, S. F.; Yang,

S.; Wang, Y. Breaking the Limit of Lignin Monomer Production via Cleavage of Interunit Carbon–Carbon Linkages. *Chem* **2019**, *5* (6), 1521–1536. https://doi.org/10.1016/j.chempr.2019.03.007.

(28) Chowdari, R. K.; Agarwal, S.; Heeres, H. J. Hydrotreatment of Kraft Lignin to Alkylphenolics and Aromatics Using Ni, Mo, and W Phosphides Supported on Activated Carbon. *ACS Sustain. Chem. Eng.* **2019**, *7* (2), 2044–2055. https://doi.org/10.1021/acssuschemeng.8b04411.

(29) Chum, H. L.; Johnson, D. K.; Black, S.; Ratcliff, M.; Goheen, D.; Posey, F.; Baldwin, R.; Cowley, S. *Liquid Fuels from Lignins*; Golden, CO, 1986.

(30) Shabtai, J. S.; Zmierczak, W.; Chornet, E. Process for Conversion of Lignin to Reformulated Hydrocarbon Gasoline. WO Pat. Appl. 99/10450, March 4, 1999.

(31) Vispute, T. P.; Zhang, H.; Sanna, A.; Xiao, R.; Huber, G. W. Renewable Chemical Commodity Feedstocks from Integrated Catalytic Processing of Pyrolysis Oils. *Science* **2010**, *330* (6008), 1222–1227. https://doi.org/10.1126/science.1194218.

(32) Lin, B.; Li, R.; Shu, R.; Wang, C.; Cheng, Z.; Chen, Y. Hydrogenolysis and Hydrodeoxygenation of Lignin in a Two-Step Process to Produce Hydrocarbons and Alkylphenols. *J. Energy Inst.* **2020**, *93* (2), 784–791. https://doi.org/10.1016/j.joei.2019.05.004.

(33) Gale, M.; Cai, C. M.; Gilliard-Abdul-Aziz, K. L. Heterogeneous Catalyst Design Principles for the Conversion of Lignin into High-Value Commodity Fuels and Chemicals. *ChemSusChem* **2020**, *13* (8), 1947–1966. https://doi.org/10.1002/cssc.202000002.

(34) Dessbesell, L.; Paleologou, M.; Leitch, M.; Pulkki, R.; Xu, C. (Charles). Global Lignin

Supply Overview and Kraft Lignin Potential as an Alternative for Petroleum-Based Polymers. *Renew. Sustain. Energy Rev.* **2020**, *123*, 109768. https://doi.org/10.1016/j.rser.2020.109768.

(35) Deuss, P. J.; Lancefield, C. S.; Narani, A.; de Vries, J. G.; Westwood, N. J.; Barta, K. Phenolic Acetals from Lignins of Varying Compositions: Via Iron(III) Triflate Catalysed Depolymerisation. *Green Chem.* **2017**, *19* (12), 2774–2782. https://doi.org/10.1039/c7gc00195a.

(36) Figueirêdo, M. B.; Venderbosch, R. H.; Deuss, P. J.; Heeres, H. J. A Two-Step Approach for the Conversion of Technical Lignins to Biofuels. *Adv. Sustain. Syst.* **2020**, *4* (10), 1900147. https://doi.org/10.1002/adsu.201900147.

(37) Sebhat, W.; El-Roz, A.; Crepet, A.; Ladavière, C.; Perez, D. D. S.; Mangematin, S.; Almada, C. C.; Vilcocq, L.; Djakovitch, L.; Fongarland, P. Comparative Study of Solvolysis of Technical Lignins in Flow Reactor. *Biomass Convers. Biorefinery* **2020**, *10* (2), 351–366. https://doi.org/10.1007/s13399-019-00435-z.

(38) Wang, S.; Li, W. X.; Yang, Y. Q.; Chen, X.; Ma, J.; Chen, C.; Xiao, L. P.; Sun, R. C. Unlocking Structure–Reactivity Relationships for Catalytic Hydrogenolysis of Lignin into Phenolic Monomers. *ChemSusChem* **2020**, *13* (17), 4548–4556. https://doi.org/10.1002/cssc.202000785.

(39) Oasmaa, A.; Alén, R.; Meier, D. Catalytic Hydrotreatment of Some Technical Lignins. *Bioresour. Technol.* **1993**, *45* (3), 189–194. https://doi.org/10.1016/0960-8524(93)90111-N.

(40) Wang, J.; Li, W.; Wang, H.; Ma, Q.; Li, S.; Chang, H-m.; Jameel, H. Liquefaction of Kraft Lignin by Hydrocracking with Simultaneous Use of a Novel Dual Acid-Base

Catalyst and a Hydrogenation Catalyst. *Bioresour. Technol.* **2017**, *243*, 100–106. https://doi.org/10.1016/j.biortech.2017.06.024.

(41) Dou, X.; Jiang, X.; Li, W.; Zhu, C.; Liu, Q.; Lu, Q.; Zheng, X.; Chang, H-m.; Jameel, H. Highly Efficient Conversion of Kraft Lignin into Liquid Fuels with a Co-Zn-Beta Zeolite Catalyst. *Appl. Catal. B Environ.* **2020**, *268*, 118429. https://doi.org/10.1016/j.apcatb.2019.118429.

(42) Huang, C.; Jeuck, B.; Du, J.; Yong, Q.; Chang, H-m.; Jameel, H.; Phillips, R. Novel Process for the Coproduction of Xylo-Oligosaccharides, Fermentable Sugars, and Lignosulfonates from Hardwood. *Bioresour. Technol.* **2016**, *219*, 600–607. https://doi.org/10.1016/j.biortech.2016.08.051.

(43) Narron, R. H.; Han, Q.; Park, S.; Chang, H-m.; Jameel, H. Lignocentric Analysis of a Carbohydrate-Producing Lignocellulosic Biorefinery Process. *Bioresour. Technol.* **2017**, *241*, 857–867. https://doi.org/10.1016/j.biortech.2017.05.207.

(44) Wang, J.; Li, W.; Wang, H.; Ogunbiyi, A. T.; Dou, X.; Ma, Q. Effects of the Novel Catalyst Ni-$S_2O_8^{2-}$-K_2O/TiO_2 on Efficient Lignin Depolymerization. *RSC Adv.* **2020**, *10* (14), 8558–8567. https://doi.org/10.1039/c9ra10675h.

(45) Zhao, B.; Hu, Y.; Gao, J.; Zhao, G.; Ray, M. B.; Xu, C. C. Recent Advances in Hydroliquefaction of Biomass for Bio-Oil Production Using In Situ Hydrogen Donors. *Ind. Eng. Chem. Res.* **2020**, *59* (39), 16987–17007. https://doi.org/10.1021/acs.iecr.0c01649.

(46) Luo, H.; Abu-Omar, M. M. Lignin Extraction and Catalytic Upgrading from Genetically Modified Poplar. *Green Chem.* **2018**, *20* (3), 745–753. https://doi.org/10.1039/c7gc03417b.

(47) Wang, X.; Rinaldi, R. Solvent Effects on the Hydrogenolysis of Diphenyl Ether with Raney Nickel and Their Implications for the Conversion of Lignin. *ChemSusChem* **2012**, *5* (8), 1455–1466. https://doi.org/10.1002/cssc.201200040.

(48) Jiang, X.; Savithri, D.; Du, X.; Pawar, S. N.; Jameel, H.; Chang, H-m.; Zhou, X. Fractionation and Characterization of Kraft Lignin by Sequential Precipitation with Various Organic Solvents. *ACS Sustain. Chem. Eng.* **2017**, *5*, 835–842. https://doi.org/10.1021/acssuschemeng.6b02174.

(49) Min, D.; Xiang, Z.; Liu, J.; Jameel, H.; Chiang, V.; Jin, Y.; Chang, H-m. Improved Protocol for Alkaline Nitrobenzene Oxidation of Woody and Non-Woody Biomass. *J. Wood Chem. Technol.* **2015**, *35* (1), 52–61. https://doi.org/10.1080/02773813.2014.902965.

(50) Chen, C.-L. Functional Group Analysis. In *Methods in Lignin Chemistry*; Lin, S. Y., Dence, C. W., Eds.; Springer: New York, 1992; p 413.

(51) Glasser, W. G.; Davé, V.; Frazier, C. E. Molecular Weight Distribution of (Semi-) Commercial Lignin Derivatives. *J. Wood Chem. Technol.* **1993**, *13* (4), 545–559. https://doi.org/10.1080/02773819308020533.

(52) Kollman, M.; Jiang, X.; Thompson, S. J.; Mante, O.; Dayton, D. C.; Chang, H-m.; Jameel, H. Improved Understanding of Technical Lignin Functionalization through Comprehensive Structural Characterization of Fractionated Pine Kraft Lignins Modified by the Mannich Reaction. *Green Chem.* **2021**, *23* (18), 7122–7136. https://doi.org/10.1039/d1gc01842f.

(53) Meng, X.; Crestini, C.; Ben, H.; Hao, N.; Pu, Y.; Ragauskas, A. J.; Argyropoulos, D. S. Determination of Hydroxyl Groups in Biorefinery Resources via Quantitative ^{31}P NMR

Spectroscopy. *Nat. Protoc.* **2019**, *14* (9), 2627–2647. https://doi.org/10.1038/s41596-019-0191-1.

(54) Hu, Z.; Du, X.; Liu, J.; Chang, H-m.; Jameel, H. Structural Characterization of Pine Kraft Lignin: BioChoice Lignin vs Indulin AT. *J. Wood Chem. Technol.* **2016**, *36* (6), 432–446. https://doi.org/10.1080/02773813.2016.1214732.

(55) Jiang, X.; Narron, R. H.; Han, Q.; Park, S.; Chang, H-m.; Jameel, H. Tracing Sweetgum Lignin's Molecular Properties through Biorefinery Processing. *ChemSusChem* **2020**, *13* (17), 4613–4623. https://doi.org/10.1002/cssc.202001125.

(56) Jiang, X.; Liu, J.; Du, X.; Hu, Z.; Chang, H-m.; Jameel, H. Phenolation to Improve Lignin Reactivity toward Thermosets Application. *ACS Sustain. Chem. Eng.* **2018**, *6* (4), 5504–5512. https://doi.org/10.1021/acssuschemeng.8b00369.

(57) Furimsky, E.; Massoth, F. E. Deactivation of Hydroprocessing Catalysts. *Catal. Today* **1999**, *52* (4), 381–495. https://doi.org/10.1016/S0920-5861(99)00096-6.

(58) Marafi, M.; Furimsky, E. Hydroprocessing Catalysts Containing Noble Metals: Deactivation, Regeneration, Metals Reclamation, and Environment and Safety. *Energy and Fuels* **2017**, *31* (6), 5711–5750. https://doi.org/10.1021/acs.energyfuels.7b00471.

(59) Koch, P. Chemical Constituents. In *Utilization of Hardwoods Growing on Southern Pine Sites, Vol. I: The Raw Material*; US Government Printing Office: Washington DC, 1985; pp 363–464.

(60) Koch, P. Chemical Constituents. In *Utilization of the Southern Pines, Vol I: The Raw Material*; US Government Printing Office: Washington DC, 1972; pp 187–234.

(61) Jardim, J. M.; Hart, P. W.; Lucia, L.; Jameel, H.; Chang, H-m. A Quantitative Comparison of the Precipitation Behavior of Lignin from Sweetgum and Pine Kraft Black Liquors.

BioResources **2020**, *15* (3), 5464–5480. https://doi.org/10.15376/biores.15.3.5464-5480.

(62) Conner, W. C.; Falconer, J. L. Spillover in Heterogeneous Catalysis. *Chem. Rev.* **1995**, *95*, 759–788.

(63) Roberts, V. M.; Stein, V.; Reiner, T.; Lemonidou, A.; Li, X.; Lercher, J. A. Towards Quantitative Catalytic Lignin Depolymerization. *Chem. - Eur. J.* **2011**, *17* (21), 5939–5948. https://doi.org/10.1002/chem.201002438.

(64) Long, J.; Zhang, Q.; Wang, T.; Zhang, X.; Xu, Y.; Ma, L. An Efficient and Economical Process for Lignin Depolymerization in Biomass-Derived Solvent Tetrahydrofuran. *Bioresour. Technol.* **2014**, *154*, 10–17. https://doi.org/10.1016/j.biortech.2013.12.020.

(65) Toledano, A.; Serrano, L.; Labidi, J. Improving Base Catalyzed Lignin Depolymerization by Avoiding Lignin Repolymerization. *Fuel* **2014**, *116*, 617–624. https://doi.org/10.1016/j.fuel.2013.08.071.

(66) Deepa, A. K.; Dhepe, P. L. Lignin Depolymerization into Aromatic Monomers over Solid Acid Catalysts. *ACS Catal.* **2015**, *5* (1), 365–379. https://doi.org/10.1021/cs501371q.

(67) Deuss, P. J.; Scott, M.; Tran, F.; Westwood, N. J.; de Vries, J. G.; Barta, K. Aromatic Monomers by in Situ Conversion of Reactive Intermediates in the Acid-Catalyzed Depolymerization of Lignin. *J. Am. Chem. Soc.* **2015**, *137* (23), 7456–7467. https://doi.org/10.1021/jacs.5b03693.

(68) Yokoyama, T. Revisiting the Mechanism of β-O-4 Bond Cleavage during Acidolysis of Lignin. Part 6: A Review. *J. Wood Chem. Technol.* **2015**, *35*, 27–42. https://doi.org/10.1080/02773813.2014.881375.

(69) Centeno, A.; Laurent, E.; Delmon, B. Influence of the Support of CoMo Sulfide Catalysts and of the Addition of Potassium and Platinum on the Catalytic Performances for the

Hydrodeoxygenation of Carbonyl, Carboxyl, and Guaiacol-Type Molecules. *J. Catal.* **1995**, *154* (2), 288–298. https://doi.org/10.1006/jcat.1995.1170.

(70) Zhu, X.; Lobban, L. L.; Mallinson, R. G.; Resasco, D. E. Bifunctional Transalkylation and Hydrodeoxygenation of Anisole over a Pt/HBeta Catalyst. *J. Catal.* **2011**, *281* (1), 21–29. https://doi.org/10.1016/j.jcat.2011.03.030.

(71) Lu, J.; Fu, B.; Kung, M. C.; Xiao, G.; Elam, J. W.; Kung, H. H.; Stair, P. C. Coking- and Sintering-Resistant Palladium Catalysts Achieved Through Atomic Layer Deposition. *Science* **2012**, *335* (6073), 1205–1208. https://doi.org/10.1126/science.1212906.

(72) Jastrzebski, R.; Constant, S.; Lancefield, C. S.; Westwood, N. J.; Weckhuysen, B. M.; Bruijnincx, P. C. A. Tandem Catalytic Depolymerization of Lignin by Water-Tolerant Lewis Acids and Rhodium Complexes. *ChemSusChem* **2016**, *9* (16), 2074–2079. https://doi.org/10.1002/cssc.201600683.

(73) Dou, X.; Li, W.; Zhu, C.; Jiang, X.; Chang, H-m.; Jameel, H. Cleavage of Aryl-Ether Bonds in Lignin Model Compounds Using a Co-Zn-Beta Catalyst. *RSC Adv.* **2020**, *10* (71), 43599–43606. https://doi.org/10.1039/d0ra08121c.

(74) Klein, I.; Marcum, C.; Kenttämaa, H.; Abu-Omar, M. M. Mechanistic Investigation of the Zn/Pd/C Catalyzed Cleavage and Hydrodeoxygenation of Lignin. *Green Chem.* **2016**, *18* (8), 2399–2405. https://doi.org/10.1039/c5gc01325a.

(75) Yu, Y.; Li, X.; Su, L.; Zhang, Y.; Wang, Y.; Zhang, H. The Role of Shape Selectivity in Catalytic Fast Pyrolysis of Lignin with Zeolite Catalysts. *Appl. Catal. A Gen.* **2012**, *447–448*, 115–123. https://doi.org/10.1016/j.apcata.2012.09.012.

(76) Vroom, K. E. The H Factor: A Means of Expressing Cooking Times and Temperatures as a Single Variable. *Pulp Pap. Mag. Canada* **1957**, *58* (3), 228–231.

(77) Overend, R. P.; Chornet, E. Heavy-Oil Cracking: The Case for Nonhomogenous Kinetics. *Can. J. Phys.* **1990**, *68* (9), 1105–1111. https://doi.org/10.1139/p90-155.

(78) Li, W.; Dou, X.; Zhu, C.; Wang, J.; Chang, H-m.; Jameel, H.; Li, X. Production of Liquefied Fuel from Depolymerization of Kraft Lignin over a Novel Modified Nickel/H-Beta Catalyst. *Bioresour. Technol.* **2018**, *269* (August), 346–354. https://doi.org/10.1016/j.biortech.2018.08.125.

(79) Infantes-Molina, A.; Mérida-Robles, J.; Rodríguez-Castellón, E.; Fierro, J. L. G.; Jiménez-López, A. Synthesis, Characterization and Catalytic Activity of Ruthenium-Doped Cobalt Catalysts. *Appl. Catal. A Gen.* **2008**, *341* (1–2), 35–42. https://doi.org/10.1016/j.apcata.2007.12.034.

(80) Kramm, U. I.; Marschall, R.; Rose, M. Pitfalls in Heterogeneous Thermal, Electro- and Photocatalysis. *ChemCatChem* **2019**, *11* (11), 2563–2574. https://doi.org/10.1002/cctc.201900137.

CHAPTER 5: Conclusions

Three parallel research projects were executed that focused on improving fundamental knowledge underlying potential industrial lignin applications. Projects involved many disciplines like polymer science and catalysis but emphasized the perspective of lignin and wood chemistry. Particular attention was paid to ensuring complete and accurate characterization of starting lignin samples to predict and explain observed phenomena. It is the hope that the following conclusions will inspire continuing efforts in these areas. Suggested future work is provided in the next chapter.

Pine kraft lignin was melt blended with polyethylene terephthalate because both have an aromatic structure. However, softwood kraft lignin has a low thermal degradation point relative to its glass transition temperature, which makes melt processing challenging. A lower molecular weight, more uniform fraction of lignin appeared to be capable of blending with PET without phase separation. Both glass transition and degradation temperature of the low molecular weight fraction were lower than the whole lignin fraction, but processing was performed at the same temperature to melt PET crystals. There was evidence that crystallization of PET was disrupted by the inclusion of lignin as a miscible polymer. Chemical structure of the low MW fraction was altered during heating, likely through degradation and condensation reactions that resulted in increased glass transition and degradation points, yet thermoplastic behavior was maintained. The same structure and property changes occurred for whole lignin and high molecular lignin, but these were converted to thermosets.

Using lignins as a macromonomer in the polymerization of novel materials is a potential alternative to blending with synthetic polymers. High processing temperatures could be avoided, and the final product would contain a higher proportion of bio-derived polymer. The first step of

this strategy is to modify lignin to improve its low reactivity, which is low relative to traditional monomers that have at least two reactive groups per unit. Amination was proposed to modify lignin as a macromonomer for the synthesis of polyamides or polyurethanes, for example. Other applications of lignin amines have been explored too. The project objective was to study factors that affect degree and location of substitution and evaluate accuracy of different analytical techniques.

A quantitative technique combining 2D HSQC NMR and ^{13}C NMR spectroscopy appeared to most accurately characterized high and low molecular weight fractions of aminated pine kraft lignin. The degree of amine substitution was two times higher for low molecular weight lignin compared to the high molecular weight fraction because of increased non-etherified units containing available C5 positions. Neither pH nor amine species were significant factors. Amine substitution of pine kraft lignin took place selectively *ortho* to non-etherified phenolic hydroxyl groups and displaced carboxylic acid groups of benzoic- and cinnamic-type subunits. Other theoretically possible pathways were sterically limited. Elemental analysis overestimated amine substitution, which was attributed to the presence of side products and impurities. Multiple methods should always be employed when characterizing complex, heterogenous biopolymers like lignins to avoid misinterpretation of results.

Finally, depolymerization of multiple technical lignins and catalysts was carried out to identify structure-catalyst-product relationships. While this was largely a separate project from the other two, depolymerization of lignin and cellulose has been considered as a route towards commercial bio-based materials, whereby monomeric mixtures are purified and repolymerized in a controlled manner. Development of lignin depolymerization technology is of additional interest because the process can be modified to generate many other bio-based products like aromatic

oxygenated fine chemicals, hydrocarbon platform chemicals, or liquid transportation fuels comprised of targeted aromatic/alkane ratios. In this project, reductive depolymerization was selected to generate a stable liquid product containing deoxygenated and partially saturated molecules. Many applied research studies use lignin model compounds, which has demonstrated the vast potential of lignins as a biochemical feedstock. Additional work is needed to determine the most effective catalyst systems and process conditions to achieve depolymerization of the various technical lignins that could be used depending on geographic location and isolation method.

Three lignin types were reductively depolymerized over three unique catalysts that were developed specifically for kraft lignin. In all cases, a high carbon yield of liquid product was achieved at relatively mild conditions compared to other thermochemical conversion processes. Liquid products were mixtures of alkylated phenolic compounds. Syringyl-type product yield increased then decreased with increasing severity, possibly because these products were more susceptible to degradation than guaiacyl-type products. Increased volatile yields supported this explanation. The biorefinery hardwood lignin monomer and dimer yields were limited when using $S_2O_8^{2-}$, K_2O/TiO_2 and CoZn/dealuminated H-beta zeolite catalysts because of high volatile losses or solid residue losses, respectively. Replacement of cobalt with ruthenium reduced solid residue losses, likely due to increased hydrogenation and hydrogenolysis activity that prevented recondensation and promoted depolymerization.

HWK lignin hydroprocessed with RuZnAc catalyst produced a liquid product that was most suitable as a feedstock to jet fuel production. Oligomers were produced in the highest yield and had a weight-average molecular weight of 1500 g mol^{-1} with low dispersity. The milder treatment by CoZn catalyst was beneficial in terms of carbon economy and minimizing losses to

volatiles, but the tradeoff was increased solid residue. Optimization of carbon yield and depolymerization is key to developing a successful hydrotreating scheme.

The heterogeneity of lignin molecules and the variety of types offer potential for a wide range of diverse applications. Comprehensive characterization of physical and chemical properties of technical lignins is critical to developing value-added applications. Analytical lignin structures have been well-characterized, but many unknowns remain for technical lignins. Most applications will benefit from fractionation to reduce dispersity and chemical heterogeneity, purification to remove inorganics, and modification to remove or add specific functional groups depending on the application. Controlled deconstruction of lignins shows promise if directed to produce a more homogeneous mixture or one that is easily separated into homogeneous fractions. High carbon yield and catalyst recyclability are essential to compete economically with petroleum refining.

CHAPTER 6: Future Work

Techniques like x-ray diffraction should be used to determine how crystalline regions of PET are impacted in lignin blends. Disruption of PET crystallization may be useful in the production of amorphous polymer materials. Lower processing temperatures may be possible in the absence of PET crystals, which would limit degradation of lignin molecules. Melt extruding under nitrogen could be another technique to limit degradation. Application testing should be performed to reveal how properties of lignin-PET blends compare with commercial criteria for strength and oxygen and water resistance.

Amination of technical lignins via the Mannich reaction appeared to result in substitution at stilbene groups, but this was not confirmed by model compounds. More importantly, additional studies validating the use of 2D HSQC coupled with quantitative NMR spectroscopy (phosphorus-31 and carbon-13) to analyze multiple technical lignins will be invaluable to further chemical structure characterization of whole lignin samples. This will require the development of independent analytical methods capable of qualification and quantification of Mannich-derived lignin structures. Lignin amines generated in this study may be applicable as monomers in the synthesis of polyamides or polyurethane. This should be tested by using a diamine to modify low molecular weight fraction and react with a diacyl chloride. Whether a thermoset or thermoplastic is produced should depend on the number of reactive groups per lignin molecule.

Other techniques to introduce amines into the structure of lignin like ammonolysis and phenolic group modification should be the focus of efforts to maximize the number of amine groups. Oxidative ammonolysis partially depolymerizes lignin to introduce more amine groups and increase reactivity, which would be useful for use either as a soil amendment or thermoset precursor. Methods like epoxidation followed by amine-induced ring opening take advantage of

the fact that phenolic hydroxyl group abundance in kraft lignins is higher than the number of Mannich reaction sites.

Alkylated phenolic mixtures of monomers and dimers were derived from technical lignins in yields up to 42% based on weight of starting lignin. Yields of individual monomers up to 5% were achieved but were generally less than 1%, and separation of phenolic compounds is likely challenging. An additional thermochemical conversion step of the entire liquid product, or possibly only the oligomeric fraction, to a liquid hydrocarbon mixture could potentially be used as is. If not, the separation of hydrocarbons is routinely achieved through distillation.

Dealuminated beta zeolite-supported zinc coupled with carbon-supported ruthenium was the most effective catalyst system for the reductive depolymerization of kraft lignins towards oligomeric products. These products were of a uniform and good average molecular weight to be used as the raw material in a final hydrotreating step to complete hydrodeoxygenation and hydrogenation to jet fuel-range hydrocarbons. Once technical feasibility is ensured, environmental and economic assessment will be critical in identifying areas for process development and commercial success. Sustainable aviation fuels should be produced using established green chemistry and green engineering techniques. Areas of improvement for the present work include the use of greener solvents (e.g., tetrahydrofuran instead of dioxane), lower severity process conditions, robust and stable catalysts to limit leaching of noble metals (or replacement with base metals), and reducing hydrogen consumption. A theoretical minimum of hydrogen is needed to ensure complete deoxygenation and saturation, but excess is required to overcome mass transfer and solubility limitations. Reactor design and solvent choice can help to overcome these challenges.

APPENDICES

Appendix A: Supplementary Information for Chapter 2

Table A.1. Summary of thermal events recorded by DSC and TGA for lignin-PET melt blends.

Sample	Lignin, % wt	PET, % wt	T_g, °C	T_m, °C	$\widehat{H}_m$, J/g	$T_{d,5\%}$, °C
PET	0	100	81.3	237	39.5	377
Whole	25	75	72.1	240	31.9	345
	50	50	74.0	239	22.2	328
	75	25	ND	238	12.0	322
	100[a]	0	ND	-	-	307
	100	0	154	-	-	255
Ethyl Acetate Insoluble	25	75	ND	NQ	NQ	
	50	50	ND	NQ	NQ	
	75	25	ND	239	17.7	
	100	0	ND	-	-	250
Ethyl Acetate Soluble	25	75	97.5	230	32.4	
	50	50	98.4	204	6.09	
	100[a]	0	145	-	-	
	100	0	103	-	-	219

a. Heat treated at 260 °C for 30 minutes.

T_g: glass transition temperature, point of inflection between the specific heat before and after the transition.

T_m: melting point of the polymer crystal phase. Does not apply to lignin because it does not crystallize.

$\widehat{H}_m$: specific heat of melting for the crystal phase, integration of endothermic peak.

T_d: degradation temperature is arbitrarily defined as the temperature at which 5 percent weight loss occurred.

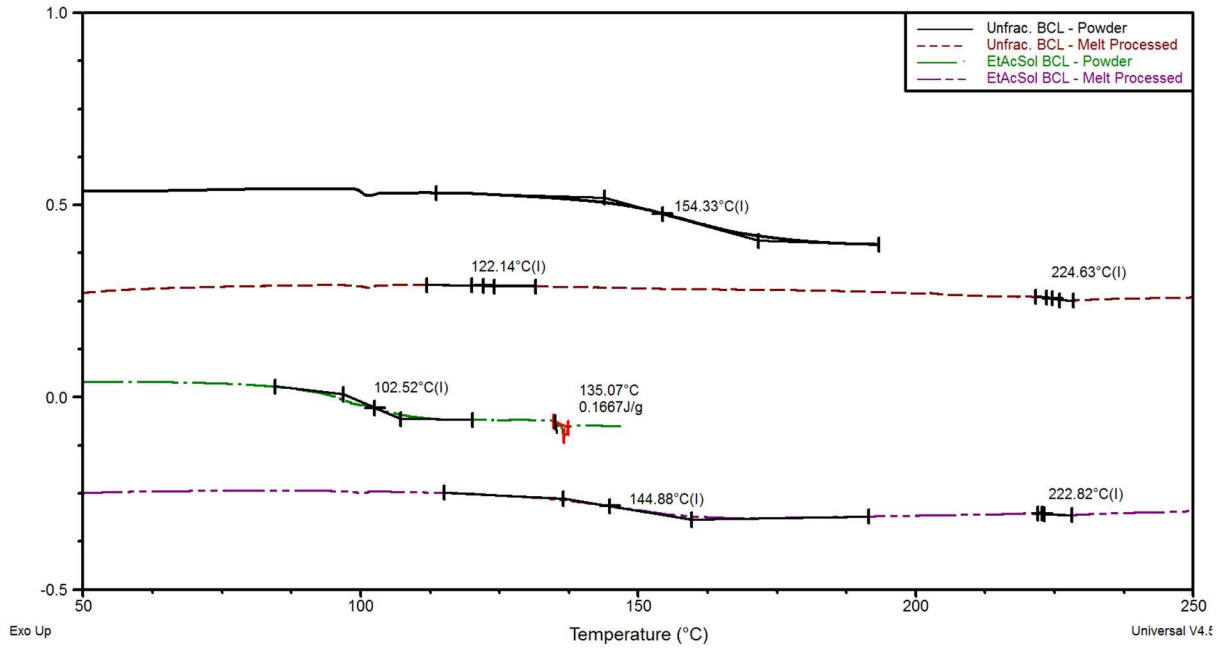

Figure A.1. Effect of thermo-oxidation and average molecular weight on transition temperatures.

Appendix B: Supplementary Information for Chapter 3

Dialysis as a method for purifying lignin amines

Dialysis was initially explored as a method for removing impurities that could be contributing to elemental analysis overestimation. The goal was to see if nitrogen contents of dialyzed aminated lignins would better agree with NMR data. When using dialysis to purify whole aminated pine kraft lignins in preliminary experiments, product recovery yields averaged 52% by mass after accounting for addition of amine groups. The presence of amine groups directly contributed to the hydrophilic nature of lignin amines, further improving their diffusion across the regenerated cellulose membrane (**Figure B.1**).

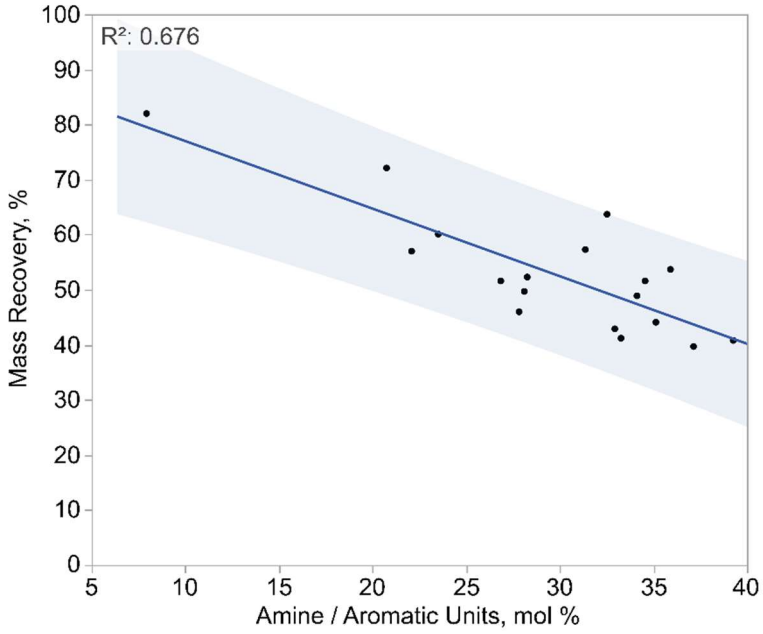

Figure B.1. Percent of starting lignin recovered after dialysis as a function of extent of amination per elemental analysis. Recovery is inversely related to diffusion through dialysis membrane. The shaded area represents the 95% confidence interval.

It was thought that dialysis losses would be mitigated by starting with a lignin sample of sufficiently high average molecular weight. A non-modified HMW lignin sample was dialyzed for three days until no lignin was observed in the dialysate by UV-Vis. Four percent by weight of HMW lignin was removed during this pretreatment. After Mannich reaction of four samples with DMA at a pH of 5, two were immediately freeze-dried and two first underwent dialysis until neutral pH was achieved. Under both work-up methods, quantification by NMR gave similar results, with 26.3 mol% amine/aromatic unit using freeze-drying and 21.3 mol% using both dialysis and freeze-drying. One explanation for the apparent reduction in amine substitution following dialysis is that 39% of the product mass was removed through the process even having pretreated the HMW lignin to prevent this. The loss of product was not as severe as when starting with whole lignin, but the increased polarity of lignin molecules after modification was apparently effective at increasing diffusion across the hydrophilic dialysis membrane. Even with the loss in mass, this test helps to confirm that the NMR analysis only quantifies lignin-amine bonds given the agreement between the two samples. Furthermore, elemental analysis overestimated amine substitution by four times, even after purifying with dialysis. So, the use of elemental analysis and dialysis once again skewed the data through loss of product when assuming all nitrogen was contained in attached amine groups.

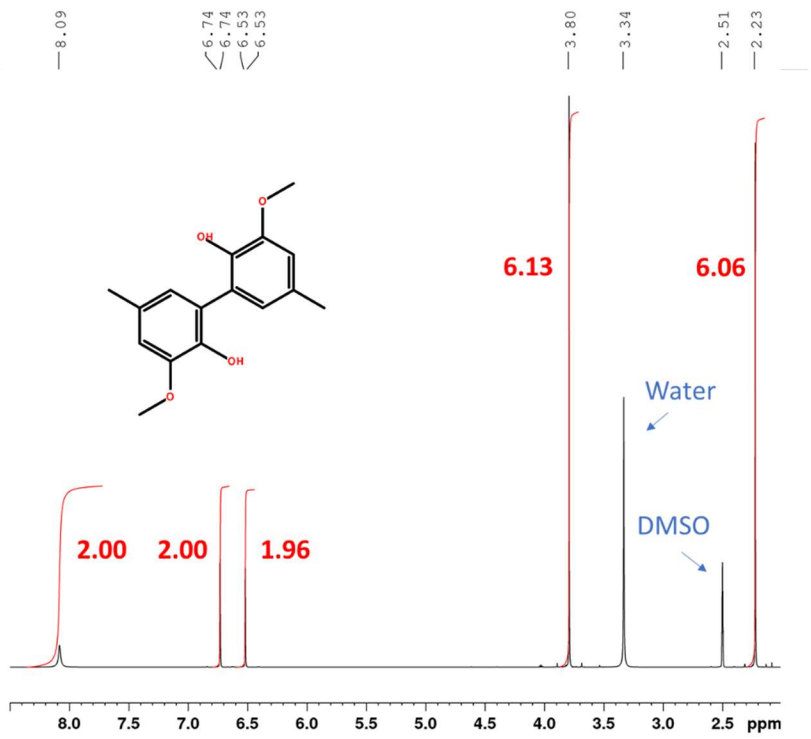

Figure B.2. ^{1}H NMR spectrum for product isolated from methyl guaiacol oxidative coupling (3,3'-dimethoxy-5,5'-dimethylbiphenyl-2,2'-diol).

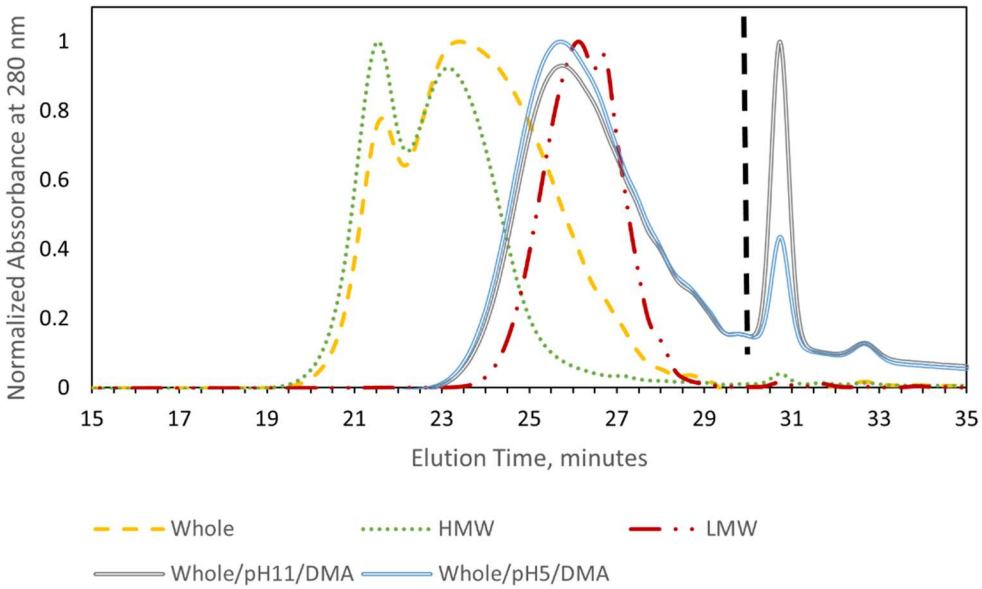

Figure B.3. Gel permeation chromatogram of whole and fractionated BCL and two samples of aminated BCL.

Aminated BCL was not entirely soluble in THF, hence the shifted molecular weight distribution and raising baseline, so it was not reported (**Figure B.3**). Amination was expected to slightly increase average molecular weight from the introduction of amine groups, but it would be useful to check for inter-unit condensation as well.

Table B.1. Chemical shifts used to quantify lignin substructures using ^{1}H-^{13}C HSQC NMR and quantitative ^{13}C NMR spectroscopy (DMSO-d_6 δ_C / δ_H = 39.52 ppm / 2.50 ppm).

Unit	**δ_C / δ_H (ppm)**
β-O-4’	α: 71.6 / 4.89
β-β’ (pinoresinol)	α: 84.9 / 4.68
β-β’ (epiresinol)	α: 81.2 / 4.78
β-β’ (secoisolariciresinol)	β: 42.3 / 1.87
β-5’ (phenylcoumaran)	α: 86.8 / 5.49
Dibenzodioxocin	α: 83.4 / 4.82
Enol ether (Z)	α: 109.1 / 5.56
Enol ether (E)	β: 142.6 / 7.29
Stilbene (β-1’)	α: 125.6 / 6.97
Stilbene (β-5’)	β: 120.1 / 7.22
Cinnamyl alcohol	α: 61.4 / 4.10
Cinnamaldehyde	α: 153.5 / 7.63
Vanillin	C2: 110.6 / 7.40
Vanillic Acid	C2: 112.6 / 7.45
Methoxyl groups	55.6 / 3.77
Syringyl	107 > δ_C > 100
Guaiacyl	114 > δ_C > 107
p-Hydroxyphenyl	128.5 / 7.1

Further discussion on the NMR spectroscopy of lignins

Quantification of ^{13}C NMR spectra requires that peak area be proportional to the number of carbon nuclei. This is not usually the case for broadband-decoupled spectra because the Nuclear Overhauser Effect (NOE) and T1 relaxation times are different for each carbon nucleus.[1] To overcome these, an inverse-gated decoupled pulse sequence can be applied that minimizes or eliminates NOE and a pulse delay greater than five times the T1 relaxation time can be used to ensure all nuclei return to equilibrium.[1–3] If nuclei do not return to equilibrium (meaning the Boltzmann distribution at equilibrium) prior to the next pulse, then the corresponding spectral peak height will be too low. In other words, if the delay between pulses is not long enough, then the quantification of nuclei with long T1 relaxation times will be underestimated. To account for this, T1 relaxation times were measured (**Figure B.4**). Chromium(III) acetylacetonate was used as a common NMR relaxation agent to shorten T1 relaxation and times. The highest T1 relaxation times were for aromatic and methoxyl carbon nuclei of HMW lignins at 0.4 s. The pulse delay for all ^{13}C 1D experiments was set to 0.4 s * 5 = 2 s.

Sufficient signal-to-noise ratio (SNR) is needed to ensure an acceptable accuracy is achieved. Probe type, spectrometer field strength, sample concentration, number of scans, and processing of collected FIDs all contribute to the SNR. Quantitative ^{13}C analysis of softwood kraft lignin has been demonstrated using a concentration of 12% to 16% (plus 0.01 M chromium(III) acetylacetonate) with a 5 mm broadband inverse (BBI) probe, 1.2 s acquisition time, 1.7s delay, and 20k to 25k scans.[4] Other ^{13}C NMR analyses of various lignin types have used similar parameters with a slightly higher concentration of 20%.[2,5,6] In this study, 20% concentration was used with a 5 mm BBO probe (more sensitive to ^{13}C), 1.5 s acquisition time, 2 s delay, and 19k scans. ^{13}C spectra were thought to be of sufficient quality given that similar

equipment, sample prep, and acquisition and processing parameters detailed in prior protocols were used. However, it has recently been suggested that an aromatic signal (163 ppm to 98 ppm) to noise (10 ppm to 0 ppm) ratio of 200 is ideal and is only achievable by doubling the sample concentration to 40%.[3] In the current study, aromatic region SNR averaged 25, much lower than 200. The authors have not seen SNRs reported before this, but it is assumed that they were close to 25 given the similarities in instrumentation and methodology. At least two recent lignin analytical studies have adopted a higher concentration (36% to 44%) for collecting quantitative ^{13}C NMR spectra (Balakshin 2016 Holz and Lancefield 2018 Chem Sci).[7,8] It is recommended that higher sample concentrations (200 mg per 500 μL) be used in the future. Derivatization and/or different solvents may need to be evaluated to dissolve aminated lignins at this higher concentration.

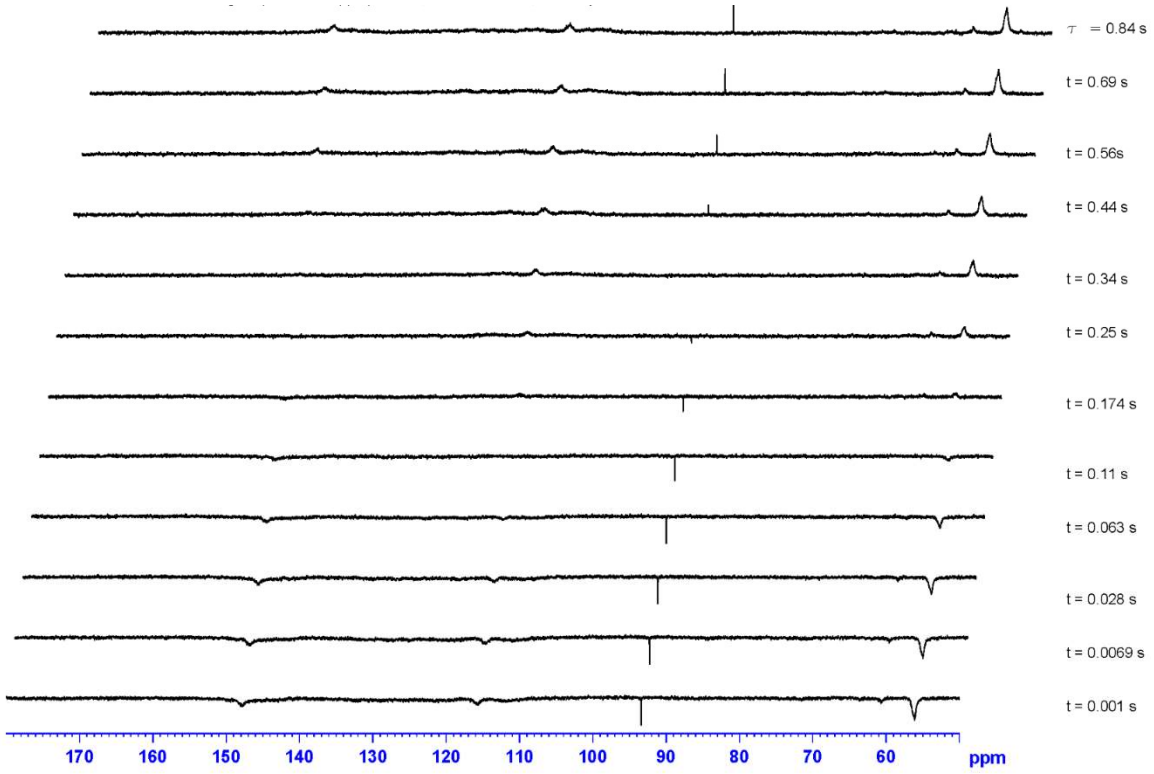

Figure B.4. ^{13}C NMR spectra from an inversion-recovery experiment on HMW lignin in DMSO-d6 to determine T1 relaxation times of the aromatic and methoxy regions. 0.016M chromium(III) acetylacetonate was added to the sample to generate the shown spectra. Calculated T1 relaxation times were 0.4 s for both the aromatic (160 ppm to 100 ppm) and methoxy (55 ppm) regions and 0.5 s for trioxane. Without adding relaxation agent, T1 relaxation times were calculated to be 0.9 s for aromatic carbons and 2.96 s for the internal standard, trioxane.

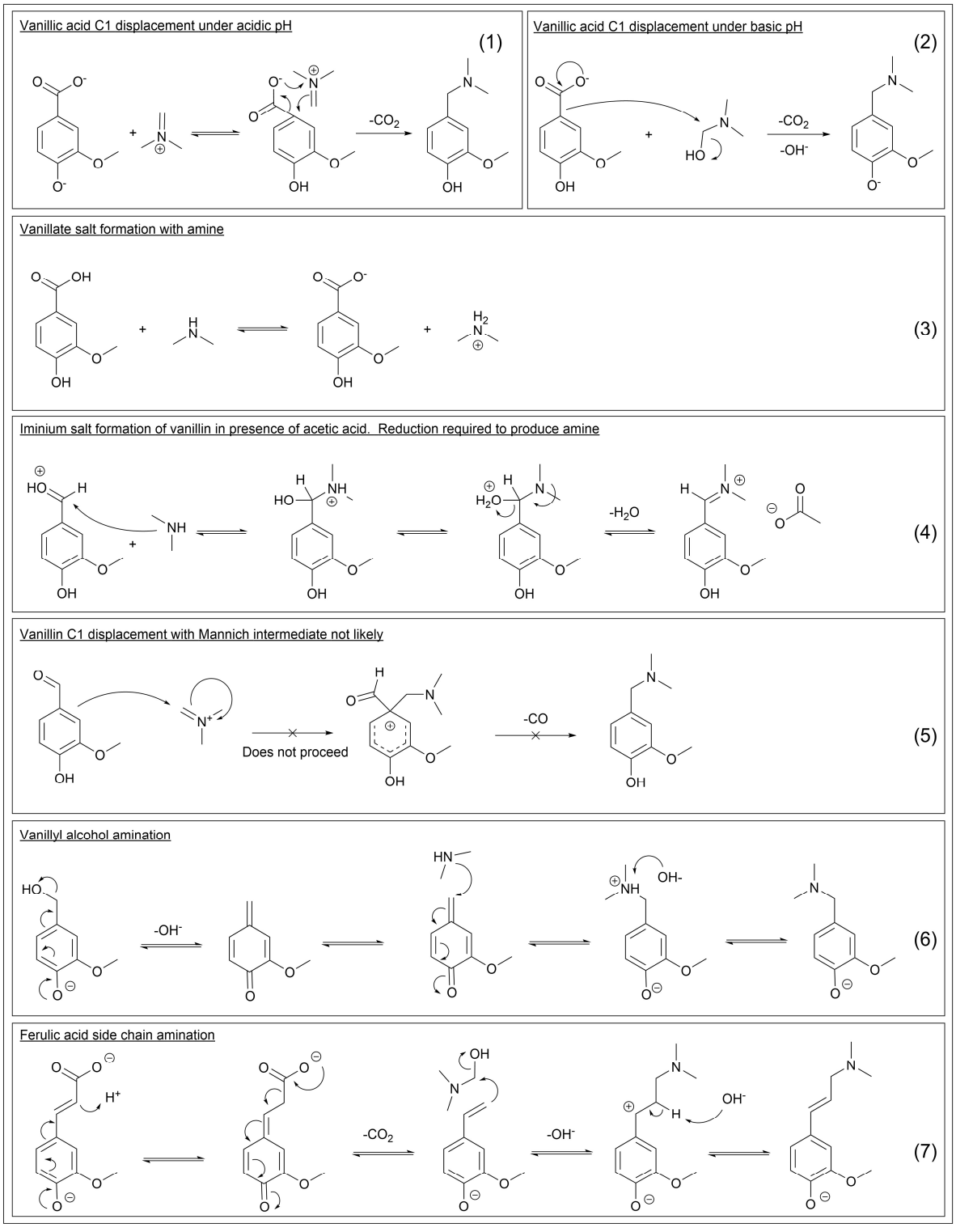

Figure B.5. Proposed mechanisms for amination of lignin side chain. All products have been experimentally verified.[9–11]

Hydroxyl Content Analysis using ^{31}P NMR Spectroscopy

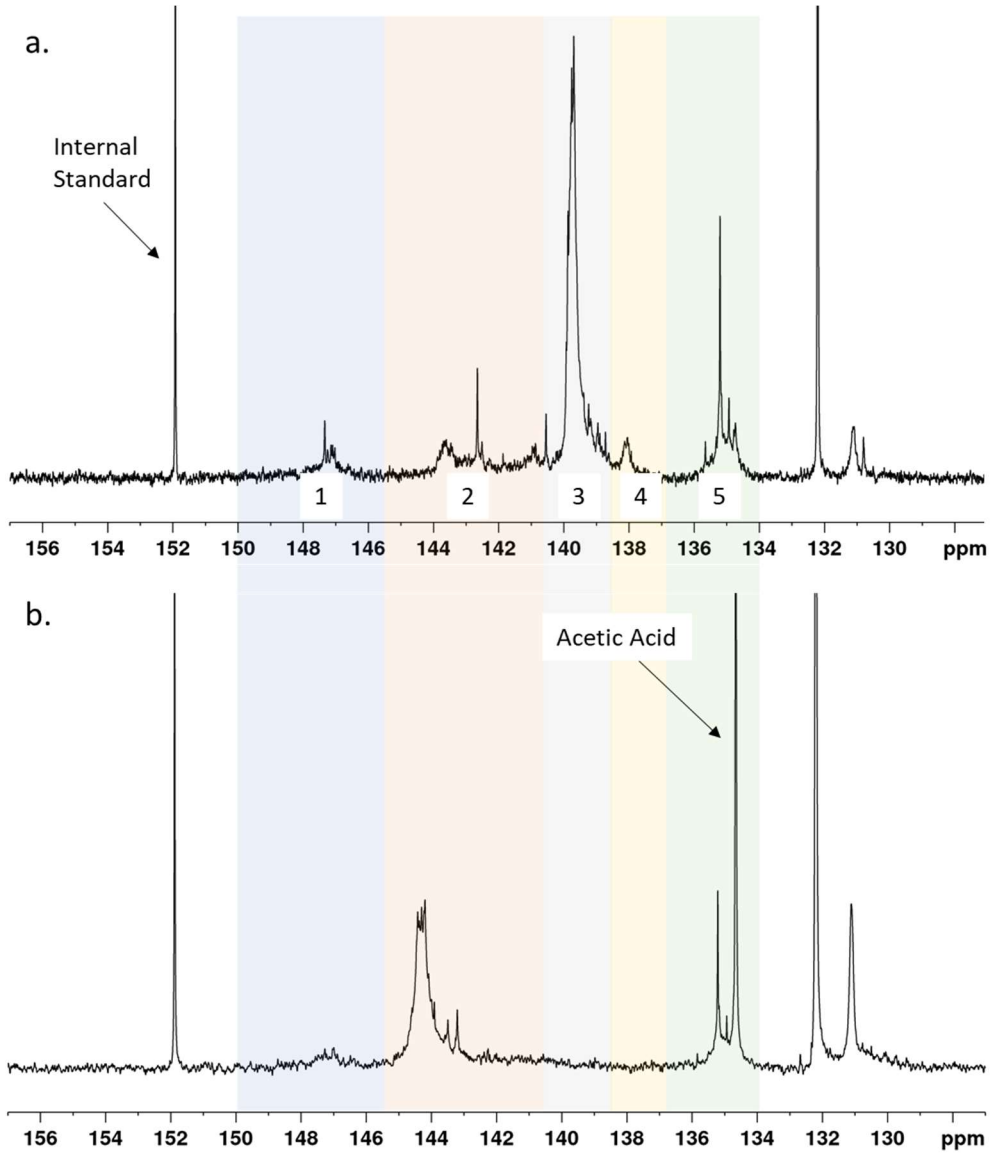

Figure B.6. ^{31}P NMR spectra for a.) LMW lignin fraction and b.) LMW lignin fraction after Mannich reaction at pH 11 using dimethylamine. Regions are numbered as follows and assigned based on a previous report: 1) aliphatic OH, 2) ortho di-substituted phenolic OH, 3) ortho mono-substituted phenolic OH, 4) ortho non-substituted phenolic OH, and 5) carboxylic acid OH.[12]

Table B.2. Original data for hydroxyl group characterization by ^{31}P NMR spectroscopy for lignin fractions before and after Mannich reaction.

Lignin sample[b]	mol / 100 mol aromatic units ± 95% CL[a]					
	Aliphatic OH	Phenolic OH				COOH[c]
		Di-substituted	Mono-substituted	Non-substituted	Total	
HMW	32	28	24	6.1	58	7.6
HMW /DMA/5	34 ± 1	48.8 ± 0.9	7.6 ± 0.4	2.5 ± 0.7	59 ± 1	ND
HMW /DEA/5	41 ± 2	49 ± 1	8.1 ± 0.3	2.7 ± 0.5	60 ± 2	3 ± 2
LMW	11	24	55	6.1	85	17
LMW/DMA/5	12 ± 2	57 ± 5	3.7 ± 0.7	1.5 ± 0.6	62 ± 6	11 ± 3
LMW/DMA/11	13 ± 3	54 ± 12	3.8 ± 0.5	2.0 ± 0.3	60 ± 12	9 ± 3

a. Where provided, the second value represents the 95% confidence limit calculated from an estimated standard deviation using student's t-distribution. Sample size = 3.

b. The sample designation is: MW fraction of lignin / amine species / pH of Mannich reaction.

c. Values for aminated samples calculated by subtracting the large, overlapping acetic acid peak.

For HMW samples, free phenolic OH abundance increased by up to 6% and LMW total phenolic OH content decreased by 5% to 37% according to original integrations of ^{31}P NMR spectra (**Figure B.6**, **Table B.2**). No reaction likely accounts for these differences, so experimental error was suspected to be the cause. Error may be introduced at several points throughout ^{31}P NMR analyses of lignins (sample prep, incomplete phosphitylation, poor spectral sensitivity or resolution, integration, or calculation errors). Troubleshooting was performed to rule out possibilities. It was determined that sample weight measurements and calculations were the most likely sources of error. Specifically, as these analyses involved lignin modifications, the exact mass gain must be known to correctly report abundances per unit original lignin. It is essential to know how much of the final product's mass is attributed to original lignin. Total free

phenolic hydroxyl content changed relatively more for LMW as compared to HMW samples per ^{31}P NMR. If the actual phenolic hydroxyl content did not change, an underestimation could be caused by a lower-than-actual product weight caused by the loss of volatile lignin molecules during freeze drying. This explains why LMW samples had an apparent decrease phenolic content, but not HMW samples.

Other explanations were also considered. The lignin amine results were normalized so the total aliphatic and phenolic hydroxyl contents (per unit original lignin) matched corresponding starting materials (normalized values shown in **Table 3.5**). This was a valid normalization for a few reasons. Aliphatic hydroxyl group content should not change in pink kraft lignin at the Mannich reaction conditions. Only vanillyl alcohol has been shown to undergo C1 displacement and no vanillyl alcohol was present according to HSQC spectra. Aliphatic hydroxyl content increased according to the original data. This fact supports the assumption that the amination conditions are too mild to cause elimination of γ-hydroxyl group as formaldehyde discussed in the previous section above. Loss of or condensation of phenolic hydroxyl groups is very unlikely. Carboxylic acid groups were shown to decrease by HSQC spectra and by model compound studies, so those groups were not included in the data normalization.

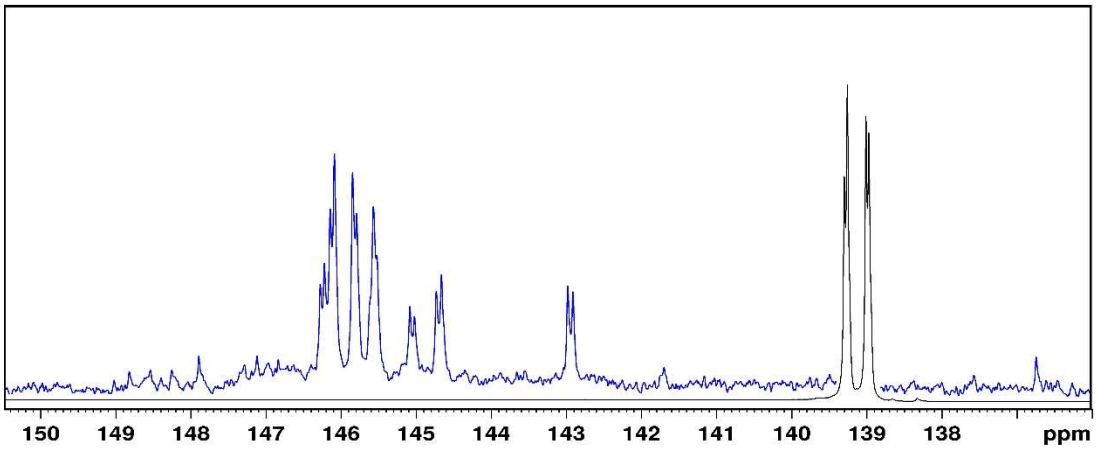

Figure B.7. ^{31}P NMR spectra for 4-methyl catechol (black) and products after Mannich reaction (blue). Hydroxyl groups of the products are all shifted downfield into the di-substituted phenolic hydroxyl region (145.5 ppm to 140.3 ppm) and aliphatic hydroxyl region (150 ppm to 145.5 ppm).

Table B.3. Comparison of results derived from different techniques across different studies.

Reference	Lignin Type	pH	Amine	Dialysis	Product Recovery, wt%	Analytical Method	Amine/Aromatic Units, mol%	Comments
Results from Du 2014[13]	Softwood Kraft Lignin from Lignoboost	5	DMA	Yes, 1 kDa	N/A	Total Nitrogen	36.0	Converted to common units assuming aromatic unit molar mass of 180 g/mol
					N/A	^{13}C NMR	28.0	using Ar-CH2-N structure
Results from Wang 2017[9]	Softwood Kraft Lignin from Lignoboost	5	DMA	No	N/A	Total Nitrogen + ^{31}P NMR	80.4	Converted to common units assuming aromatic unit molar mass of 180 g/mol
		7			N/A		26.2	
		9			N/A		19.5	
Results from Wang 2018[14]	Alkali Lignin, depolymerized to LMW. Assumed to be non-woody due to H-unit content and hydroxycinnamic acids	5	DMA	Yes, 500 Da	75	CHN Analysis	65.0	10 C/mol Ar unit given 1 mol methoxyl group/mol Ar unit
						2D HSQC	62.0	using Ar-H, note that 2D HSQC is not a quantitative technique so while this value matches CHN, accuracy is not assured
						^{13}C NMR	28.7	using Ar-CH2-N structure
This study	Pine Kraft Lignin from Lignoboost, HMW fraction	5	DMA	No	61, corrected for amine addition	CHN Analysis	78.2	
						2D HSQC + 13C NMR	73.2	using Ar-H
						2D HSQC + 13C NMR	21.3	using Ar-CH2-N structure
	Pine Kraft Lignin from Lignoboost, HMW fraction	5	DMA	Yes, 1 kDa	106, corrected for amine addition	CHN Analysis	101.7	
						2D HSQC + 13C NMR	62.7	using Ar-H
						2D HSQC + 13C NMR	26.3	using Ar-CH2-N structure

REFERENCES

(1) Silverstein, R. M.; Webster, F. X.; Kiemle, D. J.; Bryce, D. L. Carbon-13 NMR Spectroscopy. In *Spectrometric Identification of Organic Compounds*; Wiley: Hoboken, NJ, 2015; pp 191–229.

(2) Capanema, E. A.; Balakshin, M. Y.; Kadla, J. F. A Comprehensive Approach for Quantitative Lignin Characterization by NMR Spectroscopy. *J. Agric. Food Chem.* **2004**, *52* (7), 1850–1860. https://doi.org/10.1021/jf035282b.

(3) Balakshin, M. Y.; Capanema, E. A. Comprehensive Structural Analysis of Biorefinery Lignins with a Quantitative 13C NMR Approach. *RSC Adv.* **2015**, *5* (106), 87187–87199. https://doi.org/10.1039/c5ra16649g.

(4) Crestini, C.; Lange, H.; Sette, M.; Argyropoulos, D. S. On the Structure of Softwood Kraft Lignin. *Green Chem.* **2017**, *19* (17), 4104–4121. https://doi.org/10.1039/c7gc01812f.

(5) Hu, Z.; Du, X.; Liu, J.; Chang, H-m.; Jameel, H. Structural Characterization of Pine Kraft Lignin: BioChoice Lignin vs Indulin AT. *J. Wood Chem. Technol.* **2016**, *36* (6), 432–446. https://doi.org/10.1080/02773813.2016.1214732.

(6) Jiang, X.; Savithri, D.; Du, X.; Pawar, S.; Jameel, H.; Chang, H-m.; Zhou, X. Fractionation and Characterization of Kraft Lignin by Sequential Precipitation with Various Organic Solvents. *ACS Sustain. Chem. Eng.* **2017**, *5* (1), 835–842. https://doi.org/10.1021/acssuschemeng.6b02174.

(7) Balakshin, M. Y.; Capanema, E. A.; Santos, R. B.; Chang, H-m.; Jameel, H. Structural Analysis of Hardwood Native Lignins by Quantitative 13C NMR Spectroscopy. *Holzforschung* **2016**, *70* (2), 95–108. https://doi.org/10.1515/hf-2014-0328.

(8) Lancefield, C. S.; Wienk, H. L. J.; Boelens, R.; Weckhuysen, B. M.; Bruijnincx, P. C. A.

Identification of a Diagnostic Structural Motif Reveals a New Reaction Intermediate and Condensation Pathway in Kraft Lignin Formation. *Chem. Sci.* **2018**, *9* (30), 6348–6360. https://doi.org/10.1039/C8SC02000K.

(9) Mikawa, H.; Sato, K.; Takasaki, C.; Ebisawa, K. Studies on the Cooking Mechanism of Wood. XV. Mannich Reaction on Lignin Model Compounds and the Estimation of the Amount of the Simple Guaiacyl Nucleus in Thiolignin. *Bull. Chem. Soc. Jpn.* **1956**, *29* (2), 259–265.

(10) Jiang, Z.-H.; Argyropoulos, D. S. Coupling Phosphorus-31 NMR with the Mannich Reaction for the Quantitative Analysis of Lignin. *Can. J. Chem.* **1998**, *76* (5), 612–622. https://doi.org/10.1139/cjc-76-5-612.

(11) Wang, M.; Sjoholm, E.; Li, J. Fast and Reliable Quantification of Lignin Reactivity via Reaction with Dimethylamine and Formaldehyde (Mannich Reaction). *Holzforschung* **2017**, *71* (1), 27–34. https://doi.org/10.1515/hf-2016-0054.

(12) Meng, X.; Crestini, C.; Ben, H.; Hao, N.; Pu, Y.; Ragauskas, A. J.; Argyropoulos, D. S. Determination of Hydroxyl Groups in Biorefinery Resources via Quantitative ^{31}P NMR Spectroscopy. *Nat. Protoc.* **2019**, *14* (9), 2627–2647. https://doi.org/10.1038/s41596-019-0191-1.

(13) Du, X.; Li, J.; Lindstrom, M. E. Modification of Industrial Softwood Kraft Lignin Using Mannich Reaction with and without Phenolation Pretreatment. *Ind. Crops Prod.* **2014**, *52*, 729–735. https://doi.org/10.1016/j.indcrop.2013.11.035.

(14) Wang, B.; Chen, T.-Y.; Wang, H.-M.; Li, H.-Y.; Liu, C.-F.; Wen, J.-L. Amination of Biorefinery Technical Lignins Using Mannich Reaction Synergy with Subcritical Ethanol Depolymerization. *Int. J. Biol. Macromol.* **2018**, *107*, 426–435.

Appendix C: Supplementary Information for Chapter 4

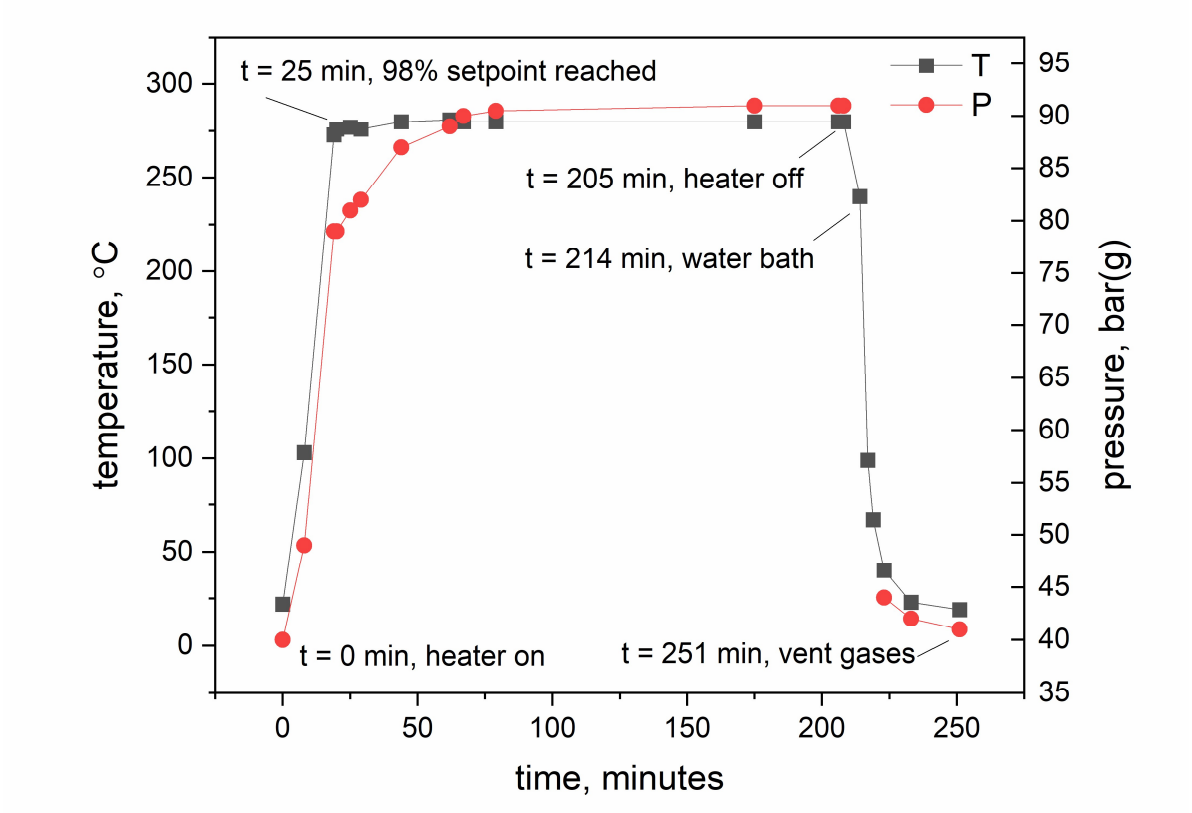

Figure C.1. Example of typical process conditions for a hydrogenolysis experiment. Lignin: 0.9 OD g BCL; catalyst loading: 0.4 g/g Zn/DeAl H-beta; solvent: 60 mL dioxane/methanol (5:1 v/v); impeller: 300 RPM; 280 °C, 3 h.

Mass balance equations

$$\text{Solid Residue, wt\%} = \frac{W_r - W_{cat}}{W_l} * 100 \qquad (C.1)$$

$$\text{Liquid Product, wt\%} = \frac{W_{es}}{W_l} * 100 \qquad (C.2)$$

$$\text{Monomers and Dimers, wt\%} = \frac{W_{ps}}{W_l} * 100 \qquad (C.3)$$

$$\text{Oligomers, wt\%} = \frac{W_{pi}}{W_l} * 100 \qquad (C.4)$$

$$\text{Volatiles, wt\%} = 100 - (solids + oligomers + monomers\ and\ dimers) \qquad (C.5)$$

W_r: weight of solids remaining after filtering reaction mixture and washing with dioxane-methanol (5:1 v/v) mixture

W_{cat}: weight of dry catalyst added to reactor

W_l: weight of dry lignin sample added to reactor

W_{es}: weight of product mixture soluble in ethyl acetate

W_{ei}: weight of product mixture soluble in ethyl acetate

W_{ps}: weight of product mixture soluble in petroleum ether

W_{pi}: weight of product mixture insoluble in petroleum ether

Nitrogen Adsorption Full Results

Table C.1. Specific surface area, pore volume and average pore diameter of samples.

Sample	S_{BET}[a]	Pore volume[b]	d_p[c]
DeAl H-beta	501.32	0.94	16.23
Zn/ DeAl H-beta	513.07	0.83	14.37
Ru/C	687.41	0.48	5.54

a. S_{BET} (m^2/g) is BET Surface Area.

b. Pore volume (cm^3/g) is BJH Desorption cumulative volume of pores.

c. BJH Desorption average pore diameter.

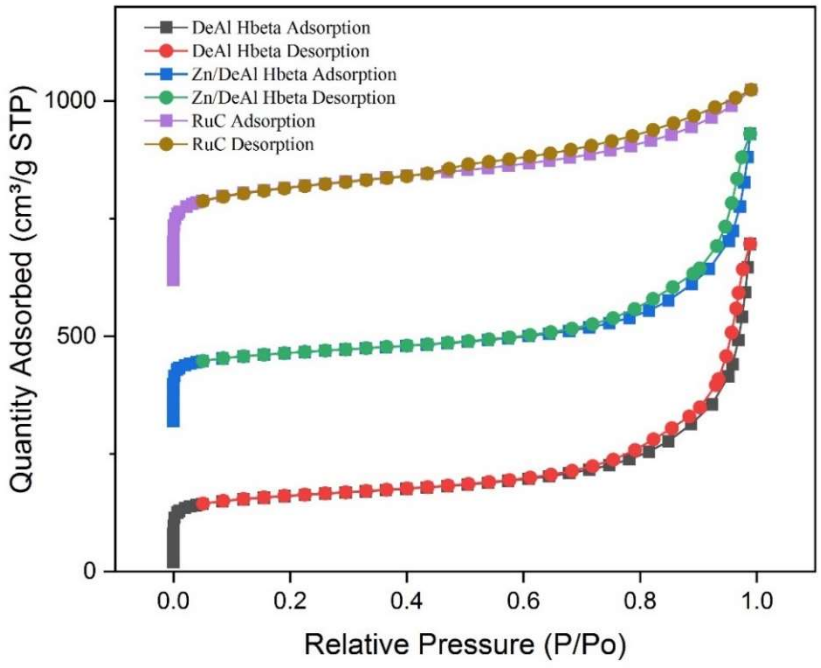

Figure C.2. Nitrogen adsorption–desorption isotherms of the samples.

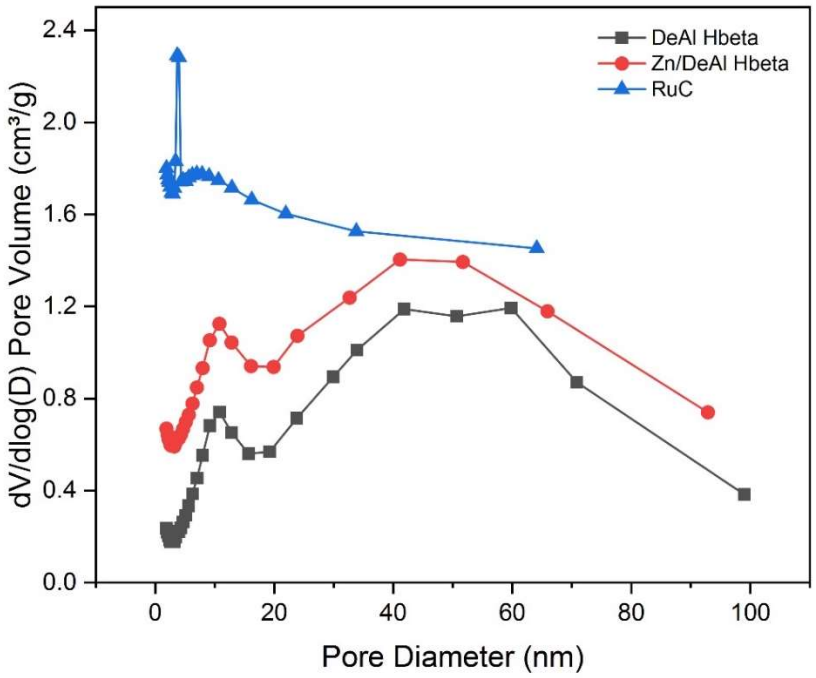

Figure C.3. Pore-size distributions of the samples.

Severity Factor

Akin to the H-factor and P-factor developed for pulping and hydrolysis of biomass, other severity factors have been devised to account for temperature and time effects while analyzing data for the conversion of complex, nonhomogeneous feedstocks like oil and biomass based on the Arrhenius relationship. The factor used here was developed by Overend and Chornet.[77] It assumes conversion is a single, first-order bulk reaction. This should not be taken to provide mechanistic insight, only as a means of presenting and discussing data and planning experiments. The temperature-corrected reaction ordinate, or severity factor, is given by:

$$\ln(R_\omega)\text{corrected} = \ln\left(\exp\left(\frac{T - T_b}{\omega}\right)\Delta t\right) - \frac{T - 2T_f + \left(T_f^2/T\right)}{\omega} \qquad (C.6)$$

T = reaction temperature, K

T_b = base temperature, K, arbitrarily set as 373.15 as a reference to which severity factors are related

Δt = reaction time, min.

ω = characteristic parameter of reaction ordinate, K

T_f = floor temperature, defined as midpoint in reaction temperature range

In determining omega for this study, lignin conversion was defined as:

$$\text{lignin conversion, wt\%} = 100 - (W_{ei} + W_r)/W_l * 100 \qquad (C.7)$$

It was determined that heating and cooling times do not affect the severity factor because the heating and cooling rates were adjusted so that the times were roughly the same, meaning the same factor would be applied in each case which does not affect the presentation of data. Two

additional assumptions were made: 1) isothermal conditions used in the determination of omega, which is assumed to be independent of temperature and related to activation energy; 2) complete conversion = 99%, because the natural log of 0 is infinity preventing calculation of a severity factor.

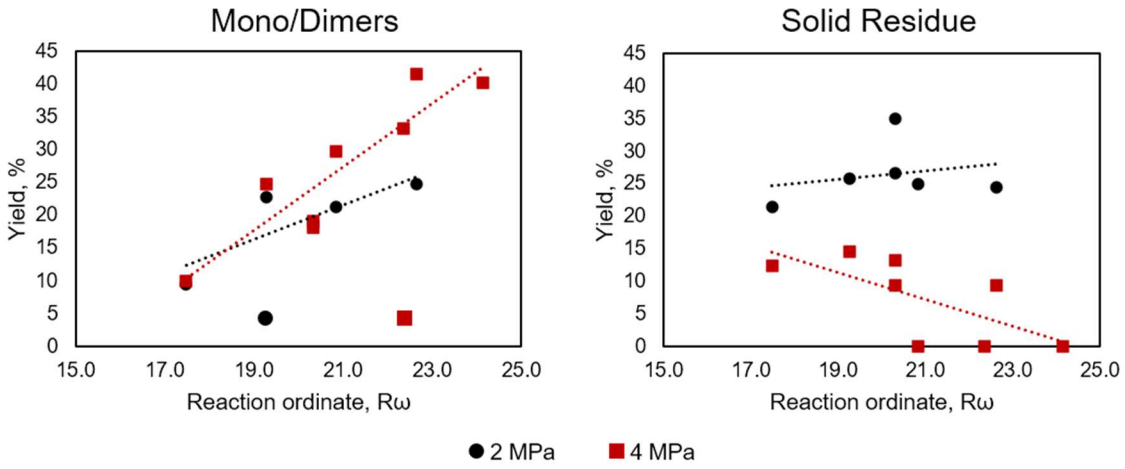

Figure C.4. Effect of hydrogen on BCL conversion plotted against reaction ordinate, or severity factor. Demonstrates the effect of hydrogen on minimizing solid residue formation at higher temperature when hydrogenation is more active. This allows for a higher monomer/dimer yield as those small molecules do not condense into coke.

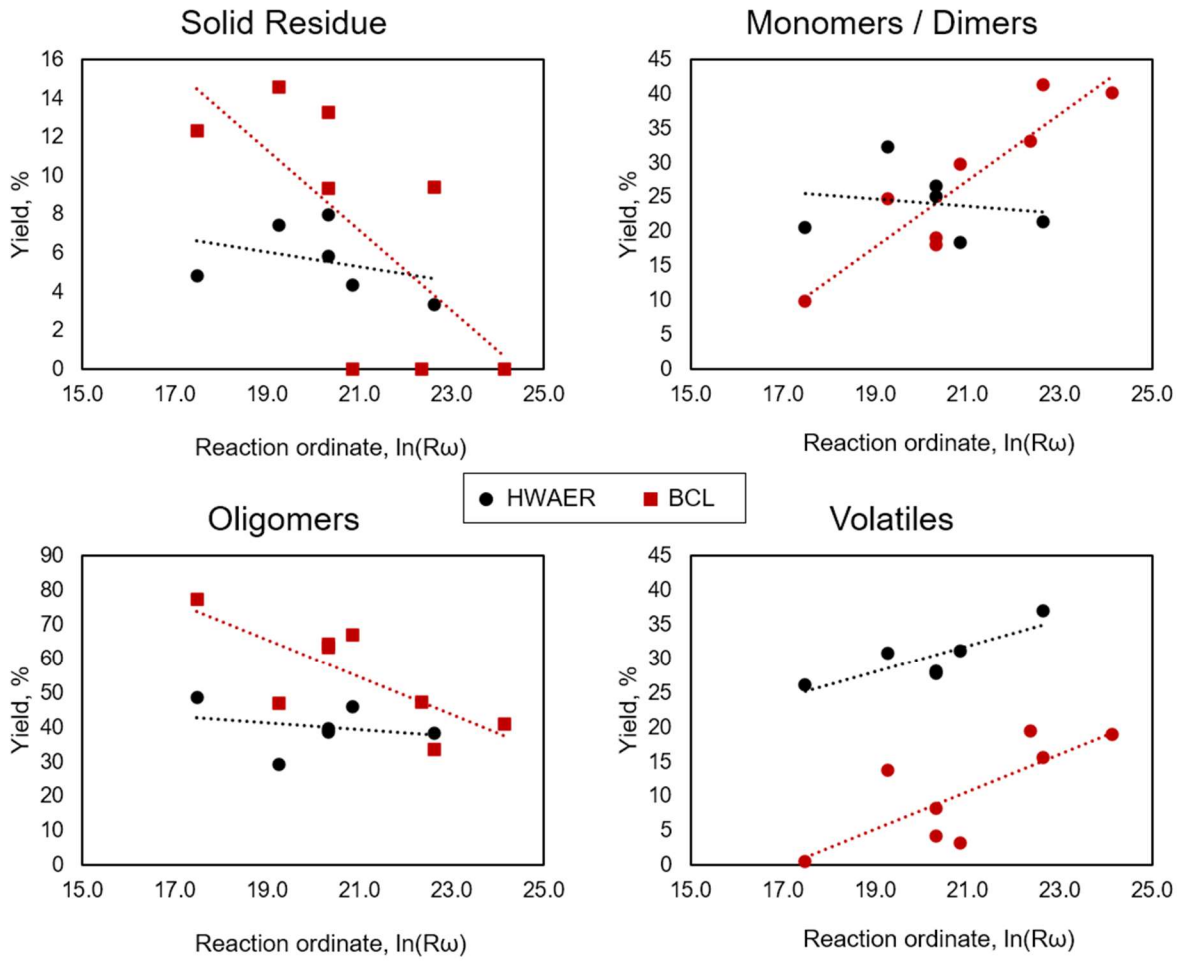

Figure C.5. Demonstration of severity factor as a method of plotting hydrogenolysis yields. Data for BCL is linearized upon transformation. HWAER data was not linearized to the same extent, mostly likely because that system has a different omega parameter, related to the activation energy. Doing some fitting to find the optimum omega for HWAER revealed that the relative severity factors were much higher for HWAER than for BCL, that is, the same time-temperature combination for HWAER was a higher severity than for BCL. Additional reactions at lower time-temperature combinations could be run to try to find the optimum omega parameter, thus an estimate of the activation energy.

Table C.2. Gas chromatography-mass spectrometry semi-quantitative yields as a function of severity (time, h * temperature, °C), weight percent on dry lignin feedstock.

Lignin Type		BCL					HWAER				
Retention Time, min	Compound / Severity	260	300	840	1560	1800	260	300	840	1560	1800
9.896	Phenol	0.04	0.08	0.00	0.09	0.12	0.00	0.00	0.02	0.00	0.00
11.508	Methyl Phenol	0.03	0.00	0.00	0.00	0.09	0.00	0.00	0.00	0.00	0.00
11.576	Cyclohexane-1,2-diol isomer	0.00	0.00	0.00	0.00	0.00	0.00	0.00	0.00	0.00	0.17
12.673	Guaiacol	1.14	2.11	1.81	2.32	2.71	0.79	1.27	1.21	1.47	1.37
12.742	2-hydroxymethyl cyclopentanol	0.00	0.00	0.02	0.00	0.00	0.00	0.00	0.03	0.11	0.00
12.833	4-Ethyl phenol	0.08	0.13	0.12	0.16	0.21	0.00	0.00	0.00	0.00	0.07
13.142	Cyclohexane-1,2-diol isomer	0.00	0.00	0.00	0.00	0.00	0.00	0.00	0.11	0.09	0.00
13.302	Cyclohexane-1,2-diol isomer	0.00	0.00	0.00	0.00	0.00	0.00	0.00	0.07	0.07	0.00
13.828	Methyl guaiacol isomer	0.09	0.16	0.16	0.39	0.55	0.00	0.12	0.17	0.35	0.28
13.885	1,2,3-trimethoxy benzene	0.00	0.00	0.00	0.00	0.00	0.00	0.00	0.00	0.11	0.11
13.988	Methyl guaiacol isomer	0.61	1.46	1.24	1.55	1.66	0.47	0.75	0.57	0.87	0.76
13.999	Catechol	0.19	0.00	0.00	0.00	0.00	0.00	0.00	0.15	0.00	0.00
14.068	Propyl phenol	0.00	0.00	0.03	0.00	0.09	0.00	0.00	0.00	0.06	0.00
15.039	Ethyl guaiacol	1.14	2.00	1.77	2.16	2.52	0.68	0.99	0.98	1.12	1.00
15.119	Syringol	0.00	0.00	0.00	0.00	0.00	2.86	4.10	3.52	3.13	2.78
15.154	Methyl catechol	0.00	0.13	0.11	0.15	0.21	0.00	0.00	0.00	0.00	0.00

Table C.2 (continued).

15.599	Unknown	0.00	0.08	0.07	0.08	0.09	0.00	0.00	0.00	0.00	0.00
15.919	4-Hydroxyphenethyl alcohol	0.00	0.19	0.16	0.14	0.00	0.00	0.00	0.04	0.06	0.11
15.976	Unknown	0.00	0.08	0.09	0.00	0.00	0.00	0.00	0.06	0.20	0.20
16.034	Eugenol	0.16	0.12	0.08	0.09	0.00	0.00	0.00	0.00	0.00	0.00
16.091	Propyl guaiacol	0.80	1.80	1.76	1.81	2.53	1.00	1.57	1.63	1.94	1.74
16.194	Methyl syringol	0.00	0.00	0.00	0.00	0.00	1.23	1.92	1.56	1.67	1.21
16.685	Bibenzyl (ISTD)	-	-	-	-	-	-	-	-	-	-
16.902	Unknown	0.15	0.29	0.30	0.18	0.19	0.00	0.00	0.14	0.13	0.20
16.948	Vanillyl alcohol	0.00	0.00	0.00	0.10	0.16	0.00	0.00	0.05	0.00	0.12
16.959	Unknown	0.00	0.00	0.05	0.00	0.00	0.00	0.00	0.00	0.18	0.00
17.040	Ethyl syringol	0.00	0.00	0.00	0.00	0.00	1.75	2.34	2.10	2.28	1.89
17.223	Isoeugenol	0.66	0.32	0.25	0.13	0.00	0.26	0.23	0.04	0.00	0.00
17.326	Isoeugenol	0.00	0.00	0.00	0.00	0.05	0.00	0.00	0.00	0.00	0.00
17.703	Unknown	0.00	0.00	0.03	0.00	0.00	0.00	0.00	0.02	0.00	0.11
17.851	Apocynin	0.08	0.10	0.09	0.00	0.00	0.00	0.12	0.05	0.00	0.00
17.943	Propyl syringol	0.00	0.00	0.00	0.00	0.00	4.09	5.64	4.90	4.98	3.94
18.091	Unknown	0.13	0.24	0.19	0.11	0.05	0.00	0.00	0.04	0.00	0.00
18.148	p-hydroxycinnamyl alcohol	0.00	0.00	0.08	0.00	0.00	0.00	0.00	0.00	0.00	0.00
18.183	Methyl vanillate	0.00	0.00	0.04	0.00	0.00	0.00	0.00	0.00	0.00	0.00

Table C.2 (continued).

18.525	Homovanillic acid	0.00	0.00	0.00	0.00	0.00	0.00	0.12	0.08	0.00	0.00
18.594	Methyl homovanillate	0.05	0.09	0.08	0.00	0.00	0.00	0.00	0.05	0.00	0.00
18.663	Unknown	0.00	0.00	0.00	0.00	0.00	0.00	0.00	0.10	0.09	0.00
18.868	Homovanillyl alcohol	0.23	0.53	0.46	0.50	0.00	0.17	0.18	0.12	0.00	0.19
18.88	Unknown	0.00	0.00	0.11	0.00	0.46	0.00	0.00	0.08	0.22	0.00
19.074	Unknown	0.00	0.00	0.00	0.00	0.00	0.12	0.00	0.00	0.00	0.00
19.634	Ethyl homovanillate	0.03	0.00	0.00	0.00	0.07	0.00	0.00	0.03	0.00	0.00
19.737	Unknown	0.00	0.00	0.00	0.00	0.00	0.16	0.00	0.16	0.00	0.00
20.034	3-Vanilpropanol	0.56	1.21	1.05	1.07	0.85	0.78	1.02	1.11	1.10	0.74
20.446	Unknown	0.00	0.00	0.00	0.00	0.00	0.24	0.28	0.23	0.16	0.00
20.560	3,4-dihydroxyphenylacetic acid	0.00	0.07	0.04	0.00	0.00	0.00	0.00	0.00	0.00	0.00
20.686	4-hydroxy-3-methoxy benzenepropanoic acid	0.00	0.05	0.04	0.13	0.13	0.00	0.00	0.03	0.19	0.10
20.789	1,2,3-Trimethoxyphenylacetic acid	0.00	0.00	0.00	0.00	0.00	0.00	0.00	0.11	0.00	0.17
21.440	4-(3-hydroxypropyl)-2,6-dimethoxyphenol	0.00	0.00	0.00	0.00	0.00	1.46	1.50	1.89	1.18	0.42
21.600	3-(4-hydroxy-3-methoxyphenyl) propane-1,2-diol	0.04	0.13	0.10	0.10	0.00	0.00	0.00	0.03	0.00	0.00
Total ID'd semi-quantitative, wt %		**6.2**	**11.4**	**10.3**	**11.3**	**12.8**	**16.1**	**22.2**	**21.5**	**21.8**	**17.7**
Petroleum Ether Soluble, wt %		**9.9**	**29.7**	**19.0**	**24.7**	**41.6**	**20.6**	**18.4**	**25.9**	**32.3**	**21.4**

Table C.3. Carbon yield on starting material for hydrogenolysis performed at 280 °C for 3 h.

Catalyst	Lignin	Solids, %	Liquid, %	Solid + Liquid, %
DAB-Ru	BCL	15.6	90.4	106.0
	HWK	5.8	87.1	92.9
	HWAER	11.7	72.2	83.8
CoZn	BCL	30.0	72.5	102.5
	HWK	9.5	-[a]	-
	HWAER	31.9	-[a]	-
RuZnAc	BCL	6.7	96.0	102.6
	HWK	4.3	102.7	107.0
	HWAER	16.6	78.5	95.0

a. Data missing or not measured.

98.6% ± 3.6% (95% CL) of carbon from lignin was retained in solid or liquid products. A goal set by the Department of Energy for biomass-to-fuel projects was 50% overall carbon balance. Apart from CoZn trials, the kraft lignins were able to retain close to 90% carbon or higher, which is a good starting point for furthering processing. HWAER/DAB-Ru solid product was 99% carbon and an estimated (by subtraction) 16% of carbon left with volatile products, therefore limiting condensation and degradation by using lower severity may help improve liquid product carbon yield. BCL/CoZn, HWAER/CoZn, and HWAER/RuZnAc solid products were 77.8%, 71.7%, and 52.1% carbon, so those feedstocks may be less coke-like in nature and more susceptible to further hydrogenolysis. In fact, using a better hydrogenolysis catalyst (Ru vs. Co) increased liquid carbon yields of both BCL and HWAER.

Correcting for catechol on kraft lignin structure analysis by 2D HSQC

Catechol is formed due to the demethylation of methoxyl groups during kraft pulping. The formation of catechol shifts the C2 signal out of the original region for both S-type and G-type units. G2 in catechol resonates in the traditional G5 region, whereas S2 in catechol resonates in the G2 region. Thus, a correction was performed to use G_2 and $S_{2/6}$ signals as a measure of aromatic units for quantitative analysis.

G2 was corrected using the following equation:

$$I_{G2-corrected} = I_{G2-2D} \times \frac{1}{(1 - catechol\%)} \quad (C.8)$$

Because BCL had a catechol content of 10.4%, mol/100 mol Ar unit values were corrected by using a factor of 0.896.

Hardwood kraft lignin

Although the distribution of catechol between S and G units is unknown, it was assumed that 1/3 of catechols are G-type and the other 2/3 are present in S-type units.

C2 (from G2) → G5 region

C2 (from S2) → G2 region

The S/G ratio was determined by the following equations:

$$x + y = 100 \quad (C.9)$$

$$\frac{I_{S_{2/6}}}{I_{G_2}} = b = \frac{2x - 2a/3}{y + 1a/3} \quad (C.10)$$

x and *y* are S and G units in mol per 100 C9 units

b is the integral ratio of [$S_{2/6}$ region] and [G_2 region]